5-15-2018

Developing of Ultrasound Experimental Methods using Machine Learning Algorithms for Application of Temperature Monitoring of Nano-Bio-Composites Extrusion

Ahmed Elseddawy
University of Windsor

Developing of Ultrasound Experimental Methods using Machine Learning Algorithms for Application of Temperature Monitoring of Nano-Bio-Composites Extrusion

By

Ahmed Elseddawy

A Dissertation
Submitted to the Faculty of Graduate Studies
through the Department of Electrical and Computer Engineering
in Partial Fulfillment of the Requirements for the
Degree of Doctor of Philosophy
at the University of Windsor

Windsor, Ontario, Canada
2018

Developing of Ultrasound Experimental methods using machine learning algorithms for application of Temperature monitoring of Nano- Biocomposites extrusion

By
A.Elseddawy

APPROVED BY;

L. Simon, External Examiner
University of Waterloo

S. Saad
School of Computer Science

M. Ahmadi
Department of Electrical and Computer Engineering

S. Chowdhury
Department of Electrical and Computer Engineering

R.Gr. Maev, Advisor
Department of Electrical and Computer Engineering/Physics

May 7th, 2018

Declaration of co-authorship / previous publication

I. Co-Authorship

I hereby declare that this thesis incorporates material that is the result of joint research, as follows:

Chapter 2 and chapter 4 was the results of co-operative work with Seviaryna I, Leshchynsky V, Tjong J, Maev R.. In All cases, the key ideas, primary contributions, experimental design, data analysis, interpretation and writing were performed by the Author, and the contribution of the co-authors was primarily through supervision on the result analysis. Dr. Seviaryna and Dr. Leshchynsky both contributied with supervison of the ultrasound and material test results. Dr. Maev provided feedback on the refinement ideas and the editing on the manuscript.

I am aware of the University of Windsor Senate Policy on Authorship, and I certify that I have properly acknowledged the contribution of other researchers to my thesis, and have obtained written permission from each of the co-author(s) to include the above material(s) in my thesis.

I certify that, with the above qualification, this thesis, and the research to which it refers, is the product of my own work.

II. Previous Publication

This thesis includes [*2*] original papers that have been previously published/submitted for publication in peer-reviewed journals, as follows:

Thesis Chapter	Publication title/full citation	Publication status*
Chapter [2]	*[*Elseddawy A, Seviaryna I, Leshchynsky V, Tjong J, Maev R. Correlation method based Bio-composite material temperature estimation utilizing Ultrasound Signals. InElectrical and Computer Engineering (CCECE), 2017 IEEE 30th Canadian Conference on 2017 Apr 30 (pp. 1-4). IEEE	*Published*
Chapter [4]	Mechanical, Thermal, and Ultrasonic Properties of Plastic Composites Reinforced with Microcellulose and MWCNT	In progress of submission

I certify that I have obtained written permission from the copyright owner(s) to include the above-published material(s) in my thesis. I certify that the above material describes work completed during my registration as a graduate student at the University of Windsor.

III. General

I declare that, to the best of my knowledge, my thesis does not infringe upon anyone's copyright nor violate any proprietary rights and that any ideas, techniques, quotations, or any other material from the work of other people included in my thesis, published or otherwise, are fully acknowledged in accordance with the standard referencing practices. Furthermore, to the extent that I have included copyrighted material that surpasses the bounds of fair dealing within the meaning of the Canada Copyright Act, I certify that I have obtained written permission from the copyright owner(s) to include such material(s) in my thesis.

I declare that this is a true copy of my thesis, including any final revisions, as approved by my thesis committee and the Graduate Studies office and that this thesis has not been submitted for a higher degree to any other University or Institution.

Abstract

In industry fiber degradation during processing of biocomposite in the extruder is a problem that requires a reliable solution to save time and money wasted on producing damaged material. In this thesis, We try to focus on a practical solution that can monitor the change in temperature that causes fiber degradation and material damage to stop it when it occurs.

Ultrasound can be used to detect the temperature change inside the material during the process of material extrusion. A monitoring approach for the extruder process has been developed using ultrasound system and the techniques of machine learning algorithms. A measurement cell was built to form a dataset of ultrasound signals at different temperatures for analysis. Machine learning algorithms were applied through machine-learning algorithm's platform to classify the dataset based on the temperature. The dataset was classified with accuracy 97% into two categories representing over and below damage temperature (190^{o}c) ultrasound signal. This approach could be used in industry to send an alarm or a temperature control signal when material damage is detected.

Biocomposite is at the core of automotive industry material research and development concentration. Melt mixing process was used to mix biocomposite material with multi-walled carbon nanotubes (MWCNTs) for the purpose of enhancing mechanical and thermal properties of biocomposite. The resulting composite nano-bio- composite was tested via different types of thermal and mechanical tests to evaluate its performance relative to biocomposite. The developed material showed enhancement in mechanical and thermal properties that considered a high potential for applications in the future.

Acknowledgment

This project would not have been possible without the kind support and help of many individuals and organizations. I would like to extend my sincere thanks to all of them.

I am profoundly grateful to the IDIR team for their guidance and constant supervision as well as for providing necessary information regarding the project & also for their support in completing the project.

- Roman Maev[1,2]
- Inna Seviaryna[2],
- Volf Leshchynsky[2]

[1]Electrical and Computer Engineering Department University of Windsor

[2]Institute for Diagnostic Imaging Research (IDIR),

Windsor, Ontario, Canada

I would like to thank all those who affect my life through the Ph.D. journey in either positive or negative way. They made me the person who I am today and am proud of that.

Thank you

Contents

List of Figures

List of Tables

Chapter One
Introduction and Literature Review

Introduction and Literature Review

Products are being highly customized with reduced production lead times. The conjugation of these factors pushes companies to continuously and quickly adapt the new technologies rapidly especially the ones related to resources, materials, and information flows [1, 2].

Extruder process

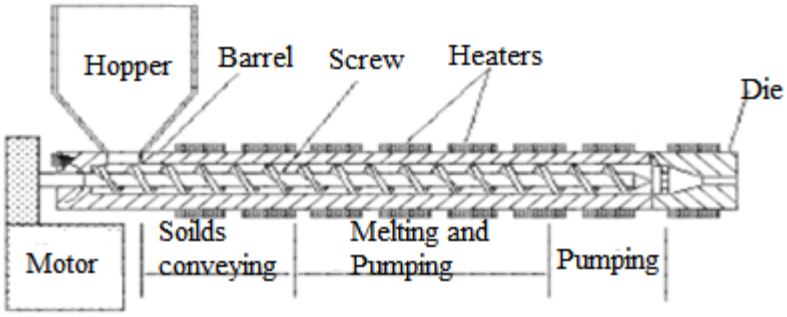

Figure 1 Extruder

https://ru.wikipedia.org/wiki/%D0%A4%D0%B0%D0%B9%D0%BB:Extruder.gif

Polymer composites are being produced via either single or twin screw extruder (Figure 1). The polymer resin is heated until it reaches molten state through a mixture of heating elements and shear heating coming from the extrusion screw. The screw, or screws as the case with twin screw extrusion, forces the resin through a die.

Main Control Parameters

- Speed
- Pressure
- Temperature

One of the essential measures to be taken into account during the composite manufacturing process is the temperature parameter. Temperature monitoring allows prediction of polymer composite material destruction during the extrusion. Controlling the temperature during production cycle helps to save material from damage; hence saving time and money of preparing another material. There are several approaches to monitor the temperature represented in different kinds of transducers and monitoring systems. The objective of this project is to provide a robust Ultrasound temperature monitoring system for material production, which allows controlling the high-temperature effect on the material preparation and preventing damage before it happens.

Composite materials

Materials which consist of two or more elements, one of them, the fiber, is dispersed in a continuous matrix phase is called composite material. The product properties that are produced are different to the properties of the elements on their own. Composites have many advantages such as lightness, resistance to corrosion, resilience, translucency and superior efficiency in construction in comparison with conventional materials. To obtain the maximum reinforcement, highly stressed fiber regions could be introduced into the polymer matrix at in a particular position, orientation and volume.

Composite Manufacturing

The primary goal is to achieve the required technical performance of the manufactured composite at an economical cost process. Hence the choice of process is essential to achieve that goal. Each process has its particular benefits and limitations making it suitable for specific applications. Composite parts can be molded via a wide range of processes including simple manual process and industrialized complex processes such as 'Sheet Molding Compound' (SMC) [3].

Technical factors like the mechanical properties, environmental performance and size, and shape of the part in addition to economic factors like cost per piece being produced and run length are the main factors that govern the choice of the process and process parameters.

Fiber

Fiber reinforcement has different grades and types. In production, attention must be taken to guarantee that the correct grade/type is used. When different grade or type of fiber is used, the composite material produced will not have the expected properties. For example, Carbon fibers of different types or grades do however have vast differences in modulus and strength.

Fiber may be broken, and sometimes bundles of fiber may be kinked or wavy rather than straight, all of which will severely affect the tensile and compressive strength of the final composite material by reducing them. Uneven distributions of fiber lead to resin-rich or resin-starved regions. Defects in fiber may make them weaker or introduce stress concentrations

Bio-composite

Biocomposites have proven their capability as an environmentally friendly replacement for polymers composites. Over the past decade, biocomposites have been used in many industries with different running applications primarily in the automotive industry[4]. Enhancing the properties of the biocomposites and providing the composites with more efficient electrical properties will open the door widely for more applications, especially with the mainstream heading towards cheaper and lighter electric vehicles.

Studies concerning fiber-reinforced composites have been focused on thermosetting matrices because of the low viscosity of the uncured resin, which results in excellent fabric impregnation, and the low curing temperature, which is beneficial to avoid fiber thermal degradation[5].

Cellulose-based natural fibers have excellent mechanical properties and a low density which can be used successfully as reinforcements for different kinds of thermoplastics. Although a weakness point of that fiber, which may cause a thermal stability problem, is that the first degradation occurs at temperatures above 180°C. Because of this, the thermoplastics typically used as the matrix are polyvinyl chloride, polypropylene, and polyethylene, which have melting temperatures below or equal to the degradation temperature [6].

Monitoring extruder temperature

In polymer extrusion, a homogenous melt output is required to achieve a uniform extruded product. The extruder temperature profile is to be taking into consideration as one significant parameter to avoid fiber degradation during the production process. Temperature disturbance in the melt leads to non-uniformity of the optical, mechanical, or chemical properties of the produced parts, or leads to extrudate containing un-molten or gelled particles[7].
The mechanical properties are the main affected properties when fiber degradation is concerned. Studies show the small or significant effect on mechanical properties (e.g., tenacity) due to fiber degradation as a result of thermal exposure for short or long time long [6].

Although the Surface temperature of the screw is known to affect the melting process [7], there are no published studies that take the surface temperature of the screw during the process into account when simulating the temperature profile of the melt inside the screw. One of the main reasons is the difficulty of measuring screw temperature during the process.

Studies investigating the temperature profile using another means of measurement can be found. Single screw extruder averaged melt temperature profiles comparison across the width of the screw at the end of the metric zone between a high-density polyethylene homopolymer (HDPE) with low-density polyethylene (LDPE) for three types of screws was measured. Data was measured with an infrared sensor at the metering section of the screw channel while other data was collected using a thermocouple grid at the end of the metric zone [8].

Results show that IR data is sensitive to the temperature and detects small variation in temperature across the channel width within 3-5℃ especially with the high speed. While larger variations can be detected through the melt (20-30℃) [9].

A twin extruder is more challenging to measure the temperature profile though. However, some studies have a temperature data analysis along the axis of the extruder by using six measuring points along the length of the extruder [10]. Measuring melt profile before the die section is highly likely to give similar results of a single screw.

As illustrated earlier, this variation of temperature may lead to degradation of fiber although the sited temperature is less than the degrading temperature. To avoid this, less temperature should be applied to the melt through the extruder. To implement real-time control of the temperature, the further measurement should be done near the screw (center of the melt) which represents the highest temperature point due to the high shear force between the screw and composite and friction between the fiber, that may lead to exposing the fiber to more heat and end with fiber degradation that affects the mechanical properties badly.

Conventional methods of temperature determination

Thermocouples

Shielded thermocouples are the most commonly used melt temperature sensors. Thermocouples are generally used in association with another thermocouple held at a known reference temperature, the differences being used to compute temperature at the measurement position. The thermocouple junction is shielded, and the tip is mounted to protrude into the polymer melt.

Although shielded thermocouples (the thermocouple junction is sheathed for robustness) are relatively inexpensive, they have several disadvantages. When the sensors are flush mounted with the extruder barrel wall, the recorded temperature is often similar to barrel temperature; the thermocouple gives a single point measurement that tends to be heavily influenced by the barrel due to its proximity. Temperature gradients along the thermocouple sheath introduce measurement error. Shear heating effects can be observed if the thermocouple tip protrudes into the melt flow, thereby indicating a local temperature increase. Also, response time is slow owing to the thermal mass of the sheath, limiting sensitivity to transient changes.

The single point measurement issue may be addressed by the use of multiple or traveling thermocouples. However, the disadvantages of shear heating errors and slow response times remain. More recently, thermocouple meshes have been proposed whereby a pattern of crossing wires forms several thermocouple junctions across the mesh, which sits within the melt flow. However, the durability of such a mesh of thin wires in high pressure and high flow rate conditions is yet to be confirmed. Some published experiments installed a thermocouple grid before the die section of the barrel to measure the temperature profile on radial positions [11].

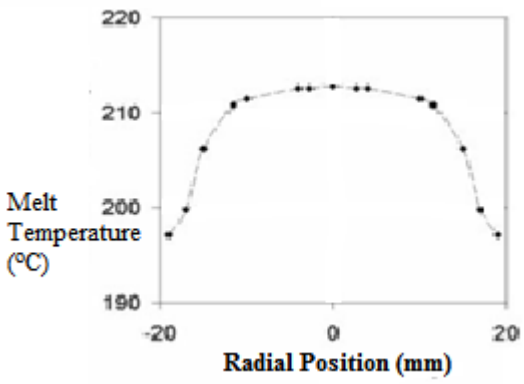

Figure 2 Temperature profiles for single screw measured by thermocouple grid

Infrared transducers

Melt temperature can also be measured using infrared techniques, with a wavelength range of ~0´8 mm to 1 mm. A polymer melt in a closed area or within an extruder or mold is assumed to behave similarly to a black body (one that completely absorbs all incident radiant energy and emits the maximum level of radiation possible at all infrared wavelengths).

The Stefan Boltzmann relationship gives the total energy emitted by a black body object $U=\sigma T^4$,where $U=W\ m^{-2}$; $\sigma=5´6687\times10{-}8\ W\ m^{-2}\ K^{-4}$ (Stefan's constant); and T =absolute temperature (K).

For specific temperature conditions, a particular wavelength has energy radiation of maximum intensity. For a particular wavelength, the energy emitted can be measured and related to the temperature of the object. The principle of operation of an infrared temperature transducer makes use of this fact, such that the transducer notes the wavelengths for which infrared radiation is strongest and relates them to the temperature of the body. The energy emission information is typically gained from an area of melt projecting inwards from the die wall such that an accurate indication of melt, rather than surface temperature, may be obtained.

Infrared transducers are thought to probe a distance of up to 8 mm into the melt. The actual distance is unknown and depends upon the material under test. Work by Obendrauf and others [8, 12] using a Dynisco MTX transducer determined penetration depth by measuring the emitted intensity of infrared from a specific material for different sample thicknesses and using the information to quantify the absorption coefficient for that material, from which an average penetration depth is obtained. The authors suggest that the measuring depth for an unfilled polypropylene is on the order of 1.6 mm. This is compared with 6.7 mm for rigid poly(vinyl chloride) PVC and 0.033 mm for a 20% talc and soot-filled polypropylene.

Recent studies, again using a flush mounted Dynisco MTX sensor with a sapphire window, have confirmed that penetration depth is affected by polymer type. For a linear low-density polyethylene (LLDPE), an average penetration depth of 4.5 mm is noted when a traversing thermocouple is used to measure temperatures, whereas for low-density polyethylene (LDPE) and high-density polyethylene (HDPE) the penetration depth is on the order of 3.2 mm.

Corrections for shear heating associated with the traversing thermocouple may mean that the infrared measurement depth is underestimated. Magnesium hydroxide filler is also shown to have a tremendous influence on penetration depth during extrusion and a smaller effect during static tests. Measured temperature apparently decreases with increasing filler content in LDPE.

The advantages of using an infrared device rather than thermocouples include [13]:

1. Much improved response time (having a typical first order time constant of 10 ms);
2. Non-intrusive design using a flush mounted sapphire window, removing the influence of shear heating from measurements;
3. The ability to make bulk temperature measurements rather than surface temperature measurements; and
4. Robust design;

However, the uncertainty of measurement depth and inability to probe the entire melt cross-section depending upon die or nozzle geometry leads to problems when estimating bulk melt temperature.

Ultrasound Measurements

Non-Destructive Testing (NDT) for material evaluation keeps gaining more interest every day for both industrial and research purposes. NDT not only saves material cost but also can be used to have quality control over the production process. Ultrasound plays a vital role as an NDT method. It has gained more interest, especially in the medical applications as a safe alternative to other evaluation methods and industrial applications and as a cheap and a high potential multipurpose testing method.

Since the early 19th century elastic constant of material has been determined extensively using acoustic techniques [14]. The ability to detect a change in acoustic properties of polymers/composites due to the environment made Ultrasonic Non-Destructive Evaluation (NDE) a very promising technique for inline monitoring [15, 16]. The need for robust process control increases especially for complex engineering components constructed from fiber reinforced polymer composites [17].

In 2000, Challis, R. E presented a paper describing the application of a group of physical techniques that used to characterize the polymer structure during cure, with the aim of relating these to phenomena measurable by ultrasound, He concluded that compression wave ultrasound systems have the potential to monitor both the progress of treatment and the development of mechanical properties [18].

Dynamic Mechanical Analysis (DMA) defines techniques whereby we apply a time-dependent sinusoidal disturbance to a specimen, and the consequential behavior is measured as a function of time [19]. Several authors have reported using ultrasound to monitor the progression of the viscoelastic moduli of polymers due to change in time or temperature. It is known as Ultrasonic Dynamic Mechanical Analysis (UDMA) [20].

Although there are still limitations on the application of ultrasound on polymer process evaluation, such as the poor long-term stability of transducers at high temperature and more reliable software analysis and interpretation of events derived from the response of polymers to ultrasonic waves, the use of ultrasound is potentially a influential method for the characterization of polymers, mainly as a tool for Inline monitoring of events occurring during the manufacture of polymer matrix composites [20].

Ultrasonic Dynamic Mechanical Analysis (UDMA) can be performed by scanning over a wide range of frequencies [21]. Mc Hugh, Jarlath (2007), presented his work to demonstrate the practical application and sensitivity of ultrasound as a high-frequency DMA technique for the characterization of polymers [17]. He was following the footsteps of Satrk. W and others at Bundesanstalt für Materialforschung und –prüfung (BAM) [22] who, at this time, had the only commercial acoustic equipment that has the capability of industrial process monitoring thermosetting molding compounds.

In his work, he employed a high-temperature sensor to obtain data over a wide range of frequencies (2 to 6MHz and 250 to 650 KHz). He used two sample measuring setups to neglect the boundary reflections. He applied Fourier transformation analysis software to determine frequency-specific sound velocity and attenuation. Applying these factor, he achieved a high sensitivity technique for DMA of polymers and demonstrated its potential for a range of applications.

Recently, ultrasonic measurements as a nondestructive, cheap and safe technique have also found it's place for process control applications either to understand equipment problems or as a way to predict the outcome of measurements proposed to control a process [23].

Acoustic properties of polymers

There is no parameter used to describe the material properties using ultrasound. For crystalline materials, a simple relationship describing elastic recovery exists $M = \rho c^2$, whereby M represents the mechanical modulus, ρ the density and c is transversal or longitudinal sound velocity. On the other hand, viscoelastic materials such as polymers dissipate energy and wave propagation is attenuated [17]. It is common to express Young's modulus as a complex quantity $E^* = E' + iE''$ [21].

Acoustic waves are characterized by sound speed and sound absorption. Sound absorption (α) is a measure of the energy removed from the sound wave by transformation to heat during the propagation of the wave through a given thickness of the material.

Varying stresses are normally expressed as a complex quantity, and the modulus is given by $M^* = M' + iM''$ [19]. M′ is referred to as the real component and describes the elastic or energy storage component of the modulus. M′′ is the imaginary part or loss modulus.

Depending on the nature of the ultrasonic wave, from measurements of velocity $\boldsymbol{c}$ and attenuation coefficient $\boldsymbol{\alpha}$ the two components of the complex modulus (shear or longitudinal, here indicated with M′ and M′′) can be calculated from the following expressions [20]

$$M' = \rho v^2 \frac{(1-(\frac{\alpha\lambda}{2\pi})^2)}{(1-(\frac{\alpha\lambda}{2\pi})^2)^2} \quad (1)$$

$$M'' = 2\rho v^2 \frac{(\frac{\alpha\lambda}{2\pi})}{(1+(\frac{\alpha\lambda}{2\pi})^2)^2} \quad (2)$$

These laws work for modulus including the complex Young's modulus E*, complex shear modulus G*, complex longitudinal modulus L* or complex bulk modulus K*. The modulus is related according to the following expressions [20, 24]

$$\begin{aligned} K^* &= L^* - 4/3G^* \\ L' &= K' + 4/3\,G' \\ L'' &= K'' + 4/3\,G'' \end{aligned} \quad (3)$$

The ratio of the imaginary part of the modulus (Young's shear of bulk) to the real part is the tangent of the phase angle between the two components and is called the loss factor, tanδ. The loss factor is approximately related to absorption (α) per wavelength (λ) by the equation[21]:

$$\tan\delta = \frac{E''}{E'} = \alpha\lambda/\pi \quad (4)$$

The longitudinal and transverse speed of sound is related to the elastic constants with the relations [21]

$v_l = \sqrt{\frac{k+4G/3}{\rho}}$, $v_s = \sqrt{\frac{G}{\rho}}$ where K is the bulk modulus, G is the shear modulus and ρ is, the density.

The calculation of attenuation and group velocity for different sample thickness is calculated from the peak arrival times according to the following equation.

$$V_{TOF} = \frac{(d_2 - d_1)}{(t_2 - t_1)} = \text{(m/s)} \quad (5)$$

t_1 and t_2 represent the time of flight of the sound wave to travel through individual samples. $_1$ and $_2$ are the thin and thick specimen respectively. The attenuation is determined by linking the peak amplitudes (e.g., negative peak) from the thin d1 and thick d2 samples and calculated according to the following Equation. Peak amplitudes are referred to as A1 and A2.

$$\alpha = 20 \log\left(\frac{A_1}{A_2}\right)\frac{1}{\Delta d} = \text{(dB/mm)} \quad (6)$$

The advantage of using Ultrasound (US) monitoring system

Previously published work by C. K. Jen discussed using ultrasound for monitoring polymer and the dispersion of the filler in a polymer matrix during extrusion [25, 26]. Experiments have shown that ultrasound can provide in-process information about the quality of dispersion. It has been confirmed that the ultrasonic sensor can be successfully operated along the extruder screw and that ultrasound can give access to the material properties while the polymer is being processed [27].

Several advantages are provided by Ultrasonic techniques over conventional methods and through ultrasonic measurements performed at the die level [27, 28]. However, since the properties of the composites are gradually changing along the extruder, there is a keen interest to access these properties at any location throughout the process.

- Ultrasound wave prevents the false increase in temperature due to interaction effect between the viscous polymer and conventional thermocouple probe, which leads to more accurate temperature measurement of the melt.
- Ultrasonic can also monitor the distribution of the reinforcement material/ additives in the composite as different distribution lead to different ultrasonic properties.
- Ultrasonic equipment can be very competitive with other techniques of measuring temperature regarding cost-effectiveness, durability, and reliability.

Machine learning

A new era of industry 4.0 based mainly on the mass production of individually customized products leads manufacturers and companies to adapt rapidly to new evolving technologies and manufacturing systems to respond quickly to market demands especially those are continuously changing [1, 29-31].

Learning is the process of converting experience into expertise or knowledge [32]. Data is the input to a learning algorithm in training. The output is experience, which usually has a form of a computer algorithm that performs particular tasks.

Machine Learning has become a cornerstone of information technology. With the ever-increasing amounts of data becoming available there is no doubt that data mining and data analysis is becoming an unreplaceable ingredient for technological progress [31].

Personal computers facilitate saving things that previously would have been trashed. Affordable multi-gigabyte storage units are postponing someone's decisions about what to do with all this data since it is easier to purchase another disk and keep it all. The world is overwhelmed with similar data. Buried in all this data is potentially useful information that is hardly taken advantage of. As the volume of data increases, inexorably, the proportion of it that people understand decreases, alarmingly [29].

Data mining is about looking for and discovering the patterns in data. Generally speaking, a scientist's job is an interpretation of data, to identify the patterns that govern how the physical world works and capture them in theories that can be used for predicting what will happen in similar or new situations. The entrepreneur's job is to recognize opportunities, that is, patterns of behavior that can be turned into a profitable business, and exploit them [29, 31, 33].

Data mining is using automated searching via computer programing or an algorithm to look at electronically stored data. However, this is not new for science, as similar techniques have been used for sorting, identification, and validation of information. The unique thing is the significant increase in chances and opportunities to find a pattern in data.

The continuous growth of databases in recent years and databases on everyday activities as customer choices puts data mining into the front of new business technologies. It has been estimated that the amount of data stored in the world's databases doubles every 20 months [33].

The opportunities for data mining increases as the flood of data continues and machines that can undertake the searching become usual. As the world overwhelms us with the data it generates, data mining becomes our only hope for revealing the patterns that lie beneath it. Similar to knowledge is power, wisely examined data is a treasured resource. It can lead to new understandings and, in commercial settings, to competitive advantages [29]. Data mining is about finding a solution to problems by analyzing data existing in databases.

There are two excesses for the expression of a pattern, either as a black box or as a transparent box. Black box innards are effectively incomprehensible while transparent box construction reveals the structure of the pattern. Valuable patterns allow us to make predictions on new data. The difference is whether or not the patterns that are mined are represented regarding a structure that can be inspected, reasoned about, and used to enlighten future decisions. Such patterns are called structural because they capture the decision structure in an explicit way that assists us to explain something about the data.

Most of the techniques that are for finding and describing structural patterns in data have developed within a field known as **machine learning.**

Task Statement

Problem definition

The fiber in Fiber Reinforced polymer composites reaches degradation temperature during processing. Fiber degradation leads to the material losing leading properties such as strength. Material reaching fiber degradation temperature is considered damaged and should not be used to the production line. The damaged material is considered a loss in both time and money.

Cause

Temperature increase and vary between inside the extruder barrel temperature (measured temperature) and material inside. Due to shear force between the extruder and material during production, temperature increases in the center of the extruder more than the settled temperature. Thermocouple does not sense the temperature change since it is loaded into the barrel to measure temperature from the surface of the extruder barrel. Hence, detection of the damage happens after the material is already processed.

Mission

The primary goal of this work is to study the Bio- composite production technology and the production process conditions (e.g., different temperature regions of production) to develop a reliable approach to solve the defined problem. Adding CNTs to the Bio- composite and following the modified composite from production to testing will be an excellent aid for understanding the technology and provide a suitable solution for future materials.

Currently, to overcome the problem of temperature increase, manual temperature adjustment is performed when damage is detected to stop the following batches of the material being ruined. The suggested approach is to find a monitoring system that can help detect damage when it happens, so it could be controlled earlier and resulting in saving time and money. This can be achieved by either directly measuring temperature near extruder screw surface instead of the barrel via different methods, or detecting temperature increase effect inside the material and have control if the damage is exposed. Although, measuring the temperature directly near the surface of rotating screw is not practically possible for either high cost or technical difficulties.

The mission is to develop and confirm the selected approach of using ultrasound to monitor the temperature increase and its effect on the material and apply machine-learning techniques to classify different Temperature US signals to detect damaged material.

Chapter Two

Ultrasound Instrumentation for experimental examination of temperature

Fundamentals of ultrasound

Acoustics (The science of sound) has become a wide-ranging interdisciplinary field covering the academic areas of physics, engineering, psychology, audiology, architecture, physiology, neuroscience, and others [34]. The branches of acoustics include architectural acoustics, physical acoustics, musical acoustics, psychoacoustics, electro-acoustic, noise control, shock and vibration, underwater acoustics, speech, physiological acoustics, etc.[34, 35].

Soundwave is generated through different techniques, such as vibrating bodies, changing airflow, time-dependent heat sources and supersonic flow. Ultrasonic Testing (UT) uses high-frequency sound waves in the range between 0.5 and 15 MHz for inspections and measurements [34, 36]. In the engineering field, UT has a wide range of applications such as flaw detection/evaluation, dimensional measurements, material characterization, etc.[37]. Ultrasound is also used in the medical field such as sonography, therapeutic ultrasound, etc. [38].

UT is based on the analysis of either the reflected waves (pulse-echo) or the transmitted waves through the transmission. Since they require one-sided contact surface to the item being examined, generally pulse-echo systems are more useful than other techniques.

Ultrasonic testing (UT) is the most commonly used non-destructive evaluation method for the inspection of composites [39]. Frequency range 20 kHz to 20 MHz is frequently used on microscopically homogenous materials (i.e., non-composite). In testing composites the frequency range is reduced due to the attenuation, so the operating frequency limit is usually 5 MHz or less [40].

In most techniques, pulses of ultrasound are sent through the composite and then received after being affected by the structure.These techniques include through-transmission, pulse-echo, back-scattering, and ultrasonic spectroscopy [21, 34, 40].

Through the manual (UT) the area is contact-tested by scanning a probe by hand; For a small inspection area is, this is suitable for fieldwork. To obtain consistent results, manual UT requires a high level of operator skill due to the signal amplitude dependence on the thickness of the coupling fluid layer, which itself is dependent on the pressure applied [39, 41]. However, variations among trained operators should not pose a problem provided a standard calibration be obtained.

For water-sensitive or absorbent composites, roller probes with water-retentive rubber tires are favored because they leave the surface dry. However, these work at the lower end of the UT frequency range and therefore are not best suited to detailed defect analysis [13, 39]. This illustrates that the probe-specimen distance must be within a narrow tolerance else the ultrasound transmitter will become de-coupled from the testing sample [13].

In non-contact UT, tolerated probe movements can be accepted without de-coupling the transmitter. Generating the ultrasound with a laser is one way of doing this [13]. The added advantage of this is that the speed and the signal can be produced and sensed in any orientation up to 60 degrees relative to the specimen. However, this approach is obviously relatively costly in addition to surface ablation risk and the required physical safety measures when using high powered lasers, which can be restrictive in a production or field environment. Using the magnetostrictive is another alternative, but these operate only at the low ultrasonic frequency range (200 kHz or less).

Immersion testing, or IUT, is to uphold a continuous buffer, preserved when the specimen probe distance changes significantly, of coupling fluid, usually water, between the probe and the testing sample. For a small specimen, an immersion test can be executed by executing the test with the probe and specimen fully submerged in coupling fluid [13, 36]. However, this approach is impractical in the case of large specimens since submersion of the specimen will cause excessive cost and also the size of immersion tanks.

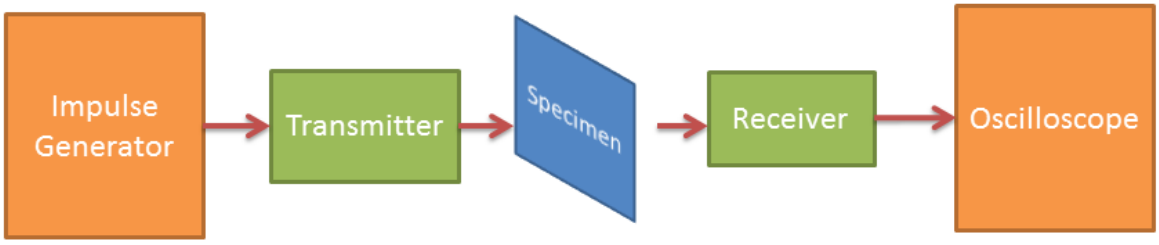

Figure 3 US non-destructive test Through Transmission setup

If the specimen is floating that will lead to another problem, large forces are needed to keep it submerged. The jet probe technique is an alternative to submersion in which two specially designed probes apply water jet and couple it to the ultrasound, one transmitter and one receiver. This is a more suitable technique for big or floating samples since it can adapt to the change in the surface contours. [13, 41, 42].

Pulse-echo UT examination system includes several units, transducer, the pulser/receiver, and a display unit. High voltage electrical pulses are generated by the electronic device or a pulser/receiver. Driven by the pulse, high-frequency ultrasonic energy is generated by the transducer [34, 39].

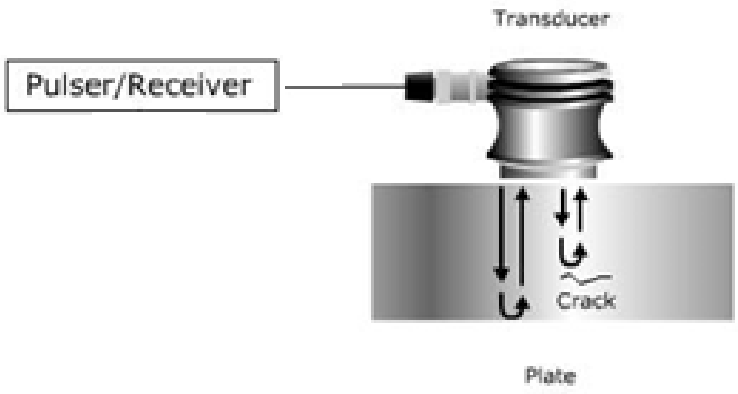

Figure 4 US Non-destructive Pulse- Eco System

https://www.nde-ed.org/EducationResources/CommunityCollege/Ultrasonics/Introduction/description.htm
https://eis.hu.edu.jo/ACUploads/10526/Ultrasonic%20Testing.pdf

The energy of sound is generated and propagates through the materials in the form of waves. When there is a discontinuity (defect /crack) in the wave path, some of that energy will be reflected back from the surface with a flaw. The transducer turns the reflected wave signal into an electrical signal, and the signal is displayed on a screen. Time of travel can be directly related to the traveled distance, Knowing the velocity of the signal. From analyzing the signal, information about the reflector location, size, orientation and other features can be gained [34, 39, 41].

Advantages and Disadvantages

compared to other NDT methods are [13, 21, 34, 36, 39, 41]:

Advantages

- An automated system produces detailed images;
- Safety;
- Other features can be obtained, such as thickness measurement;
- Portable and easy to use;
- Sensitivity to the surface and beneath the surface discontinuities;
- Penetration depth for flaw detection or measurement is superior to other NDT methods;
- High accuracy;
- Specimen preparation is minimal; and
- Instantaneous results can be obtained.

Disadvantages

- Surface must be accessible to transmit ultrasound;
- Coupling medium is required;
- Defects may be unseen if it is parallel to the sound wave beam; and
- Some samples, e.g., cast iron specimen are hard to inspect due to law sound wave and high noise level from the rough surface.

Physical acoustics involves the use of acoustic techniques in the study of physical phenomena as well as the use of other experimental techniques (optical, electronic, etc.) [34]. Since much of physics involves the use and study of waves, it is useful to begin by mentioning some different types of waves and their properties. The most basic definition of a wave is a disturbance that propagates through a medium. A simple comparison can be made with a stack of dominoes that are lined up and knocked over. As the first domino falls into the second, it is hit over into the third, which is knocked over into the next one, and so on. This suggests that we define two concepts, the average particle velocity of the individual dominoes and the wave velocity (of the disturbance) down the chain of dominoes [21, 34].

Physics of Acoustics

Properties of Acoustic Waves

The wavelength is inversely proportional to the frequency of the wave and directly proportional to the velocity of the wave. This relationship can be described by the following equation:

$$\lambda = \frac{v}{f} \tag{7}$$

Where;

λ : wavelength (m)

v : velocity (m/s)

f : frequency (Hz)

The speed of sound waves in a medium is fixed where it is a representative of that medium. As can be illustrated by the equation, an increase in frequency will lead to a decline in wavelength [34, 35].

Defects Inspection

In UT, a decision about the frequency of the transducer that will be used has to be taken into consideration to control the wavelength. The wavelength of the ultrasound plays an essential rule in detecting a discontinuity. A discontinuity should be larger than one-half the wavelength to stand a reasonable chance of being exposed as a general practice [19].

In order to define a technique's ability to locate discontinuity, sensitivity and resolution are two terms that are used in the ultrasound evaluation. Sensitivity is the ability to locate small defects. Sensitivity increases with higher frequency and shorter wavelengths. Where resolution is the ability of the system to find discontinuities that are close together within the specimen or located near the part surface. The resolution also increases as the frequency increases [39].

Material's grain structure and thickness have to be taken into account for selecting a frequency for inspection, in addition to the discontinuity's type, size, and probable location. Soundwave tends to scatter from large or coarse grain structure as frequency increases, and from small imperfections within a material.

Cast materials often require lower frequencies to be used for evaluation because they have coarse grains. Higher frequency transducers can be used for inspection of wrought and forged products with directional and refined grain structure [39, 43]. The penetration depth is also reduced.

Soundwave Propagation in Elastic Materials

Sound waves propagation is caused by the oscillatory or vibrations motions of particles within a material. Ultrasonic wave can be simulated as an infinite number of oscillating masses or particles connected by means of elastic springs. Each particle is affected by the motion of its nearest neighbor and both inertial and elastic restoring forces act upon each particle [34].

For a mass with spring constant k and its mass m, a mass on a spring has a single resonant frequency (natural frequency). Tied to the elastic limit of any material, there is a linear correlation between the displacement of a particle and the force trying to restore the particle to the position of Equilibrium. Hooke's Law describes this linear dependency. When using terms of the spring model, the relation between force and displacement is written as F = k x.

The effect of Material Properties on Speed of Sound

Because the mass of the atomic particles and the spring constants are different for different materials, sound waves propagate at different speeds through the different materials. While the mass of the particles is related to the density of the material, the spring constant is linked to the elastic constants of material. In solids, the speed of sound is connected in a general relationship to material density, and elastic constants are given by the following equation:

$$v = \frac{C_{ij}}{\rho} \tag{8}$$

Where;

v : Speed of sound (m/s)

c_{ij} : Elastic constant " in a given direction" (N/m^2)

ρ : Density (kg/m^3)

Subject to the type of wave and which of the elastic constants that are used, this equation may have different forms. The subscript "ij" linked to "C" in the equation is used to direct the directionality of the elastic constants with respect to the type of the wave and wave travel

direction. The elastic constants are the same for all directions in isotropic materials. However, most materials are anisotropic. Hence the elastic constants differ in each direction.

The velocity of the travel of an ultrasonic wave is a characteristic of a given material. The passage of a mechanical wave through a material can be thought of in terms of a stress/strain relationship, the wave transmitting a force to each element within the material encountered during its propagation and causing a corresponding elemental displacement

For longitudinal sound waves, the ratio of element displacement with time and the magnitude of that displacement in the direction of wave propagation can be related to elastic constants and material density. The ultrasonic velocity in a specific material is then determined by the elastic modulus and the material density. For longitudinal waves, the velocity can be defined in terms of the bulk and shear moduli as [44]:

$$C = \sqrt{\frac{1}{\rho}(K + \frac{4G}{3})} \tag{9}$$

Where C is the velocity of longitudinal waves (m s^{-1}); k is the bulk modulus (N m^{-2}); G is the shear modulus (N m^{-2}), and ρ is the density of the material (kg m^{-3}). For polymer melts, the appropriate modulus for material characterization is often taken as the bulk modulus k, while the shear modulus G is relatively small compared with its value for the material in its solid state.

When attenuation is small, typically correct for a melt relative to attenuation in the region of the glass transition temperature, the equation can be simplified to give:

$$C = \sqrt{\frac{K}{\rho}} \tag{10}$$

The ultrasonic velocity also changes with temperature and pressure [34, 39, 44]. This is linked to changes in elastic moduli and density with temperature and pressure. The temperature and pressure effects are related for a given material, according to pressure, volume, and temperature (PVT) equations of state, and additionally for viscoelastic materials such as polymers, a time component must be considered.

Although the temperature and pressure effects are interrelated, it is useful to separate the effects of temperature and pressure on ultrasonic velocity in a specific material for the application of velocity measurements during polymer processing, because temperature and pressure values can be individually determined by non-ultrasonic means. This allows ultrasound to be used as an alternative indicator of temperature or pressure. If the temperature and pressure influences are removed from a measured velocity change, residual velocity change can then be used to indicate variations in the material type (e.g., blend fraction or filler level).

To measure ultrasound velocity, the transit time of the signal is measured. The total change in transit time may then be thought of as being a function of the variation in temperature if all other variables (e.g., pressure, material type, filler level) were constant, plus a function of the change in pressure if all other variables were constant, and so on for each of the associated variables. This can be written in terms of a differential equation, using the Chain Rule, such that for a specific material the total change in transit time Dt is given by [44]:

$$\Delta t \approx (\frac{\partial t}{\partial T})_{P\phi} dT + (\frac{\partial t}{\partial P})_{\phi T} dP + (\frac{\partial t}{\partial \phi})_{TP} d\phi \qquad (11)$$

Where ∂t is the change in transit time due to one variable; T is the temperature; P is the pressure, and ϕ is the filler level. This assumes only that T, P, and ϕ can each be varied independently.

The values of $(\partial t/\partial T)P\phi$, $(\partial t/\partial P)\phi$ T, and $(\partial t/\partial \phi)$ TP can be obtained experimentally from the slopes of the appropriate static calibration tests.

Ultrasound as temperature measurement solution

The velocity of propagation of an ultrasonic signal through a melt varies during processing since it is dependent upon temperature and pressure conditions. Ultrasonic velocity measurement can, therefore, be utilized as a method of temperature and pressure determination [26, 34, 39, 44].

Temperature and pressure effects on velocity have been calibrated for a number of materials. If an independent source of pressure measurement is present in the die or nozzle, for example, using a mounted pressure sensor, the temperature can be inferred from the ultrasound velocity and pressure measurements. The ultrasound transducers can be used in line during processing and are non-invasive, but the ultrasonic signal is propagated across the entire melt cross-section resulting in a bulk measurement, and data are available in real time [44].

Correlation Method Based Bio-composite Material Temperature Estimation Utilizing Ultrasound Signals

In material, production temperature is considered a primary factor for monitoring and quality control [12, 45, 46]. The change in temperature during the production process can lead to degradation of the material or one of its composites. Temperature monitoring allows prediction of material destruction before it occurs. Controlling the temperature during production help is saving material from damage; hence saving time and money of preparing another material. There are several approaches to monitor the temperature represented by means of different kinds of transducers and monitoring systems [45].

Ultrasound (US) technology has been a cornerstone of many development projects over the last three decades. Many approaches to using ultrasound as production or temperature monitoring system have been reported [9, 25, 47]. In these procedures, an ultrasound signal is used to determine the speed of sound and attenuation coefficient to determine properties of the produced material. In addition to providing high accuracy results for a very computable price ultrasound has a primary advantage of penetration that can predict the temperature inside the material not only the temperature at the surface as other alternatives [48-50].

This experiment aims to estimate the temperature of biocomposites by comparing its US signal with a set of biocomposite templates with known US temperatures. The predicted temperature is determined from the knowledge of the optimum value of the correlation coefficient between the biocomposites and the templates.

Theory

Ultrasound has been widely used for the non-destructive evaluation of material [47]. Temperature also affects the speed of sound. There are specific functional relations between the propagation velocity of ultrasonic waves in gas, liquid, and solid at certain temperatures [49, 51, 52]. High attenuation in the composite at elevated temperature makes recognizing two reflections inapplicable. However, using the correlation coefficient for analysis, the signal could help estimating the temperature.

A correlation coefficient (μ) is a number that denotes statistical relationships between two or more values in vital statistics [53, 54]. The correlation coefficient measures the linear interdependence between two random variables. The μ value can range between -1.00 and 1.00.

$$\mu_{X,Y} = \frac{\varepsilon\{X,Y\}}{\sqrt{\sigma^2\{X\}}\sqrt{\sigma^2\{Y\}}} \quad (12)$$

Where X and Y are representing the digital US collected from the US transducer. Ɛ is the covariance, σ is the standard deviation.

Experiment setup

Heating Setup

One (1) MHz ultrasound transducer fixed on a melting chamber has been used to record ultrasound signals while increasing temperature of Polypropylene –fiber composite from room temperature (25^{o}C) to 200^{o}c (Figure 6). Ultrasound signal data have been saved for temperature change each 10^{o}C. An On/Off temperature control with 0.5^{o}C offset was applied to maintain the temperature while measuemnt is carried out. Data were stored in MATLAB software accessible format. The program was developed for comparing a detected signal at specified temperature with the data recorded throughout the experiment. The program used the library of the data recorded as a reference for comparison to determine which data is most similar to the compared signal using correlation coefficient function between signals at frequency domain. The program illustrates the temperature of the signal with the highest correlation coefficient.

The main potential application for this project is online monitoring of material production temperature. By switching the compared signal with the signal from the online transducer, the temperature could be determined using a previously recorded data. These data could not only be

changed or adjusted from one product to another but also could be calibrated to illustrate internal degradation temperature of the material, which is usually different than detected using conventional methods like a thermocouple.

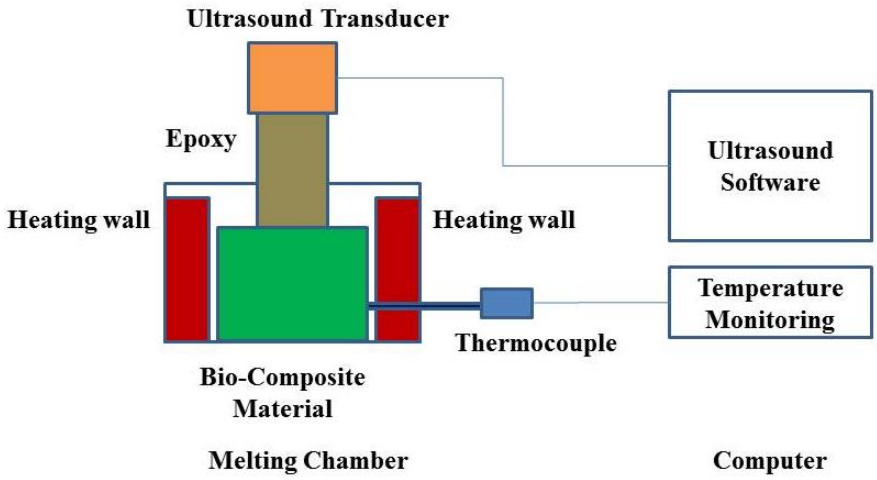

Figure 5 Block diagram of the instrumentation setup.

Figure 6 Measurement cell

Extrusion setup

Another set up was designed and built in order to simulate the fluid movement of the polymer inside the extruder (Figure 7). With the Help of Hydraulic press, a heat chamber was built from Aluminum and surrounded by heating cable to provide heat enough to melt and extrude the composite from a lower rectangular shaped hole. An epoxy material was installed in a side hole of the chamber as a waveguide. The different material was pushed via the hydraulic press through the rectangular hole where the flow can pass in front of ultrasound 1 MHz transducer. Pulser receiver mode ultrasound signal detection system was attached in order to record echo signal at a different temperature. The temperature was controlled and recorded via a temperature control unit, and a Thermocouple insulted neat the extrusion hole recording. Ultrasound signals were recorded at 500sample per second at different temperature for each composite (160^{o}c, 170^{o}c, 180^{o}c, 190^{o}c, 200^{o}c, and 210^{o}c). the signals were processed in order to determine the correlation between the temperature of the flow and the speed of sound.

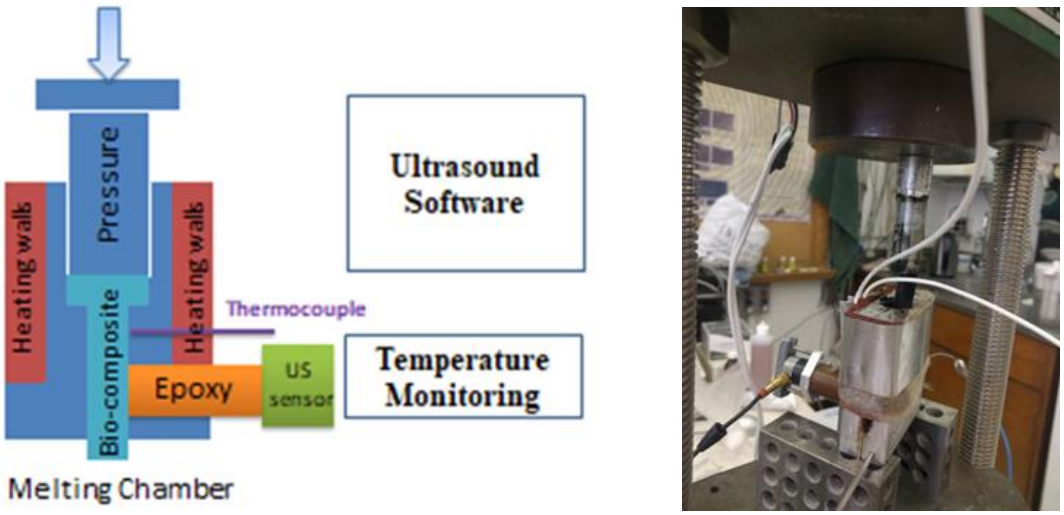

(a) (b)

Figure 7 Block diagram (a) and Measurement cell (b) of the extrusion process simulation setup

Calculations

As illustrated earlier in chapter one the calculation of attenuation and sound velocity for different the material is calculated from the peak arrival times (Figure 8) in our case equations 5 and 6 can be rewritten to be.

$$V = \frac{(2d)}{(t_B - t_A)} \tag{13}$$

Where, d is the sample thickness, t_A and t_B represent the time of flight of the sound wave to travel through individual samples. $_A$ and $_B$ are the recived peaks from the end of the buffer and the surface of the champer respectively. The attenuation is determined by linking the peak amplitudes and calculated according to the following Equation. Peak amplitudes are referred to as A1 and A2.

$$\alpha = \frac{1}{2d} \ln\left(\frac{A_1}{A_2}\right) \tag{14}$$

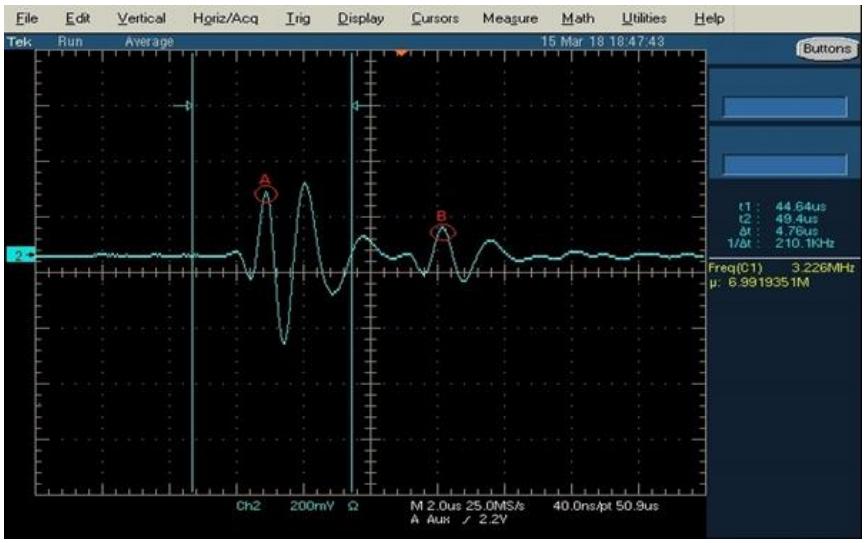

Figure 8 Sample of received US signal

Chapter Three
Applying machine learning for industrial application

Applying machine learning for industrial application

Applying machine learning in for industrial application has been a cornerstone for studies and research in the past decade especially as the industry was entering the new era of Industry 4.0 and x by internet production [55]. Applying machine learning techniques in industry shows promising potential for enhancing productivity, efficiency, and quality control in production process [56]. Many publications have discussed the effectiveness of applying machine learning techniques in different stages of production. Most of these studies have an industrial case study where a machine learning technique was applied either to overcome a problem or to create a prediction model for the results. This work is a review of some of the recent applying of machine learning techniques for different industrial fields or purposes.

In 2004 M. Aksoy et al. [57] used Rule-3 inductive learning algorithm [58] to train a system by five good cups and then tested for 113 unseen examples. The system correctly classified unseen examples by efficiency of 100% and also determines what kind of cup is being used. Compared to conventional methods the main advantages of such a system was simple, fast, low memory space is required, and orientation had no effect. This kind of system in addition to other similar systems presented at the same time but it shows lots of potential applying the machine learning in the industry to achieve better results with fewer efforts and less time-consuming.

Machine learning in the energy industry

In general, any industry is showing great interest in Energy resources and economic development. For the purpose develop and apply the machine learning approach to predict gross domestic product (GDP) based on the mix of energy resources [59], Machine learning approach was applied, and results were compared to those of a backpropagation algorithm. Lots of previous efforts were taken to investigate the relationship between energy consumption and GDP growth, although the main idea of such work was to investigate the data via applying machine learning techniques in order to deal with high nonlinearity of the data.

For their research, The World Bank Database was used as the data source. As the output parameter, the GDP growth rate (percentage) was used. Based on the results, Artificial Neural Network (ANN) can be useful in analyzing the relationship between the mix of energy resources

and economic growth and with applying of a machine learning approach it may be possible to improve predictive accuracy. Results indicate that GDP predictive accuracy can be enhanced by applying a machine learning approach.

Machine learning in material industry

Lots of efforts have been taken into building a simulation for material design for specific properties. Many material databases enhanced with many computational correlations between material properties and different desired functionalities has been studied and published [60].

An advanced material design simulation toolbox has been designed and discussed by Amir Mosavi [61]. In his work, he was trying to overcome a challenge that faces material design tools as they either depend on a single algorithm or deal with only limited ranges of design problems[62, 63]. In addition, the absence of a tool for multi-criteria decision and a significant data tool to take into account dealing with the massive material database is considered a further gap in this research area. This study proposed a toolbox for predictive simulation-based optimization of advanced materials to model, simulate, and predict the fundamental properties and behavior of multi-scale materials. With the involvement of advanced machine learning and big data technologies, the artificial systems would learn and generate knowledge from large databases of material properties to provide predictive analysis capability for unmolded materials. His methodology was using machine learning integrated optimization for predicting the three-dimensional structure multi-scale material to efficiently solve such sub-tasks and combine their outputs into a reliable 3D structure predictor.

He implemented his method on a textile design composite adapted from some referred publications. He concluded that by applying machine learning, he managed to implement a platform which is a simple yet powerful concept that reduces computation time to design application-based tailored materials.

This work is a simple yet influential concept leading to developed technology that reduces computation time to design application based custom-made materials. The toolbox is mainly considered for the virtual design and simulation of advanced material.

Machine learning for industrial reliability

Manufacturers' goal is to produce high-quality products in less time. Due to the highly competitive market, the manufacturers' interest is to put concentration more than ever before on the machines' reliability [64]. An industrial case study was presented by [65] discussed this matter. The study of how machine learning models can fit this reliability estimation function in comparison with traditional approaches (e.g., Weibull distribution). The previous work in their literature review on machine learning for reliability established that machine learning models can perform well in the industrial reliability field. However, they noted that the studies often use one well-known case study to validate their models. Therefore it was still unclear if there is machine learning model able to perform generally well across different datasets.

To predict the reliability, the study used a supervised machine learning approach on 19 industrial mechanical components obtained from real industries. Four diverse machine learning approaches were implemented: artificial neural networks, support vector machines, random forest, and soft computing methods.

The experimental set up included two failure process investigation methods via complete data or censored data. The empirical reliability function was then indicated by the machine learning models path and the traditional path for comparison.

The experimental results show the high ability of machine learning to predict the component reliability and particularly, random forest, which generally obtains high accuracy and the best results for all the cases. The data confirms that all the models improve their performance when considering censored data and shows how machine learning models obtain better prediction results with respect to traditional methods when increasing the size of the time-to-failure datasets.

The study showed the potential of the machine learning approach for technical or industrial reliability analysis. These results contribute in the field of maintenance engineering or quality control helping to define some threshold values which trigger specific maintenance action.

Machine learning in electronic industry

Technologies for inserting electronic components are necessary within the electronics industry. Visual feature recognition, robot arm insertion motion clustering, and machine learning were employed to develop a system for inserting nonconventional components [66]. A study proposed a learning system for machines-customized machines- have been mainly designed for automatic assembly- that incorporates image characteristics into the insertion motions performed by a robot arm to solve problems related to transformer insertion[66].

The operation of the investigated system was separated into three layers: Vision layer where image was filtered, and the pin image features of each transformer were preserved, Motion layer where insertion motions for transformers were manually fed to the system and a clustering algorithm was applied to search for representative motions among these manually taught motions and Decision layer where multilayer SVM modeling was applied to estimate robot arm motions according to input-image features to generate ideal insertion motions.

A large number of motions were initially fed to the system because of the variations between all transformers. However, a prominent set- back of this method is that these insertion motions must be manually trained, although automatic learning can be taught in the future. The decision layer uses one-against-rest support vector machines (SVMs) to establish classifiers for applying the collected image characteristics to the calculation of insertion motions. The concept of SVM classification was utilized to teach the relationship between image features and representative motions. Developing SVM training models involved in putting the training data set, data class labeling, and SVM parameter adjusting. Once SVM models were generated, inputting new and similar data sets enabled these SVM classifier models to estimate their respective data class. The core concept of SVM classification is binary classification.

By using 300 transformers as training samples and 200 transformers as test samples experiments were performed to validate the research methods. The experimental results showed an accurateness rate of 88%, and that the engaged SVM classifiers were more accurate than the other two classifiers.

Machine learning in pharmaceutical industry

In the pharmaceutical industry granulation processes are, more often than not, used to obtain and maintain suitable specific properties in terms of compressibility, flowability, and homogeneity [67]. In the work of A. Wafa'H et al. [68], a new systematic modeling framework which uses machine learning for describing the granulation process was presented. The ultimate aim of that research was to develop a fast, transparent, more accurate and low –cost predictive modeling framework for the twin screw granulation (TSG) process.

First, an interval type-2 fuzzy model is elicited in order to predict the properties of the granules produced by twin screw granulation (TSG). Second, a Gaussian mixture model (GMM) is integrated into the framework in order to characterize the error residuals emanating from the fuzzy model. This was done to refine the model by taking into account uncertainties and/or any other unmodelled behavior, stochastic or otherwise. All proposed modeling algorithms were confirmed by Laboratory experiments. The size of the granules formed by TSG was successfully predicted, where most of the predictions fit within a 95% confidence interval. The proposed modeling framework is a promising development in the granulation process, as it was able not only to predict the granule size successfully but also to deal with the uncertainties surrounding such a process. In the future, such a modeling framework can also be adapted to represent the production cycle of pharmaceuticals; by developing a model for each unit operation, followed by connecting these models into one single modeling framework.

Machine learning for production machines

For industry and production machines and tools, Cutting tool wears detection using multiclass logical analysis of data was presented [69]. The work shows tool wear class detection approach. Based on the recorded experiments, tool wear classes are determined using the Douglas–Peucker algorithm. Logical analysis of data (LAD) is then used as machine learning, pattern recognition technique for detecting the present tool wear class based on the latest sensors' readings of the time-dependent machining variables, and deriving new information about the inter-correlation between the tool wear and the machining variables (Feed, Cutting Force and Feed Force), by doing pattern analysis. LAD is a data-driven technique which relies on combinatorial

optimization and pattern recognition. The accuracy of LAD has compared to that of an artificial neural network (ANN) technique since ANN is the most familiar machine learning technique.

The proposed method was applied to experimental data those are gathered under various machining conditions. Based on the multiclass LAD classification algorithm, the tool wear classes are defined by finding the hidden patterns specific to each class. Through an analysis of the generated patterns, class identifiers are found. The accuracy of LAD is evaluated and validated by comparison to an ANN technique. LAD shows better classification accuracy for the tool wear phenomenon. Based on the results it the technique used was able to detect the tool wear class correctly and with high accuracy. Tool wear class detection will be used to indicate the cutting tool life when the tool is used in rough and finish cut. The objective will be the prognosis of tool wear, to find the best time to change the tool. Another point of research is to decrease the LAD's computational time to use it for online monitoring and detection of the tool wear. The accuracy of detection can be improved by including additional variables such as vibration signals, acoustic emissions, and cutting temperatures.

Machine learning in the steel industry

The core purpose of this study was to acquire a predictive model able to perform initial detection of central segregation severity in continuous cast steel slabs. Centerline segregation in steel cast products is an internal defect that can be very harmful when slabs are rolled in weighty plate mills[70]. Hence, predicting its existence is a matter of significance to prevent future risks. The study presents a hybrid algorithm, of support vector machines (SVMs) and the particle swarm optimization (PSO) techniques, to forecasting the centerline segregation from input parameters determined by experiment in continuous cast steel slabs. This technique includes kernel parameter setting in the SVM training procedure, which considerably affects the regression accuracy. also, a multivariate adaptive regression splines (MARS) and a multilayer perceptron network (MLP) approach. This last method also in combination with the particle swarm optimization (PSO) technique, was fitted to the experimental data for comparison purposes. To this end, the most critical physical-chemical parameters of this industrial process are investigated.

The study results are two main points. First, the importance of each physical-chemical variables on the segregation is obtainable. Second, predicting segregation with some models were acquired successfully. The results achieved with the MLP and PSO–MARS-based models are apparently worse than those obtained with the PSO–RBF (Radial basis function) SVM-based model. The connection between experimental data and the model confirmed the decent performance of the latter.

The main findings of this research work can be summarized as follows: The diagnostic techniques commonly used for segregation based on the traditional methods are expensive from both the material and human points of view. Consequently, the development of alternative diagnostic techniques is necessary. A hybrid PSO–SVM-based model with an RBF kernel function was successfully developed to predict the centerline segregation from the other measured input operation variables, in order to lower costs in the quality assessment of steel's bodies. A high coefficient of determination equal to 0.98 and 0.97 was obtained when this hybrid PSO–SVM-based model with an RBF kernel function was applied to the experimental dataset corresponding to two factors (Carbon and Average width).

In a word, machine learning techniques were applied successfully to provide an alternative and more reliable solution for an industrial problem and overcome an existing industrial method defects

Machine learning in the industrial chemical process

The Logical Analysis of Data (LAD) was applied as an interpretable machine-learning technique for fault detection and diagnosis (FDD) in industrial chemical processes. This classification technique discovers hidden knowledge in datasets by extracting interpretable patterns, which can be linked to underlying physical phenomena. LAD was selected as an FDD method not only on its excellent performance but also because the human expert can learn from the knowledge as it gets revealed [71]. In addition, LAD is not based on statistical analysis hence, it can deal with highly correlated, nonlinear, or time-varying variables without the need for a decorrelation procedure that is common in most statistical methods. To exemplify the difficulty in interpreting faults in complex chemical processes the LAD approach was applied to two case studies, one simulated and one real.

The LAD approach was able to interpret and diagnose the normal and faulty situations in the Tennessee Eastman Process TEP, a well-known benchmark problem in the field of process monitoring and control that uses simulated data. The second case study used a real dataset from a black liquor recovery boiler (BLRB). LAD was used to investigate and analyze the cause of low steam production by black liquor flow (SP/BLF), a critical key performance indicator (KPI) of boiler efficiency. A set of patterns was extracted from the boiler data, in a situation where the KPI was decreasing beyond an absolute lower limit set by an expert. The accuracy of the proposed LAD approach was compared to well-known machine learning methods, namely the artificial neural network (ANN), Decision Tree (DT), Random Forest (RF), k nearest neighbors (kNN), quadratic discriminant analysis (QDA) and the support vector machine (SVM). The LAD performance was comparable to the most accurate one-the Random Forest-.

The method showed substantial improvements in terms of the number of correctly classified faulty observations, and the results show that it is suitable for industrial situations with noisy measurements. Moreover, LAD is not only a classification technique, but it is also-and more importantly- a knowledge discovery tool that extracts interpretable patterns.

Such interpretable knowledge is particularly useful for fault diagnosis in engineering applications; wherein one cannot only detect and identify a fault but also relate it to the variables that contributed to its occurrence[64, 71].

Machine learning in textile industry

Data mining applications, including classification and clustering techniques and machine learning algorithms, implemented in the textile industry were investigated in this study [72] in order to provide a summary of how machine learning techniques can be applied in the textile industry to overcome the problems where traditional methods are not beneficial. That work shows that a classification technique has higher interest than a clustering technique in the textile industry. It also demonstrates that the most frequently used and practical classification approaches are ANN and SVM. As they generally deliver high accuracy in the textile applications. For the clustering task of data mining, a K-means algorithm was employed in textile studies among the others that were examined in that work. The study concluded with

some remarks on the strength of the data mining techniques for the textile industry, ways to overcome assured challenges and offer some possible further research directions.

Machine learning in research and development

In industry, it is essential to have a continues update on what compotators are doing. Machine learning can be applied to illustrate work been done for years about a specific topic into main points of interest topic[73] . It also can be used to help to have a visualization of errors and faults in order to enhance evaluation of the production process and add value to the data extracted through production an turn into valuable knowledge that can be used as a compatibility advantage. Visualization is an essential aspect of decision making. It helps in representing the knowledge that is extracted from datasets in a clear and comprehensive way [56, 73].

The primary objective of data visualization, according to standard definitions is to “amplify cognition” by externalizing thought processes. As a tool for “crystallizing new knowledge,” visualization allows us to perceive and recognize patterns in data. [56] presented some examples of visualization in the field of machining. It presented, the input data, the outcomes with respects to some specifications, and the knowledge discovered in the form of patterns. Information is extracted from experimental results and is presented in the form of characteristic patterns which are used in data visualization. Logical Analysis of Data (LAD) is used as knowledge extraction approach.

The next research challenge is to visualize big data. The field of visualization is becoming more and more significant because managing enormous amounts of data is increasing rapidly. However, the development of new visualization tools is still to be done.

Machine learning in medical industry

A) Machine learning in automata

In the field of medical industry machine learning approach to synchronization of automata were presented by[74]. The main idea is to predict the length of the shortest synchronizing words of a finite automaton by applying the machine learning approach by introducing automata features which represent the structure of an automaton and use them with machine learning algorithms. The work discusses the effectiveness of the machine learning approach in predicting the length

of the shortest synchronizing words. Several experiments were performed with different types of models and with full and restricted sets of features with the aim to answer the following research questions stated in the introduction of the research paper.

- Are the machine learning methods able to predict the reset threshold for a given automaton, described in terms of the automaton features?
- Which features have the most significant impact on the reset threshold and what are the relations between the features?
- Do the machine learning models work well when we restrict the possible features to the ones that are computed quickly (in linear time) and to simple, linear models?

Although there is a weakness in this approach appears in the strong dependence of accuracy on the machine learning method chosen and training data provided, the obtained results seem to be encouraging in terms of both algorithm effectiveness and accuracy.

They considered the novelty of the work is the analysis of different automata features and their impact on the reset threshold. Results show that these features can be utilized by the machine learning algorithms to quickly and accurately predict the reset threshold. We also showed that it is possible to use only a small set of quickly computable features and still keep the algorithm's accuracy, which makes the presented solution very practical.

Results showed that the efficient prediction of the reset threshold is possible, even when restricting to simple, linear models and features that can be computed quickly. There exist some well-known heuristic algorithms that predict the reset threshold by finding a synchronizing word for a given automaton.

B) Machine learning techniques for computer aided diagnose

Because of the high numbers of breast cancer in women significantly increased in the recent years. Physician experience of diagnosing and spotting breast cancer can be assisted by using some computerized features extraction and classification algorithms. N. I. Yassin et al. [75] presents the conduction and results of a systematic review (SR) that aims to investigate state of the art concerning the computer-aided diagnosis (CAD) for breast cancer detection.

This systematic review aims to identify various studies related to breast cancer CAD systems based on medical images and MLT classifiers. The primary intention of the study is to find the answer to these research questions. What are the Machine learning Techniques (MLT) classifiers currently applied for breast cancer CAD systems based on medical imaging?, What are the modalities of medical imaging used for the development of breast cancer CAD systems?, What are the evaluation criteria used for the assessment of breast cancer CAD systems?, and What are the data sets used for the development of breast cancer CAD systems?

Several scientific databases from different sources were used. To select those of interest inclusion and exclusion standards were defined and applied to each retrieved work. From 320 studies retrieved, 154 studies were included. the scope of this research excludes commercial interests. The survey provides a general analysis of the current status of CAD systems according to the used image modalities and the machine learning based classifiers. Potential research studies have been discussed to create a more capable CAD system.

It is noticed that there is significant diversity in the usage patterns of MLTs, some of them have been used extensively, some have been used less frequently, and others have been used at low rates. The conclusion extracted from the study was that Data Mining (DM) had been used with SVM in 50 papers; the range of achieved Acc is from 64.7% to 100%. Ultrasound (US) has been used with SVM in 14 papers; the Accuracy ranges from 75.5% to 98.3%. Also, 9 papers are using MRI combined with SVM with a maximum Acc value of 98%, and the least achieved Acc was 82.8%. And 6 papers used microscope-SVM and the ACC registered is 96.9%. Only 2 papers are using (Infrared thermography) IRT-SVM, and the achieved Acc was 88.1% and 61.8%. ANN is used with DM, US, MRI and microscopic images; it is used with DM in 34 papers and with the US in 4 papers, one of them used both DM and US, only one paper with MRI and 2 papers with microscopic. In 20 papers with DM-ANN, the Accuracy ranges from 90% to 98.14%. In the rest of the papers that stated the Accuracy values, its value ranges from 71% to 89.38%. The highest achieved Acc with US-ANN is 94%. KNN has been used in 21 papers, 14 with DM with the highest Accuracy registered 98.69%. One publication combined KNN with the US, 3 combined with MRI, and 3 combined it with microscopic modality.

According to the collected data, it is difficult to compare methods with each other due to several factors comprehensively. Some of this factors are the databases used for assessment, the samples of images selected for assessment, the number of samples used, the assessment approach (validation methodology, training and testing set) used. Moreover, the tuning of parameters involved in different methods varies from one method to the other, thus adding another obstacle for a fair comparison between various methods.

Generally, among the classifiers mentioned in the literature, SVM classifier has been used extensively for breast tissue classification purposes. The use of artificial intelligence methods is increasing because of the effectiveness of classification and detection schemes assisting experts in the medical field. Observing the pitfalls during the CADs clinical application will lead to improving their performance, thus reducing false positive that may lead to psychological, physical, and economic costs, and reducing false negative readings that may cause neglecting of treatment.

Deep learning classifier is a promising trend that appeared in the recent years. There is an increased interest in applying it in CADs systems in the last couple of years. Also, swarm intelligence is worth studying as it was rarely applied in the investigated publication in CADs systems. Developing MLT-CAD system that combines more than one image modality is a necessity. Also developing CAD systems using 3D mammography which is a new trend that may help to improve CAD efficiency is an important issue. These points should be considered to develop CAD systems in the future.

Ultrasound signal classification for fault detection

Ultrasound signal classification for fault detection has been carried out [76]. Four features were selected to determine characteristics of the signal. The mean value, root mean square value, standard deviation, and absolute value. Those four features were used to differentiate between three classes. First class related to the signal without flaw, the second one to the place with the flaw and the third class related to the weld. Support vector machine technique was used for the classification the signals. With this technique, it is possible to classify the signal with back-wall echo, a signal with fault echo and signal measured on the weld. This method is beneficial for the automated classification of ultrasound signals for industrial applications, However using this

method is limited when there is higher similarity between the two signals beginning classified since the selected features will not be enough to distinguish between signals.

Machine learning techniques have been applied extensively in different fields in the industry for the past few years. It is predicted that more application is obtained in the next decade as research is just scratching the surface of the mountains of data available to be used. Many successful attempted has been recorded in applying machine learning either to overcome a failure of the current methods that have been applied or to provide a new approach for a different solution for the problem that can not be managed using traditional approaches.

Machine learning can be applied directly for direct classification of data or as a filtration layer before or after applying the main algorithm or detecting approach in order to enhance results. Technics of machine learning can be combined and or mixed in order to create a hybrid algorithm for classification of data. Also, machine learning can be used as a single layer in multiple layer algorithm or be combined with one of these layers to form a more complex layer of classification.

The primary challenge when using machine learning is identifying the features that based on it the classification or clustering will take place. In the majority of the cases, these features are determined by the researcher based on previous knowledge of the process and the rule played by each feature affecting the results. In general, one might say the more features included, the better the results although this is not always guaranteed and strongly depends on how the features are affecting the results.

Most of the machine learning techniques have accuracy higher than 95%, some time accuracy range reaches 100%, Which is why terms like sensitivity, specificity, and Geometric mean plays an essential rule in analyzing the results especially when comparing different types of machine learning techniques.

SVM is the most frequently used machine learning technique in industry, and the Random forest is the best results technique. The primary purpose of applying machine learning in the industry and especially those two techniques is acquiring the best results of finding a solution in the most simple, reliable and cost-effective way.

With more data on analysis, machine learning is at the core of industry nearby future. Many future industry applications put data analysis either for maintenance purposes, product development or just to save time and money in high potential position. Based on the data and papers provided in this work this is no longer an option, but it has become a must to maintain a decent level of compatibility.

Using machine learning rather than direct programming

The short answer to this question is dependent on two factors

- Problem's complexity
- Need for adaptively

Complexity

Complexity means if the task is too complicated to program. Complexity can be classified into one of two categories

a) Human or animal tasks! Examples include driving, speech recognition, and image understanding. Satisfactory results can be reached using up to date machine learning programs “that learn from their experience," when exposed to sufficiently training examples.

b) Beyond human capabilities tasks! Examples include tasks related to the analysis of enormous and complex data sets: astronomical data, dealing with medical archives, weather prediction, analysis of genomic data, search engines, and electronic commerce.

There is a treasure of useful information hidden in the massive amount of data stored in electronically stored devices. Learning to search and discover patterns in these data is a promising domain with high potential market value. This domain integrates the programs that learn from these data with the unlimited memory capacity and exponentially increasing the speed of computer processors into a new field of research that opens the door for the further era of how we deal with our gained knowledge

Adaptivity.

In programming, once the coding is done, the program is ready, and we installed, it does not change. However, many factors change over time or from one user to another. Machine learning

tools provide a solution for such issues since the program behavior adapts to the input data. Example, the program can adapt to variations between the handwriting of different users, adjusting automatically to modifications like spam e-mails, and speech recognition programs.

Methods and Output presentation
Machine learning contains two main types of learning

- Supervised learning (Classification)
- Unsupervised learning (Clustering)

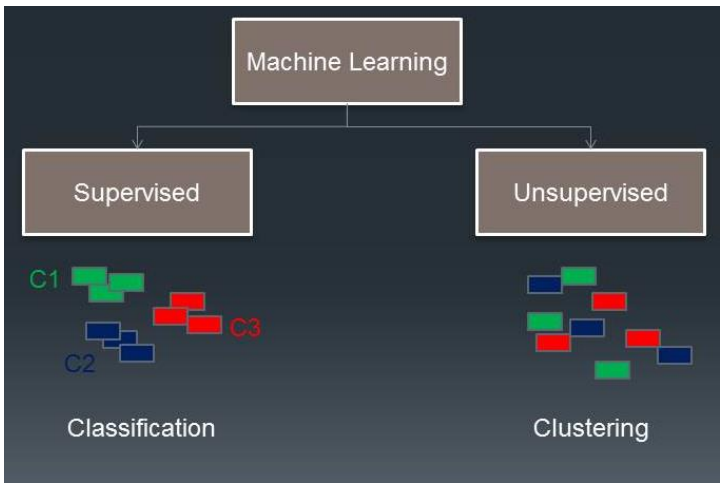

Figure 9 Types of machine learning

Supervised learning (Classification): when we know the results or the category of the training samples, the program aims to determine to which class the new sample belongs.
Unsupervised learning (Clustering): when we have uncategorized samples, the program aims to determine which samples have enough in common to be recognized as one group.

Some of the methods and techniques with which these learning types can be achieved are:

- Support vector machine
- Decision tables
- Decision trees
- Clusters
- Classification rules
- Association rules
- Rules with exceptions

Support vector machine

Support vector machine (SVM) learns a separating hyperplane to maximize the margin and to produce good generalization ability. In successful applications, one of the leading attractions of SVM is that it is capable of learning with few training samples [77].

When SVM is creating a hyperplane, there are four things to consider.

- x, data points
- y, labels for the classes
- w, weight vector
- b, bias;

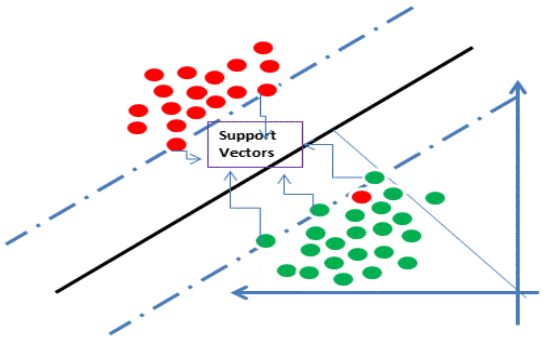

Figure 10 Support Vector Machine SVM

For a Photo classification example x would be the set of available images, y, would be the class labels (which pic contains fruits and which contains animals). To determine the orientation of the hyperplane, we will need to use w (the weight vector). The primary objective of SVM is to estimate the optimal value of w. Which one is better? A or B?

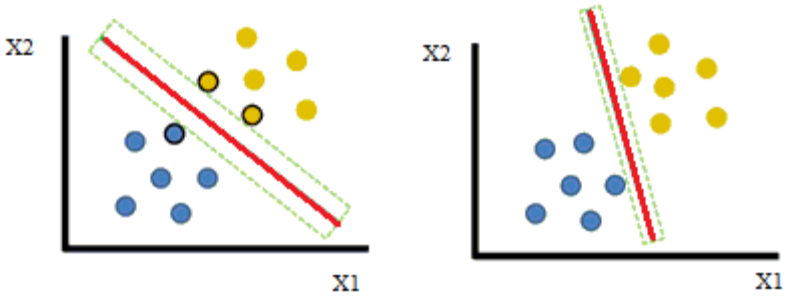

Figure 11 Different orientation hyperplanes A (Right), and B (Left)

The only difference is hyperplane function technique. Following the rule for maximum margin, we would choose the A one as it is the better one for SVM.

If we choose the B, the margin between the yellow support vector and the hyperplane is small. So in the case, that other data points that belong to the color yellow came into the left of the support vector of the yellow class, which would create a false-classification.

SVM is a promising classification and regression technique, which can be non-linearly mapped to a higher-order feature space by substituting the dot product operation in the input space with a kernel function. The method is to find the best decision hyperplane that separates the positive examples and negative examples with maximum margin. By defining the hyperplane this way, SVM can be generalized to unknown instances efficiently, which has been proven by various applications.

Decision tables

The most straightforward, most elementary technique of representing the output from machine learning is to make it just the same as the input into a decision table. For example, if we are deciding whether or not to travel using car or train. We can put the input data and the decision of that situation into a table.

Table 1 Decision table sample

Weather	Cost/person	Time	Distance	No of travelers	Kids	Decision
Rainy	>100	Day	>500Km	≤ 4	No	Car
Sunny	<100	Night	<500Km	≥4	yes	
Sunny	<100	Night	<500Km	≥4	No	
Rainy	>100	Day	>500Km	≤ 4	yes	Train
Sunny	<100	Night	<500Km	≥4	No	
Rainy	>100	Night	>500Km	≤ 4	yes	

Clusters

Clustering is to group a set of similar items closer, in comparison to other items in the same set of data.

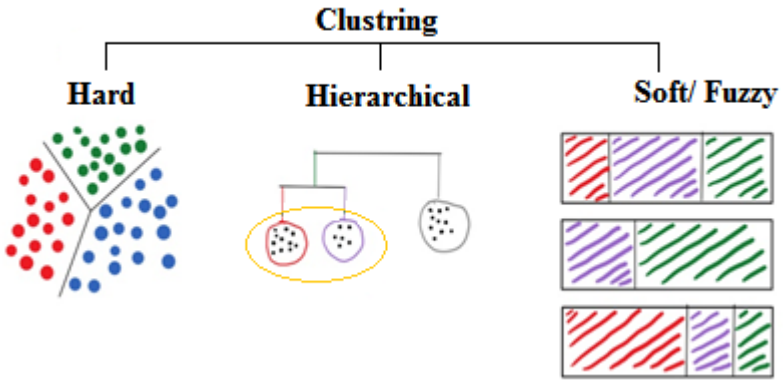

Figure 12 Types of clusters

Hard clustering: where each instance of the dataset can only fit into one cluster as there is a hard division on lines.

Hierarchical clustering: includes sub-clusters, where the clusters have ‘branches’ of subclusters

Soft clustering: where each instance can belong to each cluster with a certain degree which can be represented as a percentage or probability.

The stage that follows clustering is often a stage in which a decision tree or rule set is inferred that assigns each instance to the cluster to which it belongs. Then, the clustering operation is just one step on the way to a structural description.

Decision trees

The decision tree classifier is a predictive technique based on hierarchical node splitting using impurity of the variables. Each node in the tree tests a specific feature. However, some trees compare two features with each other or use some function of one or more attributes. To classify an unknown example, it is routed down the tree according to results of the test from the previous nodes, and when a leaf is reached the instance is classified according to the class assigned to the leaf.

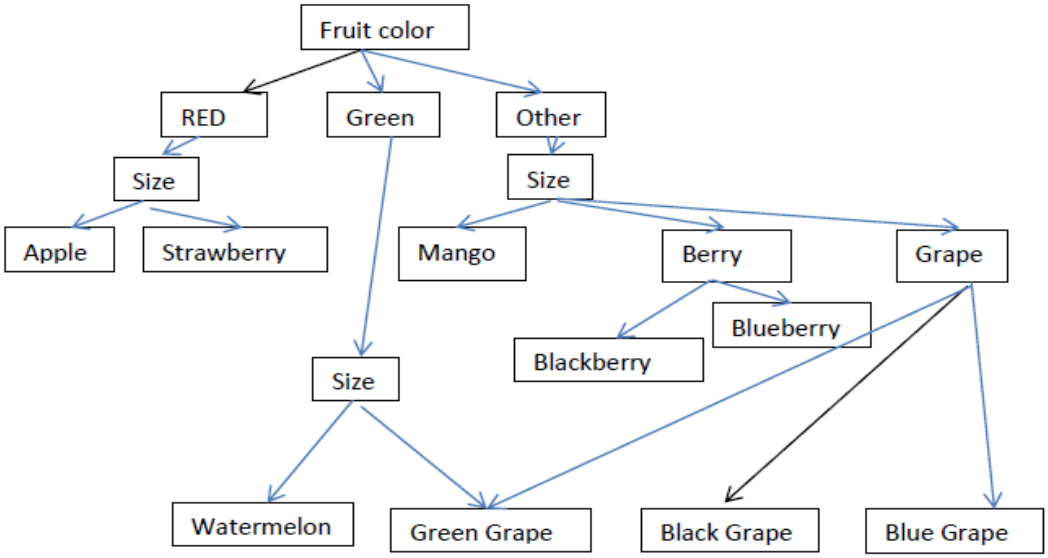

Figure 13 Decision tress sample

Random Forest Decision Trees:

Grows many different decision trees to classify sample x.

Each tree votes (classify) class for x

Forest select the class having the most votes.

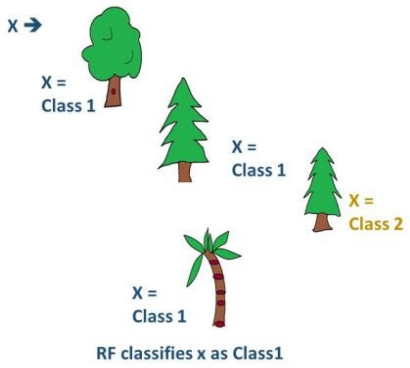

Figure 14 Random Forest sample

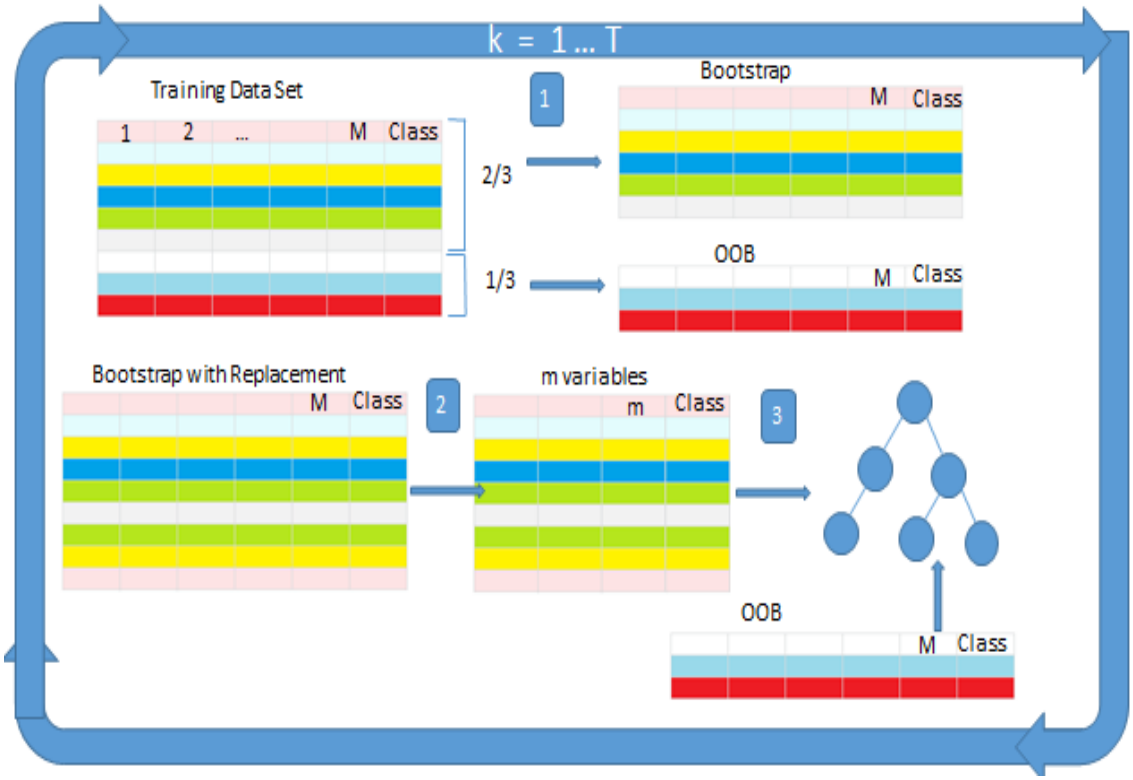

Figure 15 Random forest Algorithm

Algorithm

T : number of Trees.	N is number of samples in training dataset
M is number of Variable in N.	m is the number of selected variables, where m << M

- tree k(1..T) repeat:
- Select bootstrap samples (2/3 of N)
  - Top it to be N with replacement
  - Select m of variables randomly from M
  - On Nxm bootstrap, grow k^{th} tree
  - Gini importance to split k^{th} tree at each node
- The rest (1/3 N) is out of bag (OOB)
  - For each sample x in OOB

    classify x using k^{th} to class j

End repeat

For each sample n in Training dataset repeat

- For all time n appears in OOB. Find the class j with maximum votes
- n is classified as j
- If j != real class of n

  e =e + 1

End repeat

Error estimation

The Weka machine learning workbench

Waikato Environment for Knowledge Analysis (Weka) was developed at the University of Waikato in New Zealand. Weka is a platform that consists of a collection of up to date machine learning algorithms and data mining techniques and tools. One can say it includes almost every algorithm mentioned in books. Data mining is an experimental science, so Weka was designed to try out any existing method on new datasets rapidly and effortlessly. Starting with preparing the input data and going through evaluating learning scheme statistically, and visualizing the input data as the result of learning, Weka provides far-reaching support for the entire process. Also, it also includes a range of preprocessing tools.

What's in Weka?

Weka workbench offers learning algorithms implementations that you can easily apply to your dataset. Without writing any program code at all one can preprocess a dataset, feed it into a learning scheme, and explore the resulting classifier and its performance. Inputs are fed to algorithms in the form of a single relational table in the ARFF format. Weka workbench includes methods for all the standard data mining problems: regression, classification, clustering, association rule mining, and attribute selection.

Weka can be used for;

I. Applying a learning method to a dataset and analyze its output.
II. Using learned models to generate predictions on new instances.
III. Appling several different learners and compare their performance.

Weka interactive learning methods are called classifiers. Users select the one they want from a menu. A standard evaluation module used to measure the performance of all classifiers.

Weka is an open source platform. It is available from http://www.cs.waikato.ac.nz/ml/weka

Machine learning for Ultrasound Signal classification

Methodology

To apply a classification algorithm to ultrasound signals, a dataset containing over 180-ultrasound signals recorded at different temperature were obtained. In Chapter 2 we introduced the instrument needed for detecting and recording an ultrasound signal. Figure 5 shows the block diagram of the instrumentation and setup of the experimental equipment. The ultrasound signal is recorded as a voltage signal function in time. 500 hundred sampling rate per second is presenting the amplitude of the reversed pulse of a single ultrasound signal. The corresponding temperature at which each signal was recorded is attached to the signal file.

Ultrasound signals were put together to form one file of data containing all the recorded signals. Since 190^{o}C is the temperature at which degradation of the fiber occurs, signals were classified into two classes representing signals marked at temperatures less than 190^{o}C and the signals recorded at a temperature equal or more than 190^{o}c. The data file was saved as a Weka data file (.csv). After defining the class column of the data, different classifier algorithms were applied in order to obtain best classification results.

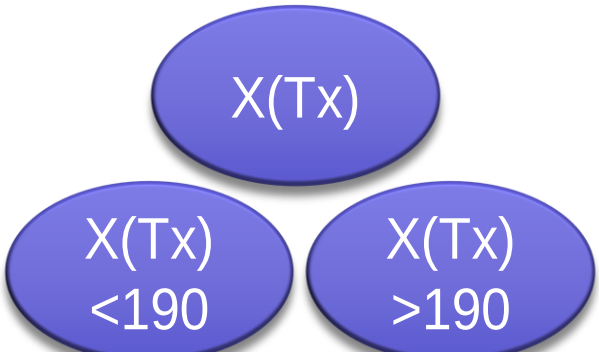

Figure 16 Signal /Temperature classification

The primary target of the classification is to identify the signals overs 190^{o}C, which represent the temperature at which material is damaged. Table 10 shows the best result outcome from a cost-sensitive random forest classifier. Compared to other classifying algorithms, it gives the highest accuracy and specificity.

Data Pre-processing

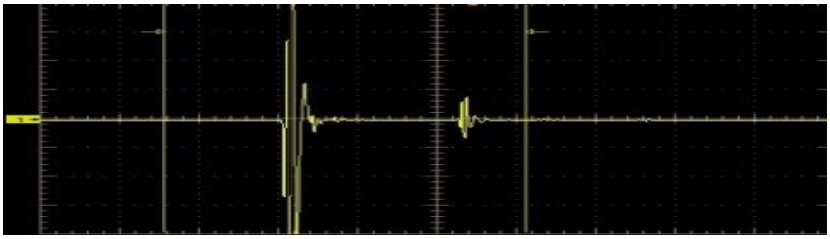

Figure 17 Step.1 Recording Ultrasound signal at different Temperatures

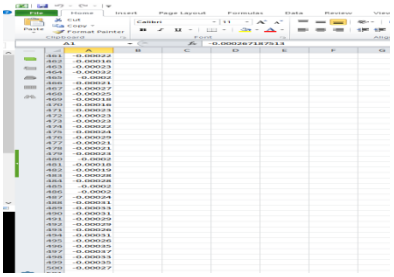

Figure 18 Step.2 Signal saved with 500 sample/sec

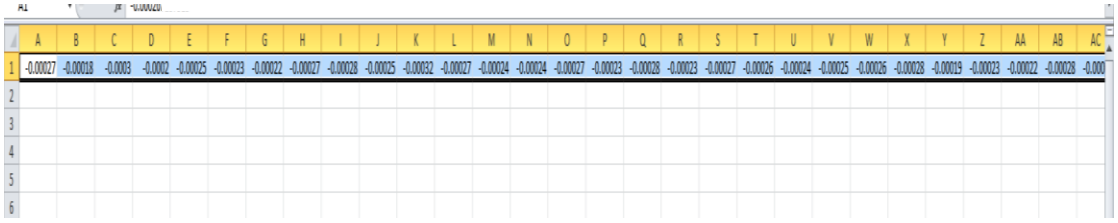

A	B	C	D	E	F	G	H	I	J	K	L	M	N	O	P	Q	R	S	T	U	V	W	X	Y	Z	AA	AB	AC
1	-0.00027	-0.00018	-0.0003	-0.0002	-0.00025	-0.00023	-0.00022	-0.00027	-0.00028	-0.00025	-0.00032	-0.00027	-0.00024	-0.00024	-0.00027	-0.00023	-0.00028	-0.00023	-0.00027	-0.00026	-0.00024	-0.00025	-0.00026	-0.00028	-0.00019	-0.00023	-0.00022	-0.00028	-0.000
2																													
3																													
4																													
5																													
6																													

Figure 19 Step.3 Signal amplitude is transferred into features

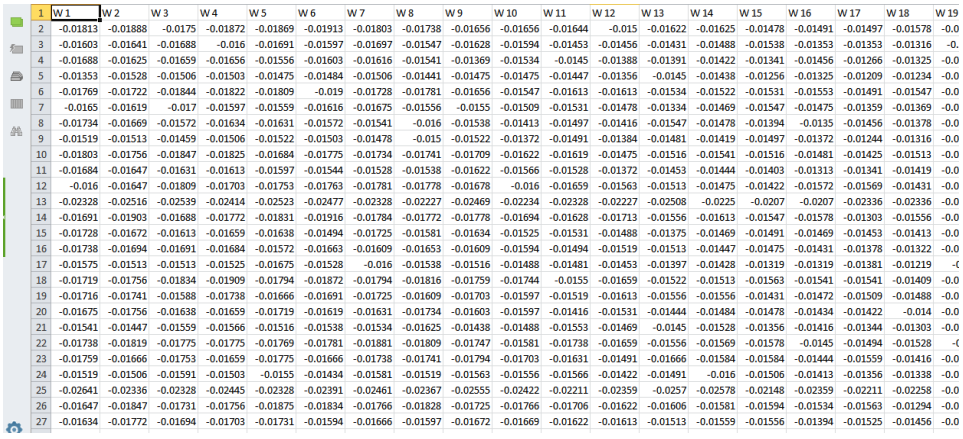

	W 1	W 2	W 3	W 4	W 5	W 6	W 7	W 8	W 9	W 10	W 11	W 12	W 13	W 14	W 15	W 16	W 17	W 18	W 19
2	-0.01813	-0.01888	-0.0175	-0.01872	-0.01869	-0.01913	-0.01803	-0.01738	-0.01656	-0.01656	-0.01644	-0.015	-0.01622	-0.01625	-0.01478	-0.01491	-0.01497	-0.01578	-0.0
3	-0.01603	-0.01641	-0.01688	-0.016	-0.01691	-0.01597	-0.01697	-0.01547	-0.01628	-0.01594	-0.01453	-0.01456	-0.01431	-0.01488	-0.01538	-0.01353	-0.01353	-0.01316	-0.
4	-0.01688	-0.01625	-0.01659	-0.01656	-0.01556	-0.01603	-0.01616	-0.01541	-0.01369	-0.01534	-0.0145	-0.01388	-0.01391	-0.01422	-0.01341	-0.01456	-0.01266	-0.01325	-0.0
5	-0.01353	-0.01528	-0.01506	-0.01503	-0.01475	-0.01484	-0.01506	-0.01441	-0.01475	-0.01475	-0.01447	-0.01356	-0.0145	-0.01438	-0.01256	-0.01325	-0.01209	-0.01234	-0.0
6	-0.01769	-0.01722	-0.01844	-0.01822	-0.01809	-0.019	-0.01728	-0.01781	-0.01656	-0.01547	-0.01613	-0.01613	-0.01534	-0.01522	-0.01531	-0.01553	-0.01491	-0.01547	-0.0
7	-0.0165	-0.01619	-0.017	-0.01597	-0.01559	-0.01616	-0.01675	-0.01556	-0.0155	-0.01509	-0.01531	-0.01478	-0.01334	-0.01469	-0.01547	-0.01475	-0.01359	-0.01369	-0.0
8	-0.01734	-0.01669	-0.01572	-0.01634	-0.01631	-0.01572	-0.01541	-0.016	-0.01538	-0.01413	-0.01497	-0.01416	-0.01547	-0.01478	-0.01394	-0.0135	-0.01456	-0.01378	-0.0
9	-0.01519	-0.01513	-0.01459	-0.01506	-0.01522	-0.01503	-0.01478	-0.015	-0.01522	-0.01372	-0.01491	-0.01384	-0.01481	-0.01419	-0.01497	-0.01372	-0.01244	-0.01316	-0.0
10	-0.01803	-0.01756	-0.01847	-0.01825	-0.01684	-0.01775	-0.01734	-0.01741	-0.01709	-0.01622	-0.01619	-0.01475	-0.01516	-0.01541	-0.01516	-0.01481	-0.01425	-0.01513	-0.0
11	-0.01684	-0.01647	-0.01631	-0.01613	-0.01597	-0.01544	-0.01528	-0.01538	-0.01622	-0.01566	-0.01528	-0.01372	-0.01453	-0.01444	-0.01403	-0.01313	-0.01341	-0.01419	-0.0
12	-0.016	-0.01647	-0.01809	-0.01703	-0.01753	-0.01763	-0.01781	-0.01778	-0.01678	-0.016	-0.01659	-0.01563	-0.01513	-0.01475	-0.01422	-0.01572	-0.01569	-0.01431	-0.0
13	-0.02328	-0.02516	-0.02539	-0.02414	-0.02523	-0.02477	-0.02328	-0.02227	-0.02469	-0.02234	-0.02328	-0.02227	-0.02508	-0.0225	-0.0207	-0.0207	-0.02336	-0.02336	-0.0
14	-0.01691	-0.01903	-0.01688	-0.01772	-0.01831	-0.01916	-0.01784	-0.01772	-0.01778	-0.01694	-0.01628	-0.01713	-0.01556	-0.01613	-0.01547	-0.01578	-0.01303	-0.01556	-0.0
15	-0.01728	-0.01672	-0.01613	-0.01659	-0.01638	-0.01494	-0.01725	-0.01581	-0.01634	-0.01525	-0.01531	-0.01488	-0.01375	-0.01469	-0.01491	-0.01469	-0.01453	-0.01413	-0.0
16	-0.01738	-0.01694	-0.01691	-0.01684	-0.01572	-0.01663	-0.01609	-0.01653	-0.01609	-0.01594	-0.01494	-0.01519	-0.01513	-0.01447	-0.01475	-0.01431	-0.01378	-0.01322	-0.0
17	-0.01575	-0.01513	-0.01513	-0.01525	-0.01675	-0.01528	-0.016	-0.01538	-0.01516	-0.01488	-0.01481	-0.01453	-0.01397	-0.01428	-0.01319	-0.01319	-0.01381	-0.01219	-(
18	-0.01719	-0.01756	-0.01834	-0.01909	-0.01794	-0.01872	-0.01794	-0.01816	-0.01759	-0.01744	-0.0155	-0.01659	-0.01522	-0.01513	-0.01563	-0.01541	-0.01541	-0.01409	-0.0
19	-0.01716	-0.01741	-0.01588	-0.01738	-0.01666	-0.01691	-0.01725	-0.01609	-0.01703	-0.01597	-0.01519	-0.01613	-0.01556	-0.01556	-0.01431	-0.01472	-0.01509	-0.01488	-0.0
20	-0.01675	-0.01756	-0.01638	-0.01659	-0.01719	-0.01619	-0.01631	-0.01734	-0.01603	-0.01597	-0.01416	-0.01531	-0.01444	-0.01484	-0.01478	-0.01434	-0.01422	-0.014	-0.0
21	-0.01541	-0.01447	-0.01559	-0.01566	-0.01516	-0.01538	-0.01534	-0.01625	-0.01438	-0.01488	-0.01553	-0.01469	-0.0145	-0.01528	-0.01356	-0.01416	-0.01344	-0.01303	-0.0
22	-0.01738	-0.01819	-0.01775	-0.01775	-0.01769	-0.01781	-0.01881	-0.01809	-0.01747	-0.01581	-0.01738	-0.01659	-0.01556	-0.01569	-0.01578	-0.0145	-0.01494	-0.01528	-(
23	-0.01759	-0.01666	-0.01753	-0.01659	-0.01775	-0.01666	-0.01738	-0.01741	-0.01794	-0.01703	-0.01631	-0.01491	-0.01666	-0.01584	-0.01584	-0.01444	-0.01559	-0.01416	-0.0
24	-0.01519	-0.01506	-0.01591	-0.01503	-0.0155	-0.01434	-0.01581	-0.01519	-0.01563	-0.01556	-0.01566	-0.01422	-0.01491	-0.016	-0.01506	-0.01413	-0.01356	-0.01338	-0.0
25	-0.02641	-0.02336	-0.02328	-0.02445	-0.02328	-0.02391	-0.02461	-0.02367	-0.02555	-0.02422	-0.02211	-0.02359	-0.0257	-0.02578	-0.02148	-0.02359	-0.02211	-0.02258	-0.0
26	-0.01647	-0.01847	-0.01731	-0.01756	-0.01875	-0.01834	-0.01766	-0.01828	-0.01725	-0.01766	-0.01706	-0.01622	-0.01606	-0.01581	-0.01594	-0.01534	-0.01563	-0.01294	-0.0
27	-0.01634	-0.01772	-0.01694	-0.01703	-0.01731	-0.01594	-0.01666	-0.01597	-0.01672	-0.01669	-0.01622	-0.01613	-0.01513	-0.01559	-0.01556	-0.01394	-0.01525	-0.01456	-0.0

Figure 20 Step.4 All signals are saved as one file .csv

Classification flow chart

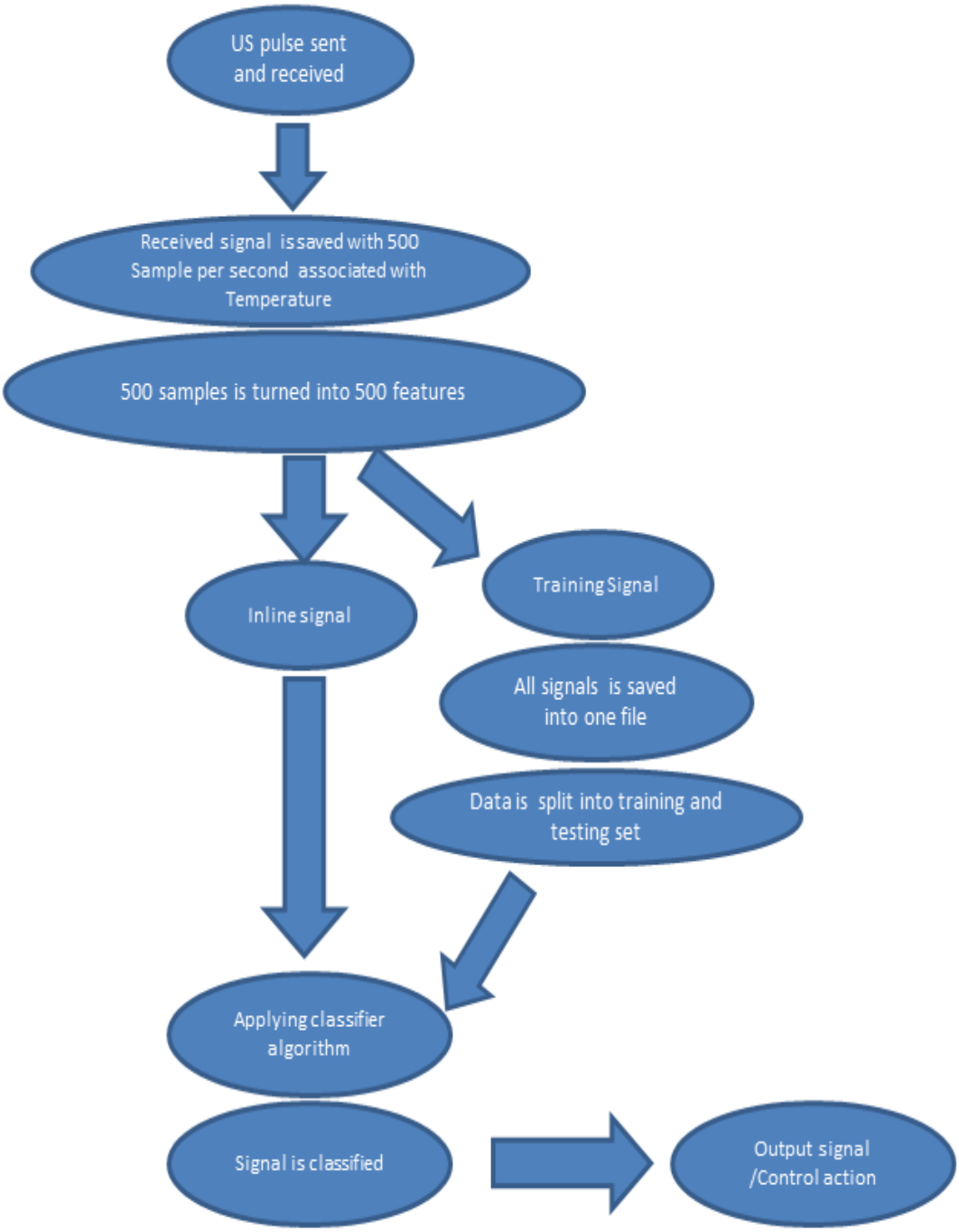

Figure 17 Flow chart of Machine learning training/classification

Chapter Four

Mechanical, Thermal, and Ultrasonic Properties of Plastic Composites Reinforced with Microcellulose and MWCNT

Introduction

Use of hybrid composites is one of the polymer science trends that are gaining attention in the automotive industry. Many automotive components are being manufactured using natural fiber reinforced composites [78]. By adding various types of reinforcements, the material can be tailored to specific needs.

Polypropylene (PP) is a commonly used thermoplastic polymer with excellent properties such as chemical inertness, lightweight, low cost, and easy processing. Despite these benefits, it has some disadvantages, such as small impact resistance and stiffness and low thermal stability [79, 80]. Thermal and mechanical properties of plastics can be significantly improved using fillers. Natural fibers are currently getting considerable attention as a new advanced material for application in automotive, building and packaging industries. The main advantage is biodegradability, sustainability, low cost, low density, high strength and lower abrasiveness. However, due to their hydrophilic nature, the natural fibers have poor compatibility with the polymer matrix, poor water resistance and produce low-performance materials. The University of Toronto has overcome several of these problems in interfacial adhesion for natural fiber composites, developing the composite that has excellent fiber dispersion on the PP matrix with excellent compatibility between the fibers and polymer [78]. Low thermal stability of the natural fibers can lead to the decomposition during material processing, which limits their applications significantly.

Monitoring the temperature during extrusion within the range of $\pm\ ^{o}C$ is believed to be very important especially for the case of processing CNT reinforced fiber-PP composites. For example, the paper results clearly demonstrate that the temperature of extrusion varies along the extruder length. Although the $150^{o}C$ is enough for melting PP during its feeding into extrusion, the melt increase of temperature is needed in order to achieve viscous property of PP melt at the entrance of the fiber (with temperature increase more than $25^{o}C$). The final temperature of PP composite extrusion defines the properties of the semi-crystalline structure of the composite [81].

The technology examination of University Toronto [82] demonstrated that the extruder temperature significantly influences the structure and the properties of the composite being formed. For example, the increase in temperature more than the settled value led to fiber degradation, hence damage to the material.

Analysis of both data shows that control of temperature region of the extruder during processing of fiber-PP Carbon Nanotube (CNT) composite is critical to achieving the high-performance materials. The work in the University of Toronto optimize the regions of the extruder of cellulose –PP- composite, so for the study of mechanical properties and structured composite we used regions defined by M. Sain [82].

Main motor Speed(rpm)	Feeder speed (rpm)	Die in place	Temperature region 1(^{o}C)	Temperature region 2 (^{o}C)	Temperature region 3(^{o}C)
150	15	Yes	180	185	190

Enhanced mechanical strength and thermal stability of natural composites can be achieved by adding nanotubes. MWCNTs become a popular choice of additives in high-performance applications. The high surface area of nanofillers provides an increase in strength even at a low content of fillers. It has been shown that reinforcing PP with CNTs gives significant improvement in thermal and mechanical properties of composites. Multi-walled Carbon Nano Tubes (MWCNTs) are a proper choice of additives to polymers that have a high Young's modulus and decent thermal and electrical conductivity. Developing multiscale composites with microscale natural fibers and nanoscale CNT provides additional benefits in reinforcing the polymer matrix [83]. Further difficulties of polymer composite extrusion technology arise due to pressure in the composites of the carbon nanotubes

When trying to understand natural fiber reinforced composites failure mechanisms, most of the results reported in publications concern the effect of fiber content and processing parameters on composite strength [84]. Little work is done on the study of deformation mechanisms of composites reinforced by natural fibers and CNT.

These mechanisms can differ from those of synthetic fibers due to different morphology and nature of fibers. The objective of this present research is to study the effect of MWCNTs on the structure and properties of natural fibers reinforced composites. The analysis of experimental data is also focused on the analysis of strengthening mechanisms and improving the mechanical performance and thermal stability of the natural fiber-based composites modified with CNTs.

Materials and Methods

Materials (Preparation of Composites)

Before the preparation, all components were dried in the oven for 24 hrs . Polypropylene/micro cellulose (PP/MC) composite developed at University of Toronto [82] (40 wt. % MC, 4 wt. % PP-g-MA (Ncell-40) and PP 4944-50) was used in this study. Polypropylene grafted maleic anhydride (PP-g-MA) was used as a compatibilizer. Three types of multi-walled CNTs (MWCNTs) were used (Cheap tubes Inc.), purity >95wt%, Ash <.5wt%. The outer diameter is 20-50 nm, the length is 15-30 μm. The composition of the materials is shown in Table 2.

Table 2 Composites

	PP-g-MA, wt.%	MC, wt.%	MWCNT, wt.%
PP	0	0	0
PP/MF	3	30	0
PP/MF/CNT-0.5	3	30	0.5
PP/MF/CNT-1	3	30	1

Masterbatch was prepared by the premixing small amount of PP/MC composite with MWCNTs at 190℃ using high viscosity mixer to ensure good distribution and reduce agglomeration. The mixed material was then poured into a flat surface, chopped to small pieces and then grinded. The composite materials were prepared by mixing a master batch and other components using twin screw extruder (TSE 25/40) at the following conditions: rotation speed of 150rpm. The composition of materials investigated is shown in Table 2. The extruded composites were pelletized and injection molded using Zangle 28 Ton into standard test specimens (Figure 18). As a reference, the neat PP without fillers was processed the same way.

Figure 18 Standard test specimens

Mechanical properties

Tensile properties were tested for three samples for each composite using the machine at the rate of 10 mm/min according to the standard.

Microhardness

The samples were mounted, and the surface was prepared and polished with series of the increasingly fine grade of the silicon carbide paper. The Shimadzu ultra microhardness tester DUH 211S equipped with Berckovich indenter was used. 200 mN load force was applied to track the load-unload behavior. Hold-at-the–peak method [85] was used to equilibrate the creep deformation. The length of impression was measured with accuracy to ±1 μm with an optic microscope equipped right after the load-unload cycle. Two types of mechanical properties were obtained through loading-unloading test. One is a dynamic hardness DHT_{115} defined as

$$DHT_{115} = 3.8584 F/h^2 \qquad (15)$$

Where F is the indentation force, and the h is the indentation depth. The other parameter is an elastic modulus E_{it} defined as a slope of the unloading curve. Elastic W_{el} and plastic W_{pl} work of deformation were determined as $W = \int F dh$ from the load-unload graphs.

Microhardness offers a bridge between microstructure and macroscopic mechanical properties. This method allows us to characterize specific parts of the material on a micrometric scale.

Thermal properties

Thermal Gravimetric Analysis/ Single Differential Thermal Analysis

(TGA/SDTA)

The thermal properties of PP-CNT composites are susceptible to the composition [86]. The thermal stability of composites was examined using TA Q500 analyzer. Samples were heated in a nitrogen atmosphere with heating rate up to 500^{o}C and held until the weight is stabilized. The mass loss and its derivative were recorded as a function of temperature.

Differential Scanning Calorimetry (DSC)

Thermal transitions of composites including melting and crystallization temperatures and crystallinity degree were investigated using 822Mettler Toledo DSC calorimeter with a cooling system under a nitrogen atmosphere. The samples were heated from room temperature up to 200^{o}C with heating rate 10^{o}C/min. To eliminate thermal history, then cooled to 0^{o}C at 10 ^{o}C/min. To detect the crystallization temperature Tc; then heated again to 200^{o}C at the same heating rate to detect melting temperature Tm and the heat of fusion (ΔHm).

Melting and crystallization temperatures were identified as peak points at the DSC curves. The degree of crystallinity, %X, was determined from;

$$\%X = \frac{\Delta H_m}{\Delta H_o w} \qquad (16)$$

where ΔHm is the enthalpy of fusion of the polymer, ΔH_0 is the enthalpy of fusion of pure PP crystals (188.9J/g), and w is the mass fraction of PP in the composites.

Microstructure

The fracture surfaces of the materials were studied using FEI Quanta Environmental Scanning Electron Microscope (SEM). The sample surfaces were coated with carbon to decrease charging.

Acoustic properties

The ultrasound properties were measured using the pulse-echo technique, which is the most frequently used methods for acoustic analysis of solid materials [87, 88]. A flat piezoelectric contact transducer with a central frequency of 1MHz was used for both transmitting and receiving the ultrasonic pulses at normal incidence. The transducer was connected to the Panametrics 5073PR Pulse-Receiver. Observation of A-scans was performed in the Techtronics TDS 5052 Digital Oscilloscope. All tests were executed at room temperature with equal input signal amplitude. Each sample was measured at 10 points with five shots per each point. The speed of sound and attenuation were calculated as

$$c = 2d / \Delta t \tag{17}$$

and

$$\alpha = \frac{1}{2d} \ln(\frac{A_1}{A_2}) \tag{18}$$

where Δd is the sample thickness, Δt is the time interval between the initial pulse and the successive pulse as the wave reflects from the lower surface of the specimen, and A_1 and A_2 are the amplitudes of these pulses.

The Archimedean method was used to determine composites ρ density. The data of sound speed and attenuation were used to calculate storage L', loss L'' longitudinal moduli as:

$$L' = \rho c^2 \tag{19}$$

$$L'' = \frac{2\rho c^3 \alpha}{\omega} \tag{20}$$

Where ω is the angular frequency. The absorption per wavelength relates approximately to the loss factor of the material according to the equation:

$$\tan \delta = \frac{L'}{L''} \tag{21}$$

Results

Mechanical properties

Many efforts have been made in describing and modeling the mechanical properties of different polymeric systems with particular focus set on the investigation of the time dependence of the viscous material behavior and the formation of irreversible plastic flow. The objective of this chapter is the examination of mechanical behavior with the aim of being able to expect the polymer composite mechanical properties.

Analysis of experimental data may be done from the viewpoint of;

A. Analysis of the test diagram and strength curves.
B. Analysis of the total stress, total strength of elastic modulus of the composites.
C. Analysis of loading/unloading behavior of the composites.

In general, the strength curve consists of two stages. Stage A at which the elastic behavior of the composite under load is observed and stage B, which associate plastic deformation of material at high stains. The yield offset indicates the initial deviation of the true stress-true stain diagrams from the linear forms, and point B is associated with the yield stress, which is located roughly at the maximum point of the curve in the true stress-true strain diagram [89]. From this viewpoint, it seems to be very important to define both parameters A and B, which reflects the process of beginning and continuation of polymer composite plastic deformation.

The generally accepted mechanism is based on the nuclear growing and motion of the defects of crystalline structure (dislocations), along with the easy crystallographic planes [89]. Adding CNTs up to 0.5 and 1.0% changes the structure of semi-crystalline PP composites and inhibit the motion of dislocations from one side and the degree of polymer crystallinity from another side. It allows increasing the yield strength of PP matrix up to 15MPa. Figure 24 shows these yield differences achieved due to change of CNT content in the polymer composite. The further deformation of the composite results in the development of strengthening effect at stage B of the strengthen curve. At this stage, there is no considerable difference of the true stress-true strain curves of the samples with different content of CNT.

Tensile test results

It is now well-known and commonly admitted that the mechanical properties of polymer nanocomposites, especially the modulus, depend to a significant degree on filler distribution and interfacial interaction, and are increased only when the excellent dispersion of the nanofiller and efficient stress transfer at the polymer/filler interface are guaranteed.

It is known from the work of M. Sain [81, 82], That the mechanical properties of PP biocomposites depend upon how strongly chemical bonds link the fiber and matrix. So, the parameters of stress-strain curves allow defining these effects.

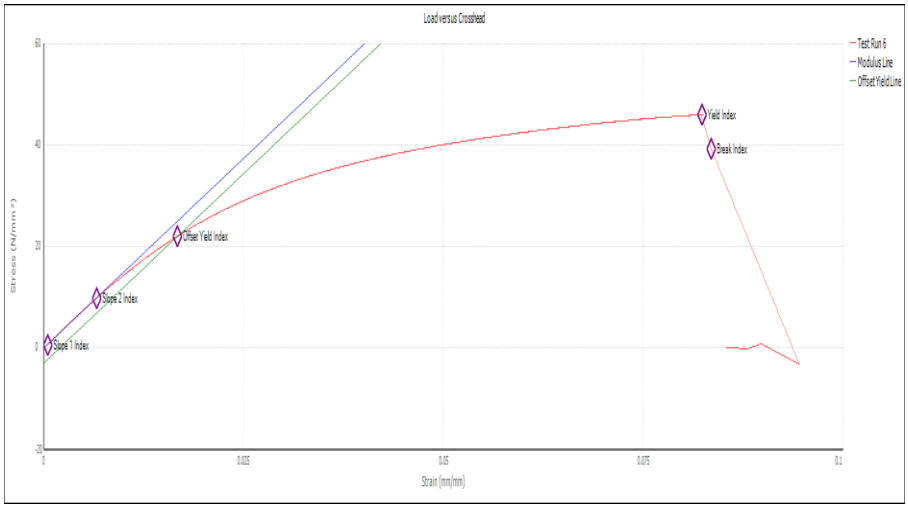

Figure 19 Tensile test

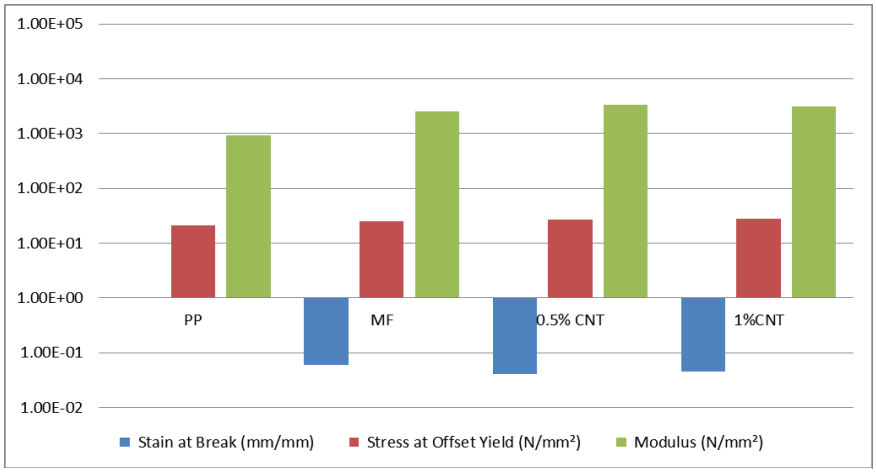

Figure 20 Tensile test results

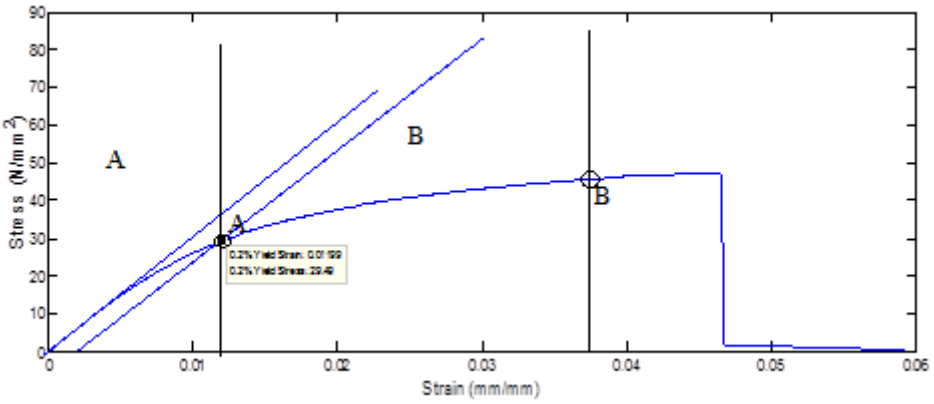

Figure 21 Stress-Strain curve

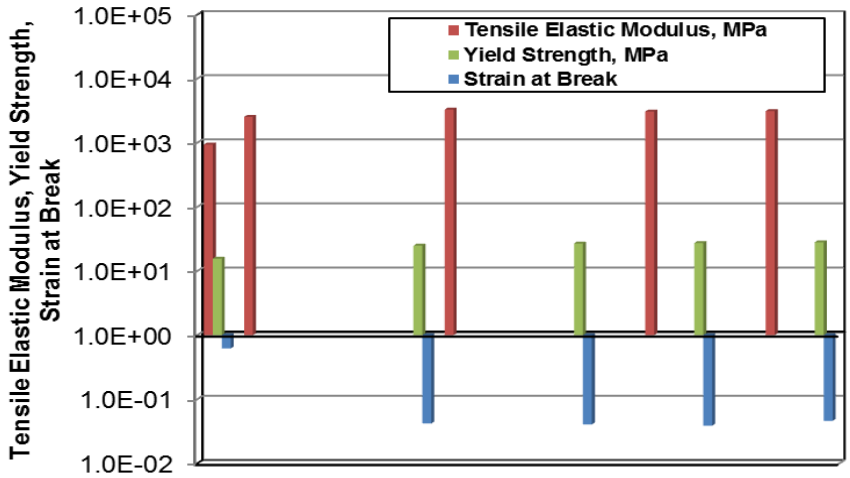

Figure 22 Tensile modulus, Yield stress and Yield strain at break

All stress-strain curves exhibit both a high stiffness as well as a brittle failure at low failure strains of about 4.5% (Figure 24). For all samples, the stress-strain curves follow a linear elastic relation up to strains of about 0.2%. They all exhibit a continuously decreasing slope, each starting with a particular initial stress value, depending on the composition, content, and type of CNTs. The Figure 24 demonstrates that yield stress of PP may be increased considerably by reinforcement with both cellulose nanofibers and CNTs.

Although yield strength of PP is about 15.1 MPa, adding cellulose microfiber results in increasing yield strength to 24MPa, adding of CNTs results in a further increase of yield stress up to 28MPa. Strengthening of PP matrix by reinforcement with microfiber and CNTs seems to be a result of modification of polypropylene matrix structure and hardening effect due to cellulose microfibers reinforcement.

Total strength of the composite depends on the content of CNTs and fibers. There is no essential difference in the total strength. It means that the further plastic deformation of prepared composite results in various similar mechanisms of deformation for both reinforced phases. Although the total strength of pure PP is about 22Mpa, the effect of the strengthening of PP during further deformation will be 6.9MPa. The effect of strengthening PP with fiber composite is 22MPa. Addition of CNT results in diminishing strength effect (19-19.5MPa). Such mechanical behavior of material during the tensile test is the result of the interaction of various structure phases (Matrix-fiber-CNTs), which will be discussed during analysis of microstructure.

The modulus of elasticity is the man sensitive parameter, which depends on modification structure by CNTs (Figure 25). Modification of PP microfiber structure with CNTs results in increasing modulus of elasticity from 2400 MPa up to 3250 MPa (32%). However, the change of the content of CNTs from 0.5% to 1.0% does not show effect. This might be because CNTs are distributed through the matrix relatively uniformly and preferably located on the surface of cellulose fibers.

The ductility of PP composite dramatically depends on the content of the reinforcement elements. Although the strain of pure PP is so high (60%), The ductility of strain at break of the composite modified with microfiber and CNTs is about only 4.5%. This means there is a need for further optimize the ductility of the composite by modification of structure by the change of extrusion technology parameters.

Loading and unloading test allows analysis of mechanical behaviors of the composite in more details. Taking into account elastic strain after relaxation and total strain after unloading, the experimental data of the test is shown in Figure 28, Figure 29. The results reveal that modification of PP with biofiber and CNTs leads to a decrease of elastic strain after relaxation phase during 1000sec. If the elastic strain of PP is about 0.003, the elastic strain for all

composites is about three times smaller (0.001). From the ratio of plastic to elastic strain we can see that this ratio for the composite diminished by five times. These results demonstrate the enormous strengthening effect of modification of PP at various stages of loading.

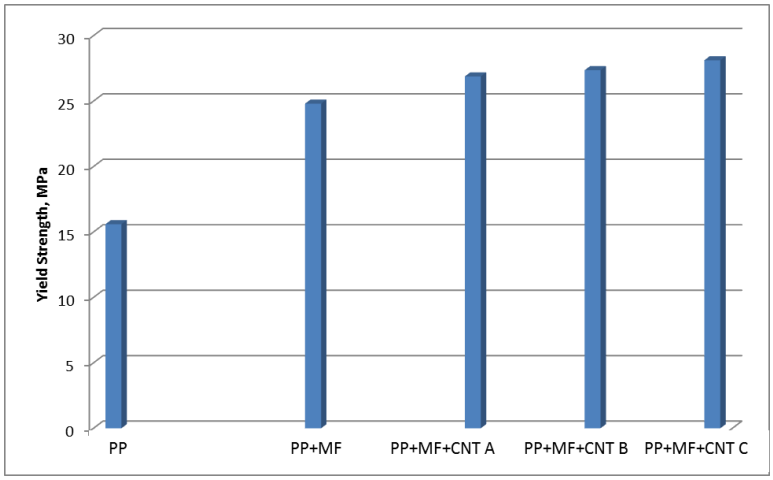

Figure 24 Yield Strength for composites

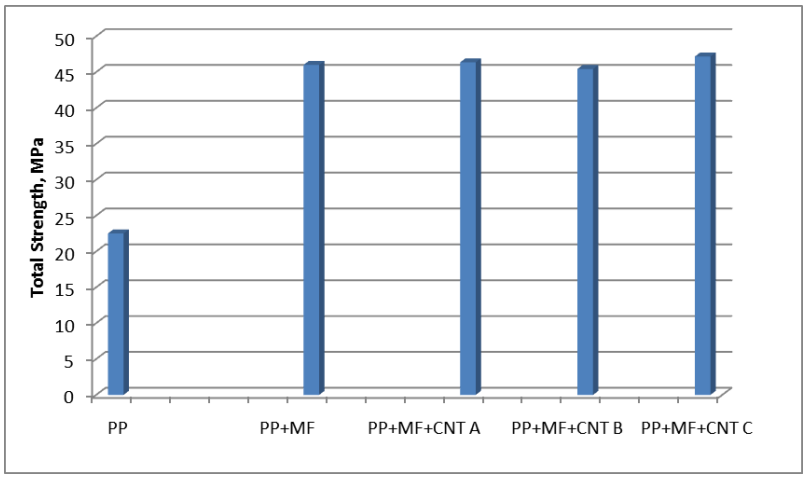

Figure 23 Total strength

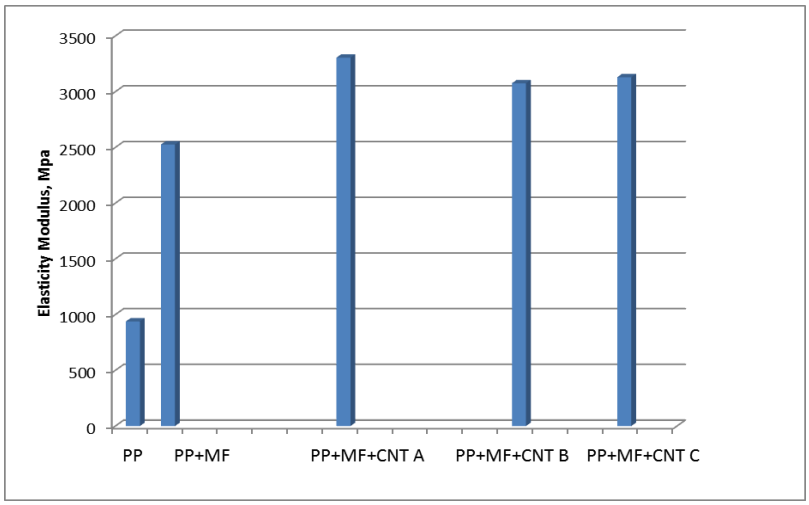

Figure 25 Modulus of elasticity

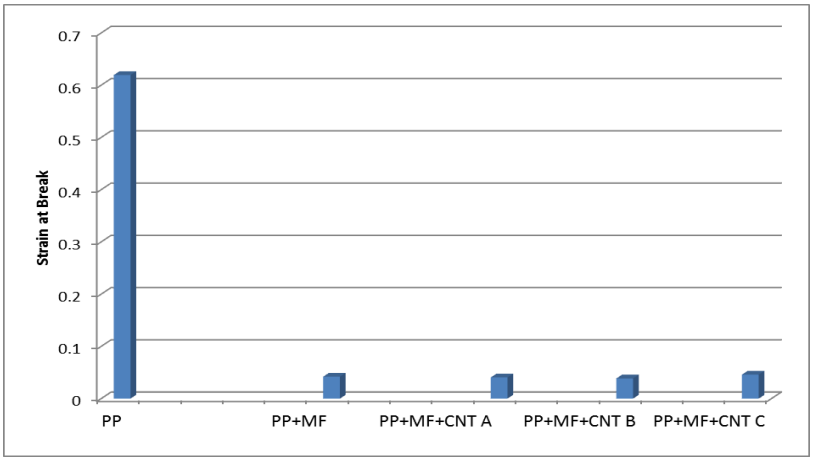

Figure 27 Strain at Break

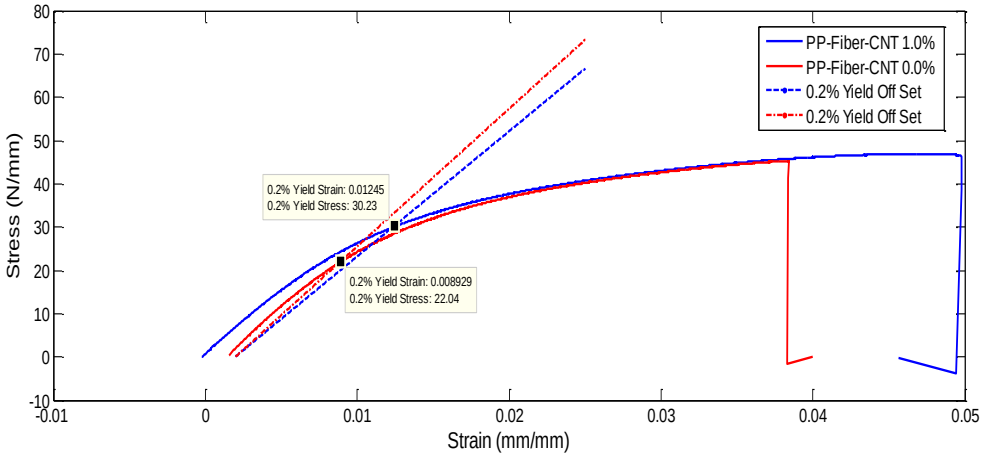

Figure 26 Yield stress difference CNT composition

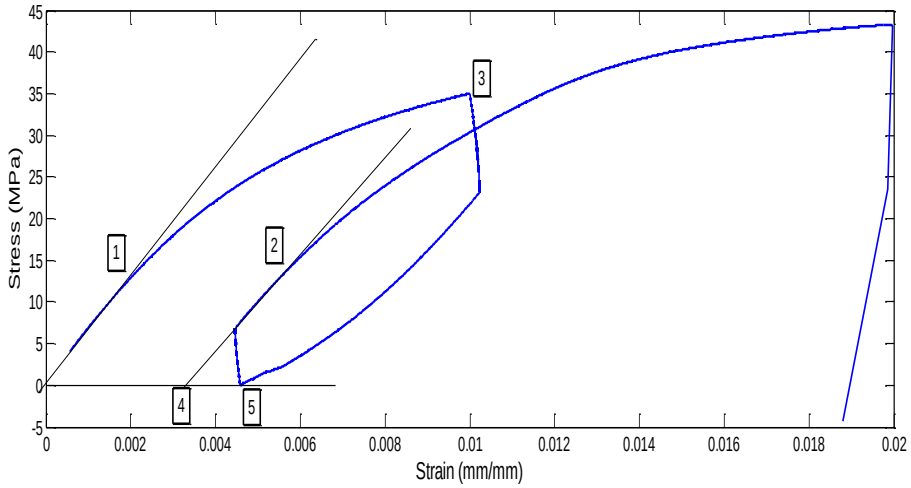

Figure 28 Stress Cycle

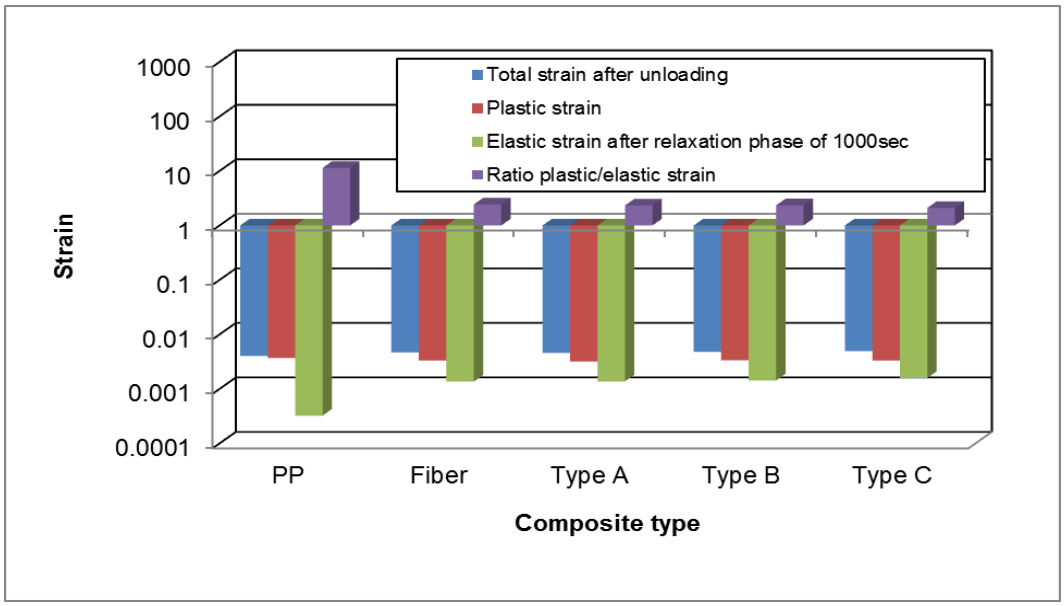

Figure 29 Total Strain after unloading, plastic strain

Uniaxial tensile tests results showing the stress-strain behavior of biofiber reinforced polypropylene with CNTs indicate for all strains: (i) a finite amount of stress relaxation leading to a quasi-stationary state. (ii) a finite amount of plastic flow with a non-linear dependence on the imposed strain, and (iii) the effect of inhibiting of stress relaxation with CNTs during unloading stage.

On the basis of these observations, some structure formation features are predicted: (i) increase of yield strength of composite with CNTs due to its possible interaction with the cellulose fibers, (ii) diminishing of total plastic strain (strain to break) of PP composite reinforced with bio fibers and CNTs.

The effects of PP composite deformation relate to the quasistatic behavior of the material including the plastic flow, the other accounts for the viscous forces leading to relaxing stress components.

Microhardness

Dynamic Micro indentation, or depth-sensing indentation testing, is a technique used primarily to obtain values of the elastic modulus and hardness of materials and involves bringing an indenter with the known geometry into contact with a sample. Three areas where selected for measurement for each sample (Figure 30). A. area with more fiber concentration (Fiber), B. area with less fiber concentration (Matrix) and C. area with a mix of fiber and matrix concentration (Matrix and Fiber). The min distance between two measurements areas has to be at least 15 times the dimension of the probe in order to avoid any effect of the measurement on each other's. Figure 31 shows the deformation after the test.

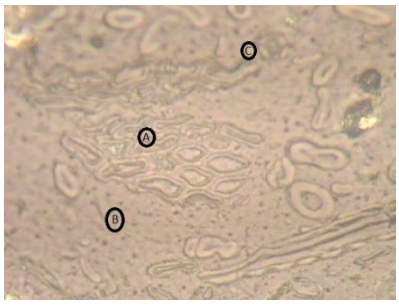

Figure 30 Image to show the selected areas of test

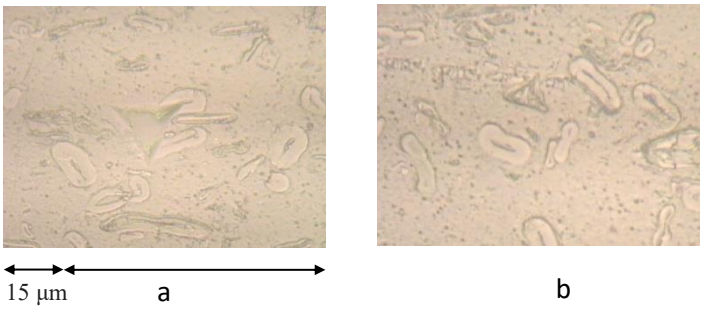

Figure 31 sample deformation after the test (a and b)

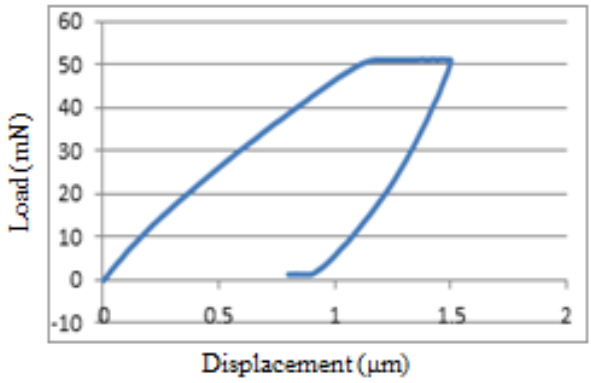

Figure 32 Typical load-unload Curve

The schematic load-unload curve is shown in Figure 32. The load-unload graph shows both elastic and plastic deformation occurs during the test. The hardness DHT115 values and elastic indentation modulus EIT are shown in Table 2. Elastic indentation modulus increases with adding fillers. It rises 85% by adding microfiber to the PP matrix; further reinforcement by MWCNT increases indentation modulus in 1.9 for 0.5% and 2.1 for 1% correspondingly.

It is important to note that due to differences in the type of loading and measuring methods, there is no direct correspondence between indentation modulus and the Young modulus from the tensile test. As seen from Table 3, the elastic work of indentation is the same order as the plastic indentation work. The ratio of elastic to the total; work is decreasing as microfibers CNT added to the PP matrix. It shows the same trend for 0.5 and 1% of MWCNT. The residual indentation depth is dependent on the composite filler and is 3.5-3.8 µm for all composites.

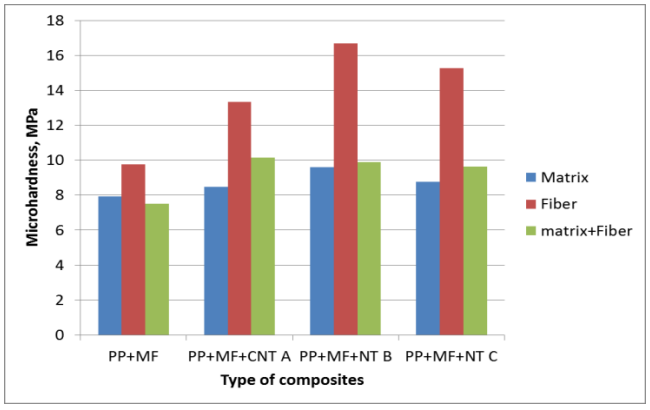

Figure 33 Micro hardness test results

The neat PP shows the most extensive indentation depth and correspondingly has the lowest hardness and indentation modulus. Addition of microfiber leads to a decrease in maximum indentation depth and raise the indentation modulus. Also, adding CNT increases microhardness and indentation modulus as it can surround the fiber and form a layer on the fiber that affect it's hardness. The diffenrce is in micro hardness between phases or areas can also be noted due to the concenrating mainly on the effect of one additive than the other.

The ratio of elastic to total work decreases slightly with adding both types of filler to the composition indicating less mobility of PP chains. This decrease in elastic function and increase in plastic work correspondingly means that the fillers affect plasticity of the PP matrix (discuss with VM). Wel/Wt parameter describes material deformation behavior.

Thus, lower indentation depth and indentation depth increase under the loading, as well as more slope of the unloading curve of the reinforced composites are indicators of higher hardness, lower creep tendency, and more elevated stiffness compared to neat PP. Lower chain mobility can explain this due to higher crystallinity rate.

Table 3 Microhardness

	DHT115	E_{IT}	W_{pl}	E_{el}	E_t	W_{el}/W_t, %
PP	16.10	4.16E+09	379	215	594	36
PP MF	26.5	7.72E+09	337	156	493	32
CNT0.5%	24.7	8.00E+09	360	138	498	28
CNT 1%	26.5	8.75E+09	378	133	511	26

Bowman et al. [17] have found the correlation between microhardness and elastic modulus/yield stress or semicrystalline polymers.

Acoustic properties

Although the ultrasonic method is well-known for non-destructive analysis, its application for measurements of dynamic mechanical properties of polymers has also been utilized [90, 91]. It is beneficial for describing the viscoelastic behavior of polymers and composites.

As sinusoidal stress is applied, modulus can be expressed as an in-phase part, the storage modulus (E‘) and out of phase part, the loss modulus (E"). The storage modulus E’ is the measure of the elastic response of the composite and measures the stored energy; whereas the loss modulus E” is the measure of the viscous response of the material which measures energy dissipated as heat. A loss factor *tan*Δ*,* which is a ratio of loss to the storage module, works as a quantity of the energy dissipation of the composite material. This parameter reports us how good the composite material will be at absorbing energy,

As known, the longitudinal modulus L is related to bulk K and shear moduli G as

$$L^* = K^* + 4/3G^* \tag{22}$$

Piche showed that below Tg, the thermal behavior of the material’s sound velocity is governed by the shear modulus G* while at Tg and higher temperatures, the bulk modulus K* is more significant and dominates the velocity’s temperature dependence.

The storage modulus E’ denotes the material’s stiffness and proportional to the energy that is stored during the load cycle. The loss modulus E” is proportional to the energy that is dissipated during the load cycle in the form of heat.

Table 4 Acoustic Properties

	PP	MF	CNT 0.5%	CNT 1%
Speed of sound, m/s	2500	2813	2880	2880
Attenuation, mm^{-1}	0.12	0.24	0.24	0.27
L’, GPa	5.66	7.97	8.39	8.45
L”, GPa	0.52	1.74	1.87	2.1
Tan δ	0.09	0.22	0.22	0.25

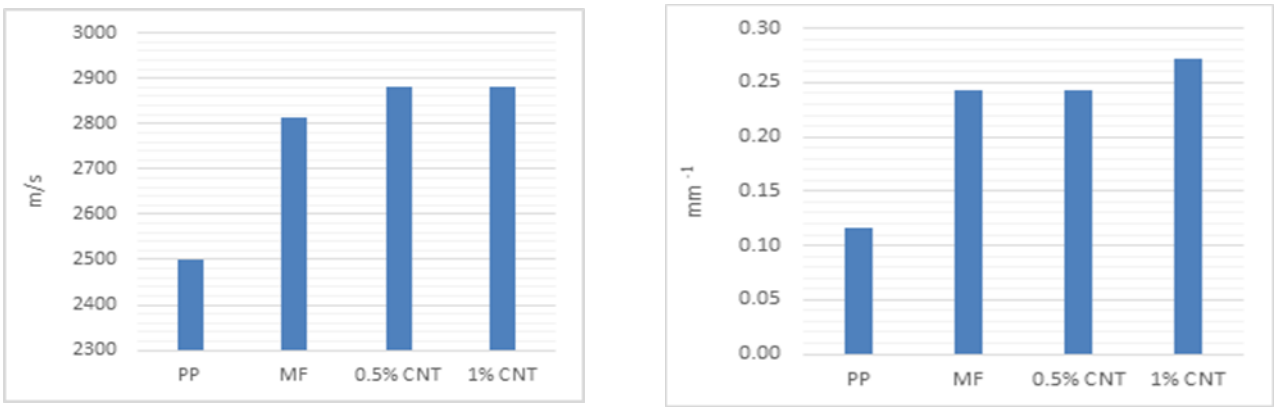

a b

Figure 34 Speed of sound (a) and attenuation (b) in neat PP and microfiber and MWCNT composites.

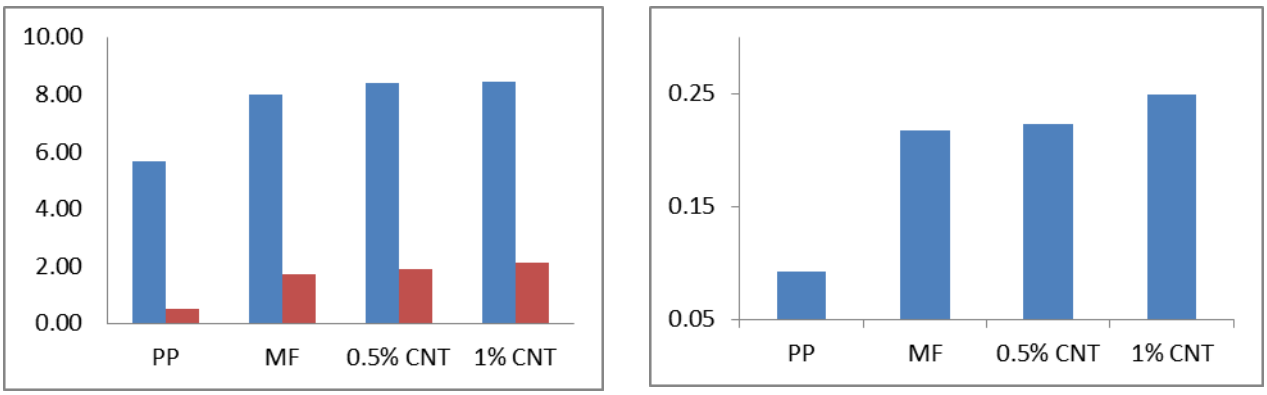

a b

Figure 35 Elastic moduli E' and E" (a) and loss factor tan δ (b) in neat PP and microfiber and MWCNT composites

The increase of storage modulus indicated that the composites show the better interaction between the fiber or CNT and the polymer matrix.

Thermal stability

Natural fiber degradation is the severe drawback in biocomposites production. Thermal degradation of natural fibers leads to the poor mechanical performance of the composite, changes in composite appearance. Thermal stability of neat PP and composites was studied using TGA. The difference in mass of the composite specimen was monitored as heat applies to the sample. Figure 36 shows the thermal degradation of the PP/MF/MWCNT composites. The first derivatives of the TGA curve are shown in Figure 36. This type of graph should show the inflection point as a maximum. Thermal degradation parameters are summarized in Table 5.

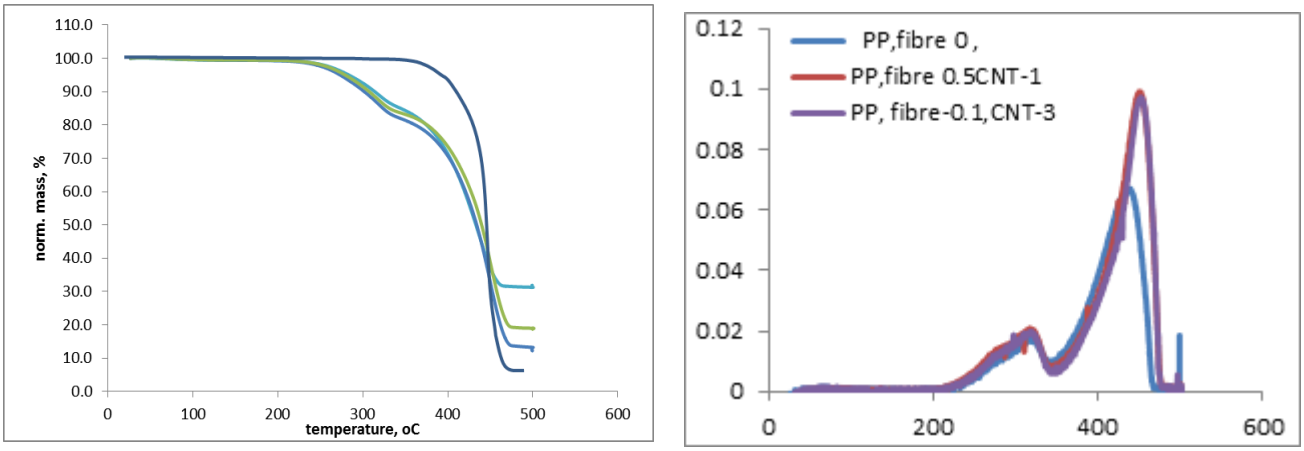

a b

Figure 36 TGA (a) and DTA (b) of composites

The TGA of the neat PP shows one degradation step, starting 370^{o}C and completed at 480^{o}C. This step is attributed to degradation of the PP matrix with the mass residue of 6%. The thermal degradation of polypropylene occurs by chain scission with radical chain mechanism. All TGA curves of composites show similar degradation pattern for all types of composites. The composite mass change has two sigmoid shapes, the degradation of cellulose and PP. The minor weight loss at the temperatures below 100°C corresponds to dehydration. All samples showed 0.5% of weight loss.

The cellulose-containing composites start to degrade at approximately 260, 265, 268^{o}C for the composites with 0, 0.5, and 1% MWCNT correspondingly. The maximum rate of fibers decomposition occurs at 320^{o}C for all composites. The mass loss of 87, 83, and 85% were measured for materials with 0, 0.5, and 1% of MWCNT. The Derivative thermo-gravimetric

(DTG) curve shows the small shoulder presence that is assigned to the degradation of the hemicelluloses and cellulose [92].

Table 5. Decomposition characteristics of composites

sample	TG/DTGA						
	Dehydration, %	T_{onset}	T 1 (peak)	$T_{onset\ 2}$	T 2 (peak)	D_{50}	FR, %
0% MWCNT	0.5	260	320	376	440	432	20
0.5% MWCNT	0.5	265	320	392	450	433	12
1% MWCNT	0.5	270	320	408	455	439	19

The second degradation step (PP degradation) occurs between 360^{o}C and 480^{o}C and corresponds to PP thermal degradation. Similar two-step degradation was observed for orange tree fibers-reinforced PP composites [88]. Thermal degradation of PP usually happens at 400^{o}C due to C-C chain bonds rupture[93, 94]. The PP in the composites starts degrading at 370 ^{o}C in PP/MC composite, the beginning of the degradation temperature shifts toward the higher temperatures with adding MWCNT to the composite, 392 and 408^{o}C correspondingly for 0.5 and 1% of CNT. The maximum degradation rate for PP also occurs at higher temperatures with adding nanoparticles. Similar behavior was reported by other authors [Chipara et al., 2008]. This effect may be due to the interaction between PP chains and CNT revealing the interface formation. MWNTs dispersed throughout the matrix may act as a barrier to heat and resistant to volatile degradation products. Improved resistance to thermal degradation has also been reposted for nanoclay/PP composites [95]. The proposed mechanism includes higher thermal conductivity of composites that facilitates heat dissipation [96]. Another mechanism attributes the increase of decomposition temperature to the hindered diffusion of volatile decomposition products caused by the nanoparticles [97]. The total mass loss was measured 20, 12, and 19% for biocomposites with 0, 0.5, and 1% of MWCNTs correspondingly. No additional mass loss was observed after reaching 470^{o}C. Due to the absence of oxidizing phase, the degradation of CNTs is not present at the curve.

Thus, MWCNT reinforcement of PP improves the thermal stability of the PP matrix by delaying the volatilization of the products of C-C bonds scission.

Crystallization and melting of PP on composites

Changes in crystallinity degree of the polymer phase of composite lead to significant changes in the composite's mechanical performance, especially in creep and compression. The DSC thermograms of the PP and composites for the cooling and the second heating are presented in Figure 37. The primary thermal behavior parameters (crystallization temperature, melting temperature, and crystallinity degree) for each specimen are summarized in Table 6. Only one exothermic peak was observed on cooling thermograms for all samples. Pure PP shows a sharp crystallization peak at 121^{o}C with onset 126^{o}C. MF composite has the peak at the 123^{o}C while adding CNT to the composite shows an additional shift of the crystallization temperature (126^{o}C). Onset temperatures also are shifted to higher values indicating the earlier start of the crystallization process. Higher T_c values indicate the earlier start of crystallization in the presence of MF and, especially, MWCNT. Spolijaric et al. [98] have reported little increase of Tc onset and peak temperatures with the rise of MC content. These data indicate that MF and CNT may act as centers of nucleation propelling PP matrix crystallization [99]. Adding MF and CNT increases the number of nucleation sites and promote PP to crystallize at slightly higher temperature.

The second heating thermograms are presented in Figure 37(b). Only one endothermic peak is observed at each thermogram. Melting onset temperature of pure PP is 144^{o}C with peal temperature 165^{o}C. This peak corresponds to melting of the α-crystalline phase of PP [100]. Adding MF and MWCNT increase the onset temperatures for both melting and crystallization processes but does not affect the peak temperature values. Other authors have reported slightly lower T_m for natural fiber-based PP compared with neat PP [101]. Adding both reinforcing agents (MF and MWCNT) lead to significant increase in the melting peak area normalized to the PP content and calculated the heat of fusion. The effect of MWCNT is more noticeable compared to the microfibers effect. This suggests that interaction between the fibers, CNT and PP are restricting the flowability of PP molecules during the melting process [100]. The crystallinity of PP has increased from 32% for pure PP to 35% for MF-containing composite. Adding MWCNT further shifts crystallinity degree to 40%. Small Angle Light Scattering analysis of glass reinforced PP has shown that adding fillers to the polymer matrix supports the crystallization process of PP matrix by creating the nucleation sites on the filler surface and

initiate the trans crystalline layer formation [87, 102]. Similar nucleation effect on PP crystallization was observed for other types of natural fibers[101, 103] and CNT.

Table 6 Thermal properties of PP and its composites

Material	Crystallization		Melting		Crystallinity degree, ΔX
	onset, ^{o}C	peak, ^{o}C	peak, ^{o}C	ΔH_m, J/g PP	
PP	126	121	165	60.7	32
0% MWCNT	127	123	165	65.3	35
0.5% MWCNT	130	126	164	75.5	40

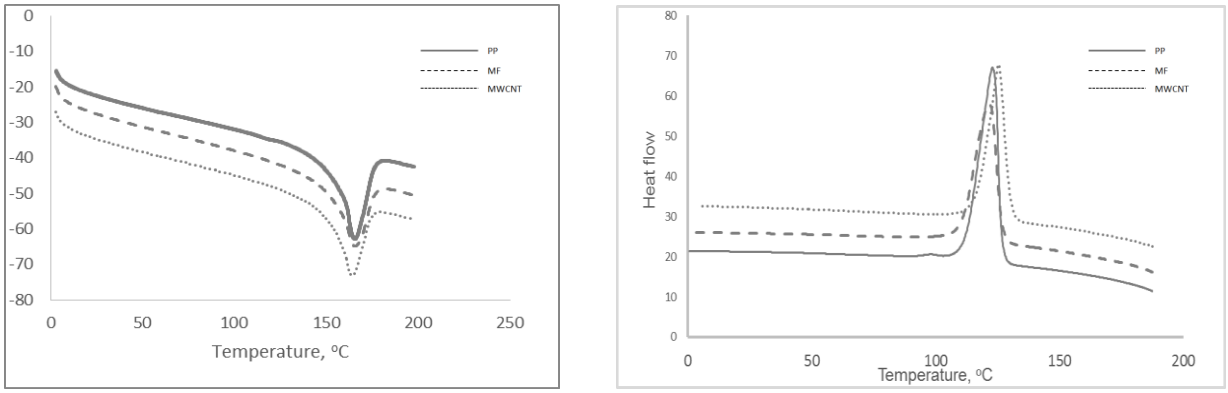

Figure 37 DSC of the composites. Cooling (left) and heating (right) plots

SEM

The fiber- matrix adhesion is the essential factor to enhance the mechanical performance of the composites. By using Scanning electron microscopy (SEM) to inspect the fracture surface of the composites with cellulose and CNT, the SEM analysis shows fibers dispersion in the matrix. Excellent adhesion between natural fibers and the matrix with random pullouts was also observed. No agglomeration occurs providing the efficient stress transfer between the fibers and the matrix.

The dispersion of CNT in polymer matrix governs the reinforcing power of CNTs. The shown SEM images are a representative illustration of fiber and CNT dispersion. A uniform arrangement of fibers can be observed without bundles. The diameter of the nanofibers was measured as nm. The increased diameter is assumed due to PP-g-MA wrapped around CNTs. Due to carbon nanotube surface interactions with grafted maleic anhydride groups, the PP-g-MA adsorbs onto the nanotubes resulting formation of the coat of PP-g-MA a few nanometers thickness. This coating remained undamaged after fracture.

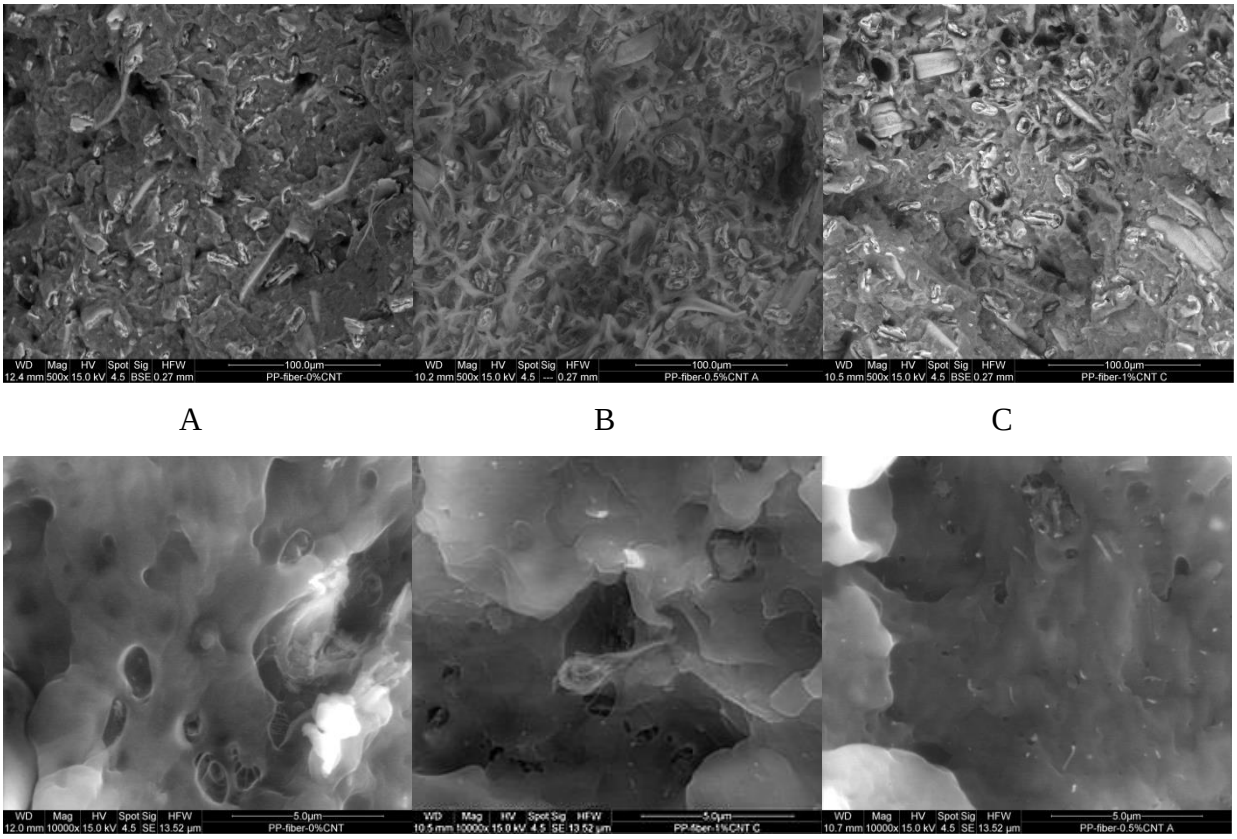

Figure 38. The fracture surface of the composites. A- PP+MF, 2- PP+MF+0.5%MWCNT, C- PP+MF+1%MWCNT

The specific feature of fracture of tension samples are seen at the SEM and optical microscope images In This cases some fractures of Bio fibers are seen, some pull off effects of Biofiber may be observed. The low ductility of the PP MF and PP-MF-CNTs composites may be explained by high loading capacity of microfiber within withstand higher stress than these of PP matrix. MF fracture details are shown in (Figure 39) the adhesion of MF to PP Matrix is perfect (Figure 40). For this reason, the total effect of the increase of PP-MF-CNTs composite mechanical properties

is high. The addition of CNTs increase the Mechanical properties of the composite due to additional strengthen to MF.

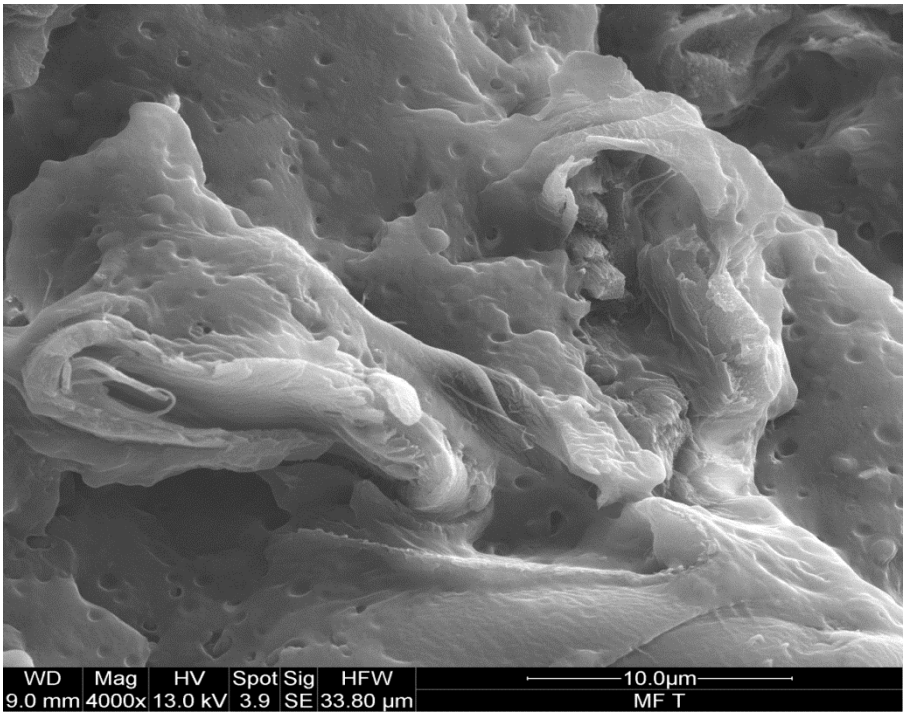

Figure 39 SEM image of Fracture surface of PP- MF composite

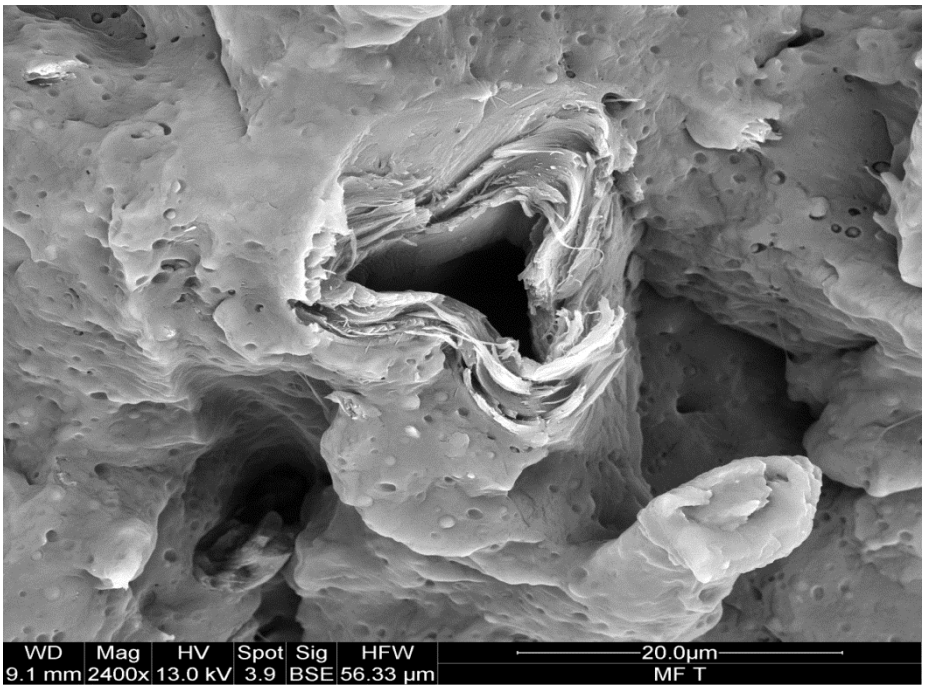

Figure 40 SEM image showing good adhesion of MF and PP

Chapter Five

Results and discussion

It is important to note that this project is multi-discipline projects that require a min understanding of all the disciplines involved including material science, physics of ultrasound and machine learning. The work in this project has covered as much as necessary from the knowledge needed to achieve the stetted tasks required to achieve the goal of that work.

The results of this work can be classified into three main categories:

A. The results of material development, which included the results and conclusion from the material evaluations tests and studying the effect of adding CNT to the bio composites.

B. The results of ultrasound measurements of the different composites at heating and extrusion temperature.

C. The results of applying machine learning techniques to classify the ultrasound signal for two temperature classes above and below 190^{o}C.

The integration of these results demonstrates the completion of the tasks and the accomplishment of the project goal to provide a system by which fiber degradation in the bio-composite process could be prevented.

Results of material evaluation tests

Polymer microfiber reinforced nanocomposites have received much attention [78, 81, 104] , and their modification with the carbon nanotubes allows to change their structure and the mechanical properties. The obtained experimental data reveal that a small amount of the carbon nanotubes results into an improvement of the properties, such as elastic modulus, strength, and others. Using the carbon nanotube reinforcement is believed to provide an improved balance of stiffness and toughness. Many studies [105] have been performed to find a relationship between the structure and the properties of the polymer-based nanocomposites to understand mechanisms of increasing the properties of the polymer. Study of the mechanical behavior of the polymer-based nanocomposites is of great importance from this viewpoint.

Characterization of the mechanical properties and study of the viscous material behavior of different polymer materials have been performed in many works (see, for example, [106]). The particular attention was devoted to the investigation of the time dependence of the formation of irreversible plastic flow [106] which may be determined by precision tension tests. It is well known that at the present time, the studies of deformation response and accompanying structural

changes of semicrystalline polymers are being performed during uniaxial tension tests prior yield point (plastic strains of about 0.01-1%). This is because straining of semi-crystalline polymers prior to yield point is the stage preceding dramatic changes of polymer structure beyond yielding [89] .The study of PP based nanocomposite mechanical behavior in microstrain area of loading is more adequate than at the large strains because the structural transformations induced by small deformations are negligible as compared to that of the composite virgin structure.

The two types of tension tests with plastic strain measurement in the range of ε=0.01-1% (Figure 24Figure 21Figure 43) allow defining the deformation behavior of nanocomposites prior the yield point. The polypropylene (PP) and polypropylene-microfiber-CNT composite C (1.0% CNT) stress-strain curves in the area of yield point are shown in Figure 41 as an example. The micro-strain area of stress-strain curves may be approximated with three lines and characterized by critical points A, B. The polypropylene-based materials exhibit deformation behavior similar to that of semi-crystalline polymers. Point A indicated the initial deviation of the stress-strain curve from the elastic line, and point B is associated with real yield point at the plastic strains of about ε=0.002. Relationships of the composite structure and properties characterized by critical points A, B are established by authors[106, 107] The possible reason of deviation of linear dependence at point A of the stress-strain curve is believed to be sliding of lamella blocks. The point B is associated with the yield point which is located at the field of maximal curvature of the stress-strain curve in the micro-strain area. The yield stress values are believed to be defined by the processes of cooperative motion of the blocks of crystalline lamellae [89]

It is interesting to note that the critical strains of the A and B points vary in the narrow ranges for all examined composites in spite of their different composition (εA=0.002, εB= 0.006, Figure 41). It means that the micro-strain deformation mechanisms proposed by [89]are similar for composites with different content of reinforcement phases (both cellulose fibers and CNTs). It allows suggesting that the micro-strain deformation mechanisms are controlled solely by semi-crystalline polypropylene matrix structure. The stress-strain response is known to be coupled with structural transformations in accordance with models developed in works[89, 108] The basic model is based on the concept of pseudoelasticity [89]which is defined by the semi-crystalline structure of the polymer. That is why a crystallinity degree c and distribution of

crystalline and amorphous phases both at initial and deformation stages are the main structure parameters controlling the stress-strain response.

True stress is calculated by dividing of the real load P_x at the certain absolute strain-Δl ($\Delta l=L_x-L_o$) on real cross-section area F_x of the dog-bone sample being tested. At this case P_x is defined from P-Δl diagram, and real cross-section area is defined on the base of the rule of constant volume of working part of the sample during tension. So $F_x = V_{sample}/L_x$. This calculation is made by the test machine, and the curve true stress-true strain is obtained by same machine. Total stress is calculated more simply: stress=P_{max}/F_o. P_{max} is the maximal load on the tension diagram, and F_o is the initial area of the tension sample, Hence the true stress is more accurate characteristics as its variation reveals about strengthening behavior of the material.

The results of precise evaluation of critical stresses and strains of the points A and B are shown in Figure 42 as the stress and strain dependences on crystallinity degree of the composite. The results reveal that modification of composite structure by its reinforcing with cellulose nanofibers and CNTs leads to following effects:

i) Reinforcing with cellulose nanofibers do not change both critical stresses and strains of the points A and B considerably in spite of variation of crystallinity degree;

ii) The main effect of CNT modification is an increase of both critical stresses and strains of the points A and B which is believed to be the result of specific features of semi-crystalline structure formation arisen due to CNTs presence;

iii) The strengthening effect of CNTs (inclination of the curves $\sigma A,B=f(c)$) in the range of c=40-50% is similar to points A and B (Figure 42) that reveals about the influence of CNTs on the polypropylene matrix crystallinity and structure at the initial stage of the PP composite deformation.

A relatively small effect of cellulose nanofiber reinforcement (30% content of the cellulose nanofibers) on the composite tensile strength (Figure 42) is similar to that defined in[104] The main reason of such a PP composite deformation behavior seems to be considerable strains of the PP matrix at the maximal tension stresses which are used for tensile strength calculation. The mechanical properties of cellulose fibers and stress transfer in the fiber-matrix interface at the significant strains are believed not to influence the total tensile strength considerably[109]. We

observe the similar behavior for critical stress (point A) and yield stress (point B) at small strains (εA=0.001 and εB=0.004). Perhaps, the interfacial stress transfer at the fiber-matrix interface is not sufficient to achieve the valuable strengthening effect of the composite structure due to the high strength of the cellulose fibers.

Modification of PP composite with CNTs with the content of 0.5-1.0% change the PP-fiber composite deformation behavior at the small strains (Figure 42) because of two possible effects: i) dispersion strengthening of PP matrix with CNTs, and ii) increase of crystalline fracture in the semi-crystalline matrix. The matrix strengthening effect due to an increase of crystallinity degree of PP matrix seems to be of great importance. Indeed, the yield stress (point B) of PP-fiber-CNT composite is obtained to be twice higher than that of PP-fiber composite (Figure 42). The Raman spectroscopy is used to investigate the deformation behavior of the nanocomposites[109] A noticeable shift of Raman peaks at the strains of about ε=0.03 reveals about two possible ways of the stress transfer: whisker-whisker and whisker-matrix interactions[109] However, our experimental results of tensile tests at the smaller strains (εA=0.001 and εB=0.004) do not demonstrate the effect of the whisker-whisker and whisker-matrix interactions on the critical stresses at points A and B. It allows to suggest that the matrix strengthening effect due to increase of crystallinity degree of PP matrix is responsible for increase of critical stresses at the points A and B.

As shown by [110] many polymers, such as, e.g., polyethylene, polypropylene, polyamide, etc. only to a certain degree (between 10% and 50%) which are called as semi-crystalline ones. The general feature of the microstructure of the semi-crystalline polymers is the presence of crystalline lamellae (blocks) which are stacked with a break of about 10…50 nm. The crystalline blocks usually have a thickness of 5-10 nanometers and a lateral size of 1-5μm [110] . The specific feature of semi-crystalline polymer crystal structure (at nano-scale) is that the polymer chains in the crystalline phase are oriented perpendicular to the lateral direction of the lamellae, and their length is much larger than the lamellar thickness [107, 108, 110]. Thus, the numerous chains arisen from the crystalline blocks into the areas between the blocks form an amorphous network as shown in [108] The structure of are assumed to be highly entangled since most of the entanglements of the molten state are preserved upon rapid cooling[110] The crystalline block

network available at the crystal phase content of about 35-50% is believed to be responsible for the effects of increase of critical stresses at the points A and B, and the deformation mechanisms at these small strains will be studied in detail in the future work.

From another side, the elastic and plastic deformation of the amorphous network of PP matrix influence of the mechanical behavior of the composite. To investigate these effects, the tensile specimens were loaded to the defined strain and subsequently unloaded into the stress-free state and kept for 1000sec similar to the procedure of [106]. The experimental results reveal that the total strain reached by the loading of the samples is composed of the elastic and irreversible plastic strain. The plastic strain is available after the long relaxation time in the unloaded state. The reversible elastic strains which achieved by relaxation in the unloaded state is believed to be the result of the composite amorphous network transformation.

The reversible elastic strain dependence on the PP matrix crystallinity shown in
Figure 44 clearly demonstrate the effect of the material composition. Indeed, the PP matrix relaxation processes are inhibited by cellulose microfibers due to a decrease of amorphous phase content. However, CNTs addition results in a slight increase of elastic relaxation strain due to possible restoration of amorphous phase structure during a stress-free state in spite of higher crystallinity of the composite. The mechanism of this effect will be studied in future work.

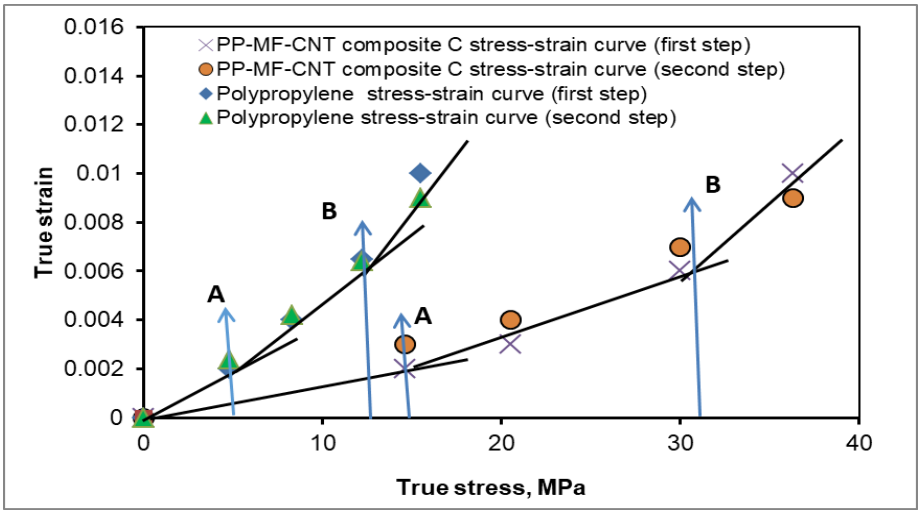

Figure 41 Critical Points A, B on True Stress vs True Strain curve

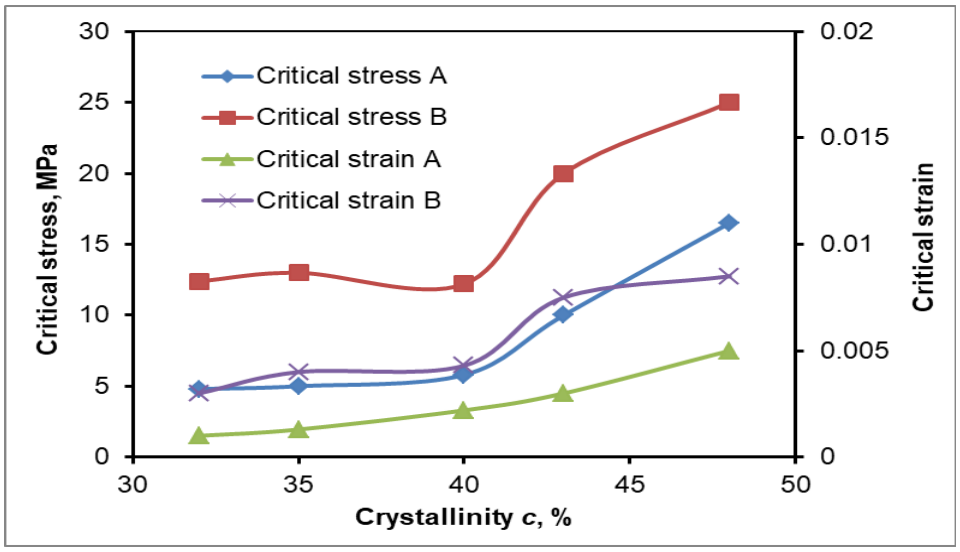

Figure 42 Critical stress vs. Crystallinity

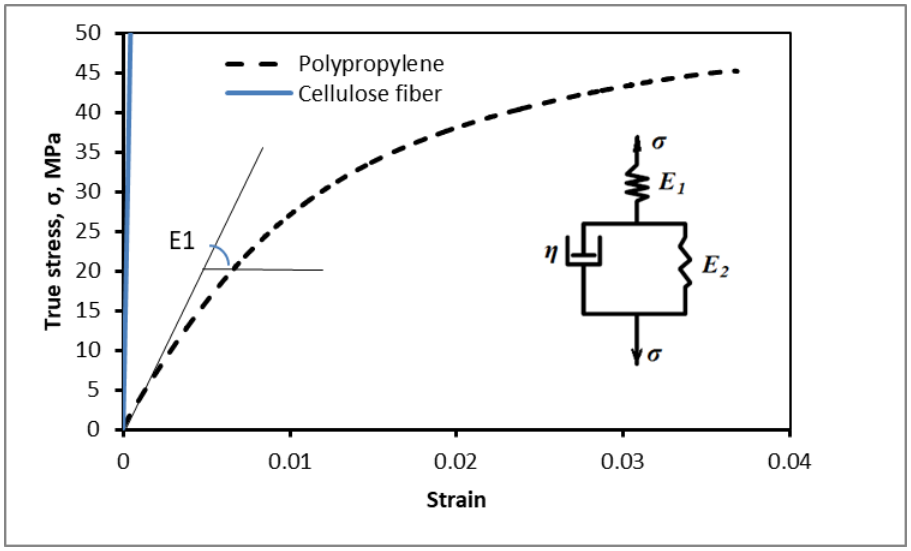

Figure 43 True Stress vs. True Strain

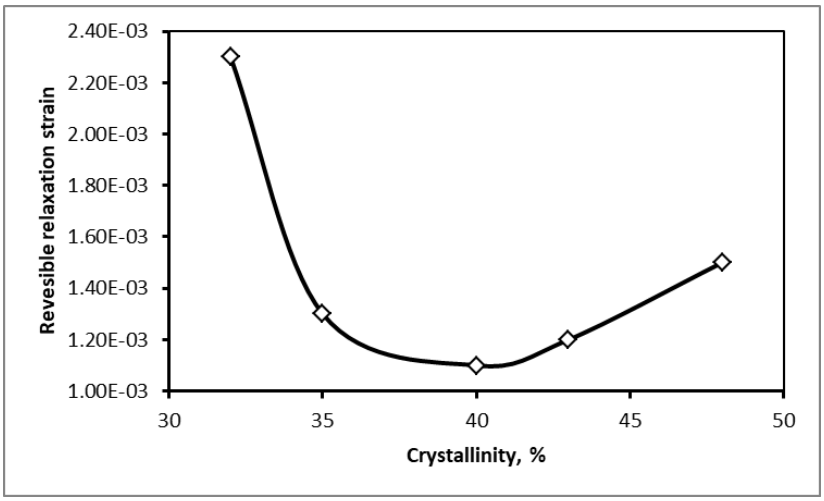

Figure 44 Reversible relaxation strain vs. Crystallinity

Results of Ultrasound measurements

The main point of US parameter measurements is the establishment of the relationships between technology parameters of melted polymer composite during the extrusion into the mold, the temperature, and structure formation processes. For this reason, the temperature dependences on the speed of sound and attenuation are determined by two methods. Both methods are explained in the experimental procedure in chapter 2 where sound speed and attenuation are defined at various temperatures of extrusion and ambient temperature after solidification of polymer material.

The dependence of sound velocity on extrusion temperature of PP itself is shown in Figure 45. It is precisely seen that the scatter of US speed for each temperature is in the range (15-30 m/s). It means that variation of sound in the temperature range of 160^{o}-200^{o}C is possible to be determined by such measurement with sufficient accuracy. The dependence of sound velocity shown in Figure 45 does not demonstrate that destruction processes of melted composite occur because curve shown in Figure 45 is smooth. It is known that PP-Microfiber composite destruction temperature is higer than 180^{o}C. because of degradation of cellulose fiber (see the data of TGA analysis). it means that increase in temperature above 180^{o}C will result in some decrease in polymer strength so, determination of the temperature regimes preventing such degradation may be made by analysis of dependences of sound velocity/ attenuation on extrusion temperature.

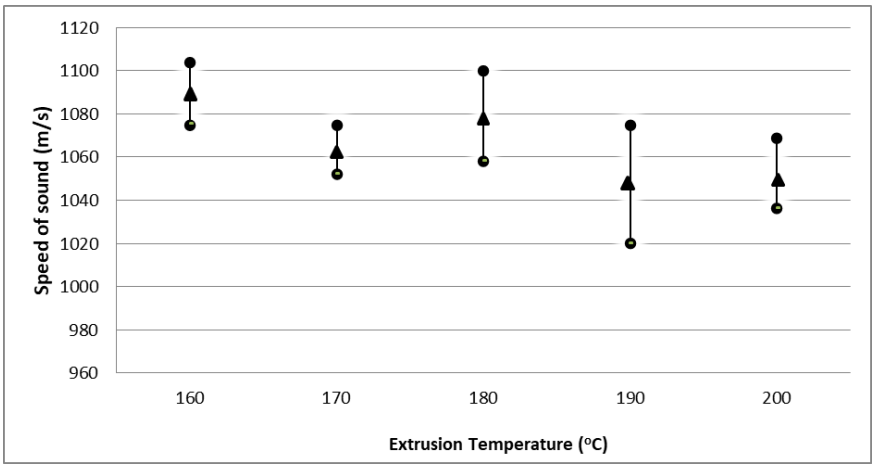

Figure 45 Variation of sound speed for PP at different temperatures

The comparison of measurements of the speed of sound during the extrusion process and directly after heating (Figure 46) we would note that polymer matrix structure formation at the different extrusion temperature does not lead to a change in speed of sound (smooth curves).

Modification of polymer (PP) with micro cellulose fiber does not change a trend of temperature dependance of speed of sound. This suggests that the polymer matrix properties have major contribution to the mechanism of ultrasound propagation (Figure 37). The absolute values of sound speed for all material are in correlation for both heat and extrusion measurements

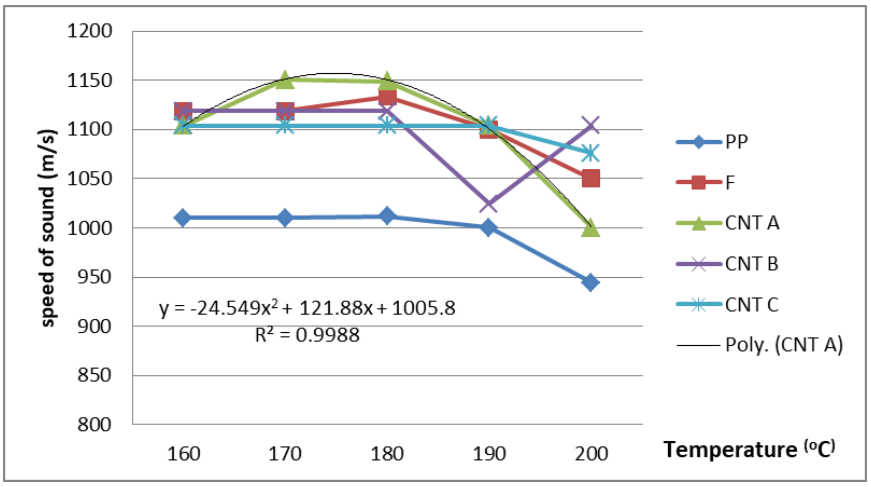

Figure 46 Sound speed vs. heating temperature

The attenuation parameter slightly increases with temperature is shown on (Figure 48). It has to be noted that attenuation is a sensitive parameter to the characteristics the structure formation of the filled composite and this parameter should be used alonf with sound speed for online monitoring of the extrusion process. The mechanisms of sound attenuation in polymers include a. scattering by fillers, and b, intrinsic absorption by conversion to heat in a viscoelastic material [111].

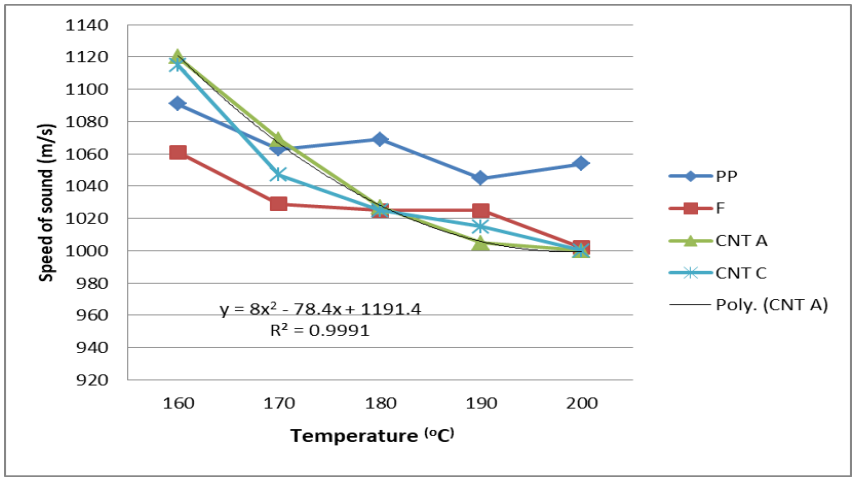

Figure 47 Speed of sound vs, extrusion temperature

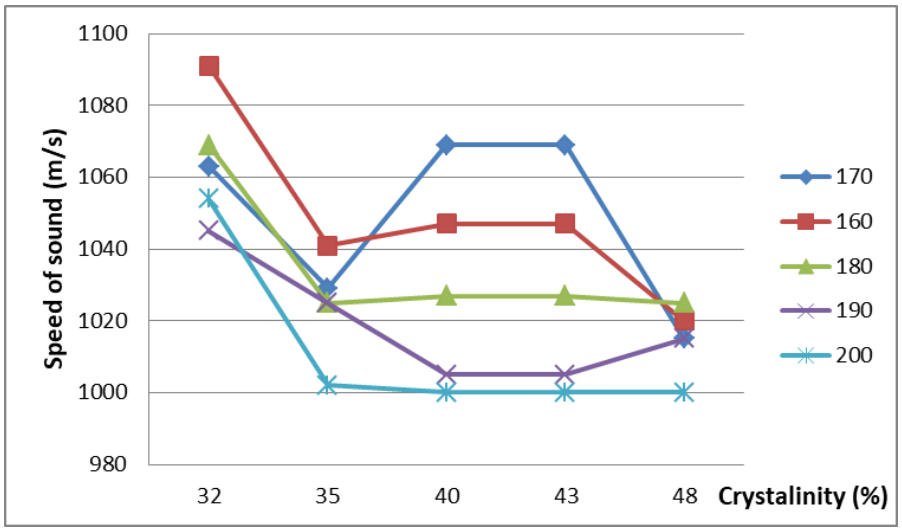

Figure 48 Speed of sound vs. crystallinity of composites extruded at various temperature

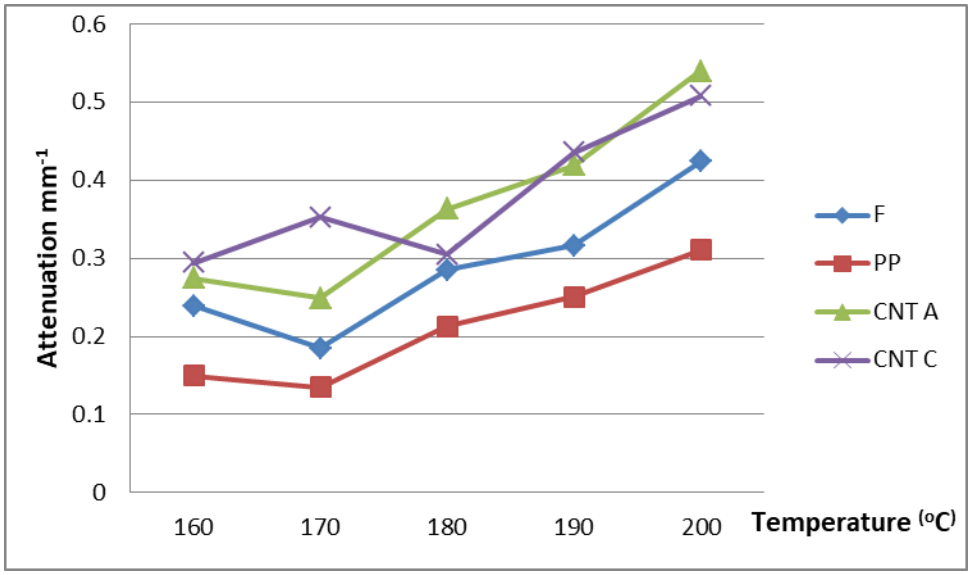

Figure 50 US Attenuation at different Temperature

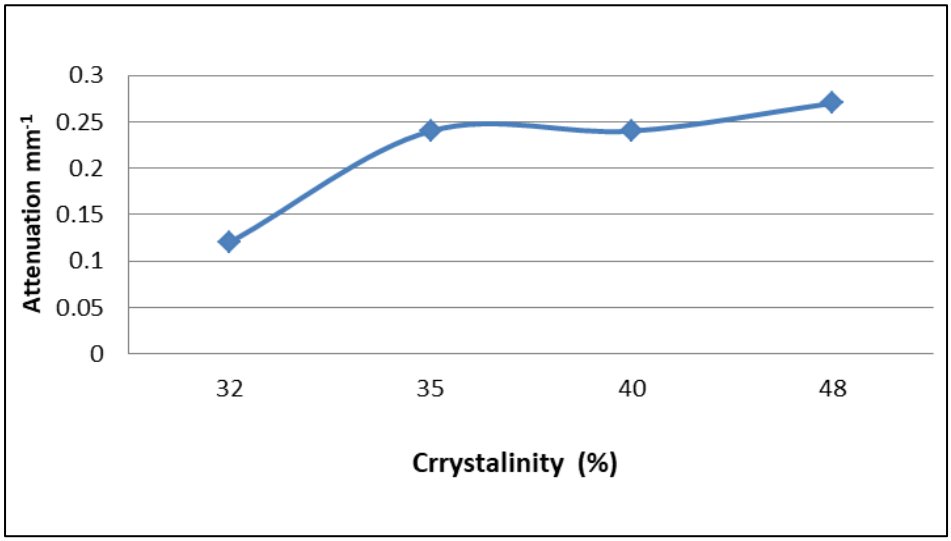

Figure 49 Attenuation vs. crystallinity of PP based composites

The speed of sound in a material relates to the elastic moduli of the material, which is considered a characteristic of each material since the propagation of the US in the material depends on of the material density and structure as seen in (Figure 47, Figure 49).

As shown from the US graphs and analysis US signal can be used as an indication of changes in the material during extrusion. However, the change in US signal is minimal and can not be directly used to monitor the processing of the material. A signal enhancement system able to detect minor changes and differentiate between different -yet so similar- US signal can be used to obtain and form monitoring conditions and characteristics that could be used for online fault detection for the Bio-composite material production process. Such a system should be able to detect and classify signals of damaged-undesirable- the structure of a material by indicating the difference in US signals with a comparison of the desired structure signal.

Establishment of a relationship between us signals and mechanical properties of the examined composites may be performed based on a comparison of data shown in (Figure 42Figure 48Figure 49). The results revealed about the dependence of both US speed and attenuation on the crystallinity of the composite matrix. These dependencies are in agreement with those of critical stress and strains obtained by mechanical tests Figure 42. It may be stated that US signal measurement during inline monitoring of extrusion process allows characterizing the mechanical properties of the material of real components. Creation of a database of US signals and mechanical properties for various compositions is required that is planned to do in future work.

In order to prove the concept of our approach of comparing and classifying signal based on the temperature. A data of ultrasound signals with sampling rate 500 samples per second is collected for each saved at a different temperature. Knowing the frequency, sampling rate and signal time the signal can also be shown in both time and frequency domain.

The correlation coefficient is calculated between signals at a different temperature. Table 7 shows the correlation coefficient between samples forms temperature range 110°C-120°C. Comparing two signals at the same temperature gives the highest μ = 1.0000.

Figure 52 illustrates two signals at a different temperature. The first signal is at 50°C and while the second signal is at 80°C. The comparison between these two signals gives low μ = 0.9122. The top graphs show the same amplitude with respect to time, and the lower graphs are the signal is frequency domain.

Table 7 μ value between signals at different Temperatures

T °C	90	110	130	150	170	190
70	0.8654	0.3570	0.3400	0.3317	0.3207	0.3023
90		0.3867	0.3733	0.3648	0.3518	0.3318
110			0.9972	0.9966	0.9965	0.9945
130				0.9987	0.9977	0.9971
150					0.9987	0.9979
170						0.9989

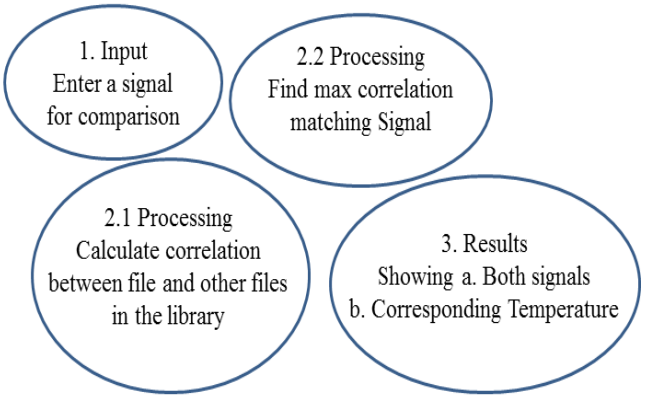

Figure 51 Software Flowchart

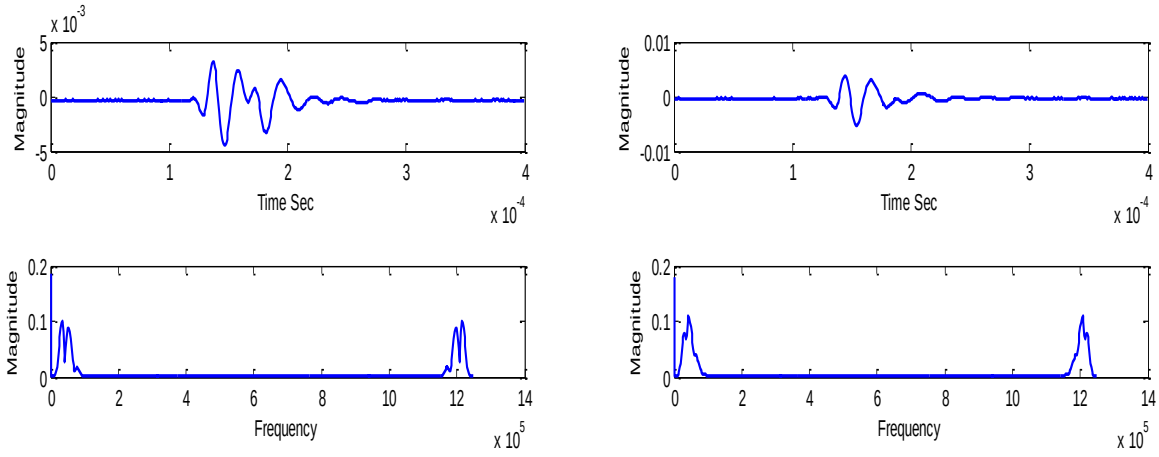

Figure 52 US signal at Different temperature 50°c (Right), 80°c (Left)

Figure 53 illustrates the comparison between the same signal at same temperature T = 100°C. The correlation between these signal gives the highest μ = 1.000.

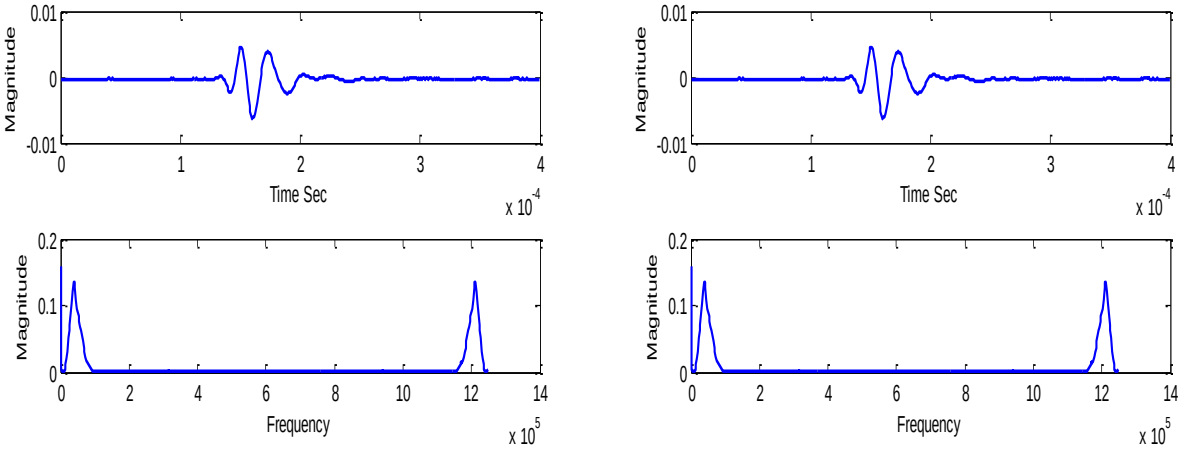

Figure 53 US signal at same temperature 100°C

The result of calculating and comparing the correlation coefficient between signals at different temperature shows that correlation coefficient between signals at near temperatures is much higher than between signals at a different temperature. Although this confirms that signals can be compared in order to determine temperature from the compared signal, it shows that correlation coefficient is a not a sufficient approach for that comparison since higher correlation coefficient

can be detected between two different materials at a different, yet near temperatures. A MATLAB algorithm that can calculate the correlation coefficient and reveal the corresponding temperature of the highest correlation coefficient confirmed these results.

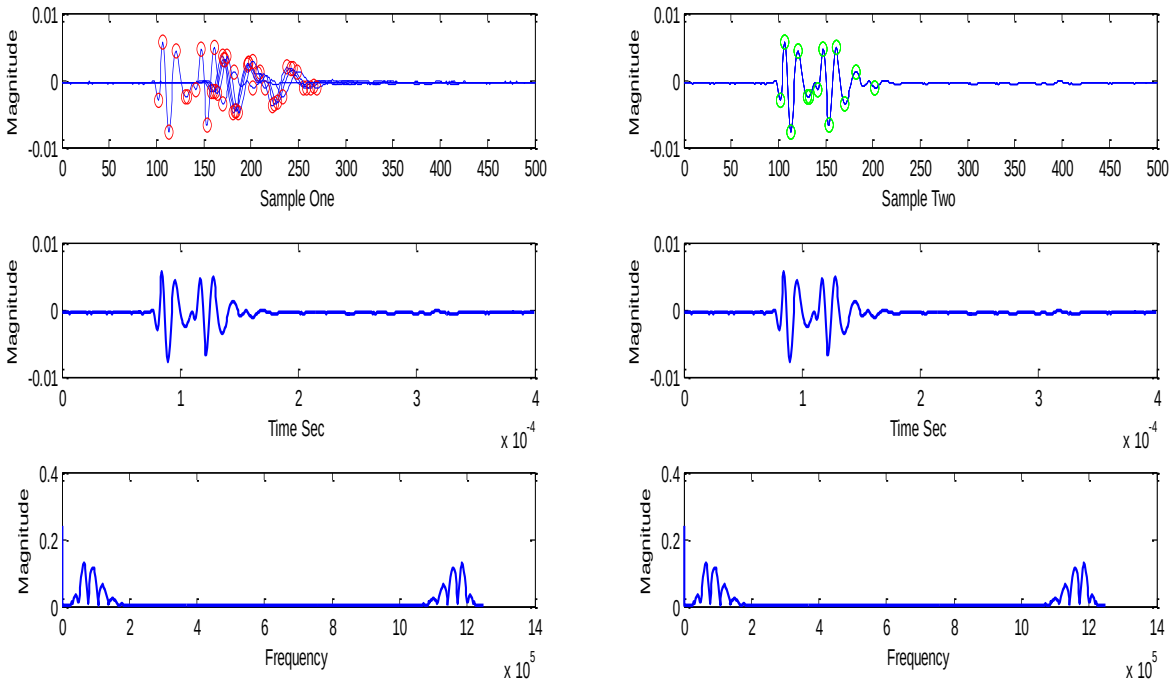

Figure 54 Finding Matching US signal

Figure 54 illustrates a comparison between the US signal on the right and multi known temperature ultrasound signals on the left. The software starts calculating μ between the signals till it reaches the max μ then it shows the temperature that matches this coefficient. The software then shows the two signals in both time and frequency domain.

The main conclusion of these results is confirming the need for machine learning techniques to classify the signal according to temperature, which make us, uses the main advantage of machine learning, which is the simplicity in finding a prediction model in order to be used to determine the temperature of the signal from previous experiences for a complex problem.

Results of Machine learning classification

A data file of 60 ultrasound signals at different temperatures was exported to Weka program to apply a classification algorithm. The ultrasound signal was classified using the cost-effective random forest classifier into two classes below and equal, or over 190^{o} C the result of this classifier was as follows.

Correctly Classified Instances	58	97 %
Incorrectly Classified Instances	2	3 %

= Detailed Accuracy By Class ===

Table 8 Detailed Accuracy of classifier By Class

TP Rate	FP Rate	Precision	Recall	Class
0.981	0.125	0.981	0.981	1
0.875	0.019	0.875	0875	2

=== Confusion Matrix ===

a b <-- classified as

51 1 | a = 1

1 7 | b = 2
2

By applying machine learning, A success of classifying the US signal according to temperature with 97% accuracy was obtained. This indicates that machine learning is a successful approach to be used to monitor the change in temperature during the extrusion. By applying machine learning techniques and use dominant ultrasound advantages over other techniques we can obtain a go-no go gage for the extrusion process that can predict material damage and alarm the operator for a required response. By using machine learning techniques, we successfully transferred the problem from a sophisticated signal analysis and modeling to find an empirical solution to a simple data classification one. These results are considered the required solution for the defined problem and the accomplishment of mission stated in the task statement.

For more reliable results, different classifiers were applied to the dataset file containing 184-ultrasound signal. Table 9 and Figure 55 show the results of the different classifiers used for comparison.

Table 9 Detailed Accuracy of different classifiers

Classifier	TP	FN	FP	TN	Sensitivity (%)	Specificity (%)	Geometric mean (%)	Accuracy (%)	Precision (%)
Linear LSVM	154.00	1.00	15.00	14.00	99.35	48.28	69.26	91.30	91.12
LSVM	155.00	0.00	29.00	0.00	100.00	0.00	0.00	84.24	84.24
NaïveBayes	106.00	49.00	3.00	26.00	68.39	89.66	78.30	71.74	97.25
Random Forest	155.00	0.00	5.00	24.00	100.00	82.76	90.97	97.28	96.88
Cost Sensitive Random Forest	154.00	1.00	3.00	26.00	99.35	89.66	94.38	97.83	98.09

Where;

Positive = ($<190^{o}$c), Negative = ($\geq 190^{o}$c), TP= True Positive, FN= False Negative, FP= False Positive, TN=True Negative

Sensitivity or true positive rate

TPR =TP/P = TP/ (TP+FN)

Specificity or true negative rate

SPC= TN/N=TN/(TN+FP)

Precision or positive predictive value

PPV= TP/(TP+FP)

Accuracy

ACC= (TP+TN)/(TP +FP+FN+TN)

Geometric mean

$$GM = \sqrt{TPR - SPC}$$

Specificity and the geometric mean play a more dominant rule of choosing the classifier in our case. Since our main interest is the minority class (Signals over 190^{o}C), it is important not to choose the classifier based only on accuracy. As higher accuracy, in this case, may not be a good indication for the strong classifier.

Results of the Classifiers

Results in changes based on the classifier algorithm and parameters tunning to deal with the specific dataset. Following is the used classifiers Strengths and weakness points.

Support Vector Machines (SVM)

As explained in chapter three SVM use Kernels mechanism, which essentially calculates the distance between two remarks. The SVM algorithm then finds a decision margin that maximizes the distance between the nearby members of separate classes.

- Advantages: with many kernels to choose from it can model non-linear decision boundaries. They are also reasonably strong against overfitting, especially in high-dimensional space.
- Disadvantages: SVM's are memory concentrated, delicate to tune due to the significance of choosing the correct kernel, and don't scale well to more massive datasets.

Naive Bayes

Naive Bayes (NB) is a straightforward algorithm based on conditional probability and counting. The model is, in fact, a probability table that gets updated through training data. To predict a new incident, just "look up" the class probabilities in "probability table" built on its feature values. "Naive" because of its core assumption that all input features are independent, which hardly holds true in reality.

- Advantages: even though the conditional independence assumption rarely holds true, NB models actually perform amazingly sound in practice, mainly for how simple they are. They are easy to implement and can scale with your dataset.
- Disadvantages: due to their sheer simplicity, models adequately trained and tuned using the previous algorithms listed often-beat NB models.

Classification Tree (Random forest)

- Advantages: classification tree ensembles also perform very well in practice. They are robust to outliers, scalable, and able to model non-linear decision edges thanks to their hierarchical structure obviously.
- Disadvantages: unconstrained, individual trees are likely expected to overfit, but this can be alleviated by ensemble methods.

For many application, random forest classifier has been showing the best results over other classifiers, which is why it is well known to be usually preferred over SVM's in the industry [112].

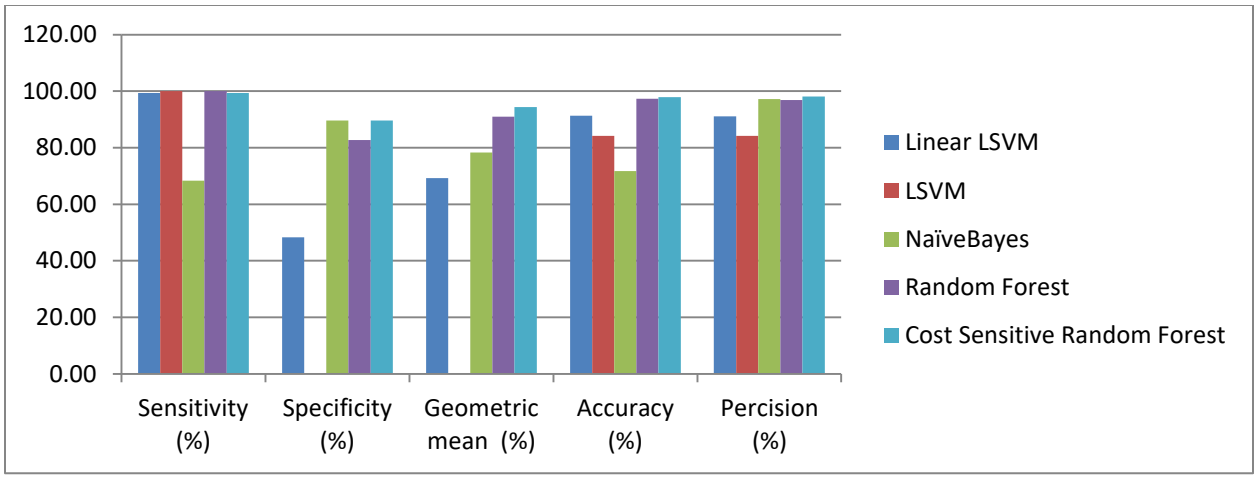

Figure 55 Comparison between classifiers

Table 10 Comparison of approaches

	Current (Thermocouple)	Conventional Approach	Machine Learning
Simplicity	✓✓✓✓✓	✓✓	✓✓✓✓
Accuracy	✓✓✓	✓✓✓✓✓	✓✓✓✓
Reliability	✓✓	✓✓✓✓✓	✓✓✓✓
Sensitivity	✓	✓✓✓✓	✓✓✓✓✓
Cost	✓✓✓✓✓	✓✓✓	✓✓✓✓
Calibration	✓	✓✓✓	✓✓✓✓✓
Adaptability	✓	✓✓	✓✓✓✓✓
Specificity	✓✓	✓✓✓	✓✓✓✓
Compatibility	✓✓	✓✓✓	✓✓✓✓✓
Practicality	✓✓✓✓	✓✓	✓✓✓✓✓
Response Time	✓	✓✓✓	✓✓✓✓

Table 10 shows a comparison between the current methods used for temperature monitoring (Thermocouple), the conventional approach of using ultrasound (signal analysis), and the studied approach of using machine learning for signal classification. This compassion could be seen as the advantages of machine learning approach over current and conventional approaches from an industrial point of view.

Regarding simplicity, monitoring the temperature using thermocouple may be the most straightforward way, since the thermocouple is already attached to most of the extruders. On the other hand, Although both conventional and machine learning approach need a transducer to be installed, the time needed for preparation of the system in comparison with machine learning is much longer. Also, the complexity of the algorithm needed to deal with the signal and analysis of the peaks and determine the speed of sound and find the correlated temperature is much harder than simple classifier technique, which from an industrial viewpoint will be as a go-nogo gauge for the processed composite.

Thermocouple approach also shows superiority over the other techniques in terms of cost. It is also very competitive with the machine learning regarding practicality, since for mass production reducing the temperature when damage is detected may be the most straightforward approach to save time and money and avoid stopping the production line. Of course, having a system that tells you whether or not this is a damaged composite will add more value to the practicality of the system. The conventional approach may achieve better accuracy and reliability since it is an empirical model, but machine learning is very competitive in the same terms since it also uses the experience to learn.

Machine learning is more superior to other techniques in many ways, especially regarding response time. Since thermocouple has a long response time and ultrasound monitoring of the temperature gives a more direct measurement of the temperature change or the temperature change effect on the material. In addition to that, machine learning techniques are more straightforward to calibrate and adapt to new material or process parameters. Machine learning is also better in terms of specificity as the primary concern for the industry is to avoid material damage and maintain a continuous composite production process. Hence, the more concern is to target the damaged material when damage occurs and prevent the cause from repeating.

Conclusion

The modified methods of US monitoring of sound speed and attenuation during heating, extrusion of PP Nano-Bio-composites is developed, and relationships between US signal and temperature parameters are established. It is found that characterization of the extrusion processes by sound velocity and attenuation allows monitoring and prevent the cellulose fiber composite destruction.

The correlation coefficient between ultrasound signals was obtained to confirm the relation between change in temperature and ultrasound signals. It is was noticed that signals at near temperature have high correlation coefficient, which makes it hard to use an empirical model to detecting the change in temperature. Machine learning classifier algorithm was used to classify 184 datasets of ultrasound signals of biocomposite material at different temperatures. The classifier was used to classify the signals into over and below 190^{o}C, which is the temperature at which the fiber degradation takes place. Five classifier results were obtained for comparison and to choose the best outcome. The results show that the best classifier is the cost-sensitive random forest classifier with accuracy 97.8%. This technique could be used in monitoring temperature during biocomposite production in order to contain fiber degradation during the extrusion. The system can be enhanced for industrial purposes to adapt different kinds of materials and to predict possible temperature increase. It is found that modification PP composite with CNTs with the content of about 0.5-0.1% changes the PP – fiber composite behavior at the small strength and this effect is controlled by structure of semi crystalline polymers.

iv) Reinforcing with cellulose nanofibers do not change both critical stresses and strains of the points A and B considerably in spite of variation of crystallinity degree;

v) The main effect of CNT modification is an increase of both critical stresses and strains of the points A and B which is believed to be the result of specific features of semi-crystalline structure formation arisen due to CNTs presence;

vi) The strengthening effect of CNTs (inclination of the curves $\sigma_{A,B}=f(c)$) in the range of c=40-50% is similar to points A and B (Figure 42) that reveals about the influence of CNTs on the polypropylene matrix crystallinity and structure at the initial stage of the PP composite deformation.

The effect of CNTs on both these parameters is especially pronounced. DSC analysis showed that adding microfibers and MWCNT in PP matrix leads to increase in the crystallization temperature and the crystallinity degree in PP. The thermal degradation study shows an increase in thermal stability of the PP matrix in the composite with added CNTs. The increased crystallinity degree of the PP matrix in composites with adding microfibers and MWCNT is shown. Thus adding fibers and especially CNT vigorously promotes the nucleation of PP.

The mechanical and thermal behavior of nitrocellulose/PP and micro cellulose/MWNT/PP composites was studied. For all systems, the increase in yield stress has been observed supporting the existence of an interaction between nanotubes and the polymer matrix. The addition of fibers and CNT increased the temperature of crystallization and crystallinity degree.

The obtained results allow developing the extrusion temperature monitoring technique and inline evaluation of the mechanical properties of the PP-MF-CNT composites.

Future work

The machine learning techniques can be used in online monitoring for ultrasound signal classification based on the temperature. The following flowchart shows that same technique used for classification for over and below 190^{o}c can be followed by similar classification for lower or higher temperatures. After classification, the system can be connected to a control system to provide a control signal that can adjust the temperature online automatically. The system could also be connected to a local or vast area network to share the data and learning experiences with other similar systems in the network. The machine learning can also be used as a prediction model to determine when the temperature is expected to be increased by obtaining more training data at different processing conditions.

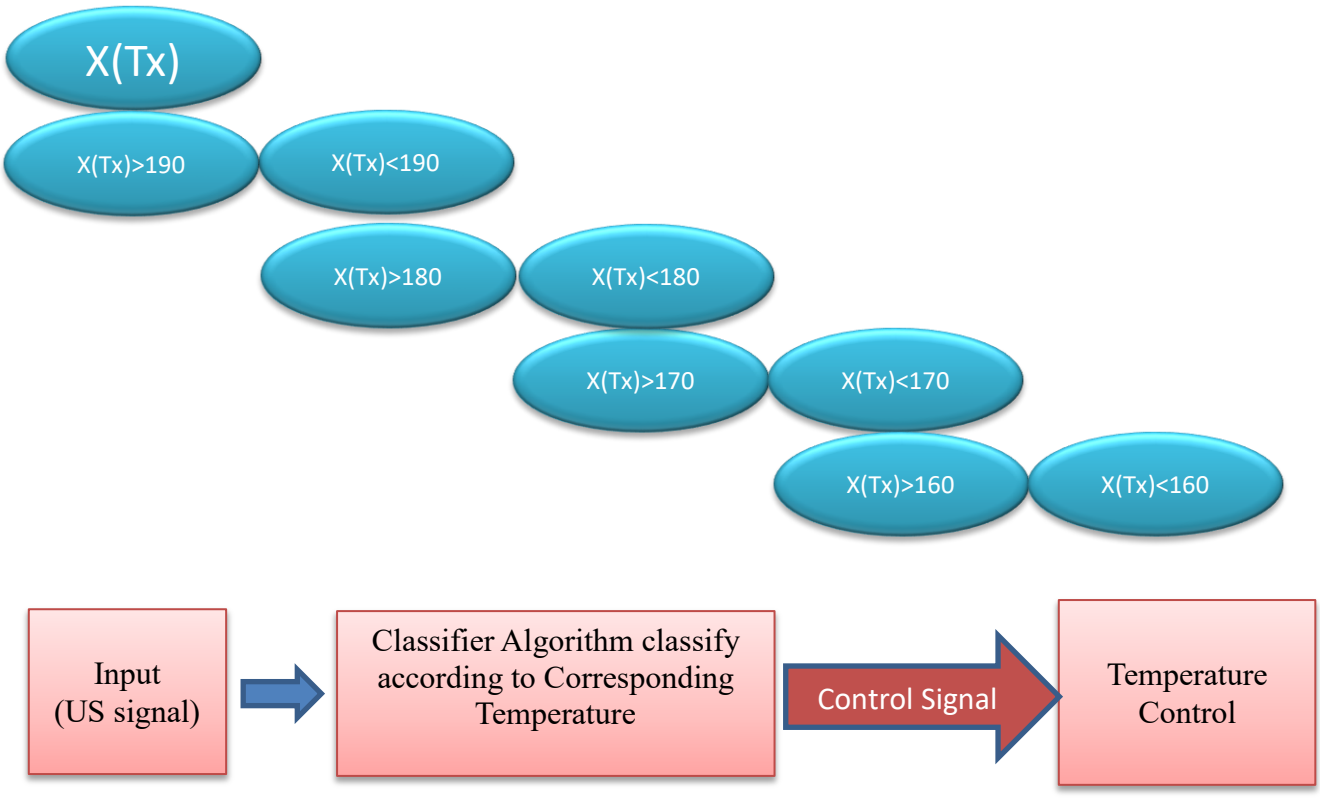

References

[1] P. Malaca, L. F. Rocha, D. Gomes, J. Silva, and G. Veiga, "Online inspection system based on machine learning techniques: real case study of fabric textures classification for the automotive industry," *Journal of Intelligent Manufacturing,* pp. 1-11, 2016.

[2] M. Khorram Niaki, M. Khorram Niaki, F. Nonino, and F. Nonino, "Impact of additive manufacturing on business competitiveness: a multiple case study," *Journal of Manufacturing Technology Management,* vol. 28, pp. 56-74, 2017.

[3] Z. Huang, H. Ge, J. Yin, and F. Liu, "Effects of fiber loading and chemical treatments on properties of sisal fiber-reinforced sheet molding compounds," *Journal of Composite Materials,* vol. 51, pp. 3175-3185, 2017.

[4] S. Ariadurai, "Bio-Composites: Current Status and Future Trends."

[5] S. Liang, H. Nouri, and E. Lafranche, "Thermo-compression forming of flax fibre-reinforced polyamide 6 composites: influence of the fibre thermal degradation on mechanical properties," *Journal of Materials Science,* vol. 50, pp. 7660-7672, 2015.

[6] J. Gassan and A. K. Bledzki, "Thermal degradation of flax and jute fibers," *Journal of Applied Polymer Science,* vol. 82, pp. 1417-1422, 2001.

[7] C. Abeykoon, P. J. Martin, K. Li, A. L. Kelly, E. C. Brown, and P. D. Coates, "Melt temperature consistency during polymer extrusion."

[8] J. Vera-Sorroche, A. Kelly, E. Brown, and P. Coates, "Infrared melt temperature measurement of single screw extrusion," *Polymer Engineering & Science,* vol. 55, pp. 1059-1066, 2015.

[9] B. K. Nguyen, G. McNally, and A. Clarke, "Automatic extruder for processing recycled polymers with ultrasound and temperature control system," *Proceedings of the Institution of Mechanical Engineers, Part E: Journal of Process Mechanical Engineering,* vol. 230, pp. 355-370, 2016.

[10] O. S. Carneiro, J. A. Covas, and B. Vergnes, "Experimental and theoretical study of twin-screw extrusion of polypropylene," *Journal of applied polymer science,* vol. 78, pp. 1419-1430, 2000.

[11] A. L. Kelly, E. C. Brown, and P. D. Coates, "The effect of screw geometry on melt temperature profile in single screw extrusion," *Polymer Engineering & Science,* vol. 46, pp. 1706-1714, 2006.

[12] M. Emin, T. Teumer, W. Schmitt, M. Rädle, and H. Schuchmann, "Measurement of the true melt temperature in a twin-screw extrusion processing of starch based matrices via infrared sensor," *Journal of Food Engineering,* vol. 170, pp. 119-124, 2016.

[13] M. Lizaranzu, A. Lario, A. Chiminelli, and I. Amenabar, "Non-destructive testing of composite materials by means of active thermography-based tools," *Infrared Physics & Technology,* vol. 71, pp. 113-120, 2015.

[14] A. Nolle, "Acoustic Determination of the Physical Constants of Rubber-Like Materials," *The Journal of the Acoustical Society of America,* vol. 19, pp. 194-201, 1947.

[15] M. Villanueva, L. Cabedo, E. Gimenez, J. Lagaron, P. Coates, and A. Kelly, "Study of the dispersion of nanoclays in a LDPE matrix using microscopy and in-process ultrasonic monitoring," *Polymer Testing,* vol. 28, pp. 277-287, 2009.

[16] N. SAMET, E. B. NDIAYE, P. MARECHAL, and H. DUFLO, "Polymerization monitoring using ultrasound," in *13th International Symposium on Nondestructive Characterization of Materials (NDCM-XIII),< www. ndt. net,* 2013.

[17] J. Mc Hugh, "Ultrasound technique for the dynamic mechanical analysis (DMA) of polymers," 2007.
[18] R. Challis, R. Freemantle, R. Cocker, D. Chadwick, D. Dare, C. Martin, *et al.*, "Ultrasonic measurements related to evolution of structure in curing epoxy resins," *Plastics, rubber and composites,* 2013.
[19] J. Mc Hugh, J. Döring, W. Stark, and J. Guey, "Relationship between the mechanical and ultrasound properties of polymer materials," 2006.
[20] F. Lionetto and A. Maffezzoli, "Polymer characterization by ultrasonic wave propagation," *Advances in Polymer Technology,* vol. 27, p. 63, 2008.
[21] M. Sinha and D. J. Buckley, "Acoustic properties of polymers," in *Physical Properties of Polymers Handbook,* ed: Springer, 2007, pp. 1021-1031.
[22] J. Döring, W. Stark, J. Bartusch, and J. Mc Hugh, "Contribution to ultrasound cure control for composite manufacturing," 2000.
[23] L. C. Lynnworth, *Ultrasonic measurements for process control: theory, techniques, applications*: Academic press, 2013.
[24] D. Lellinger, S. Tadjbach, and I. Alig, "Determination of the elastic moduli of polymer films by a new ultrasonic reflection method," in *Macromolecular Symposia*, 2002, pp. 203-214.
[25] J. Tatibouet and M. Huneault, "In-line ultrasonic monitoring of filler dispersion during extrusion," *International Polymer Processing,* vol. 17, pp. 49-52, 2002.
[26] D. Wang and K. Min, "In-line monitoring and analysis of polymer melting behavior in an intermeshing counter-rotating twin-screw extruder by ultrasound waves," *Polymer Engineering & Science,* vol. 45, pp. 998-1010, 2005.
[27] D. Françla, C. K. Jen, K. Nguyen, and R. Gendron, "Ultrasonic in-line monitoring of polymer extrusion," *Polymer Engineering & Science,* vol. 40, pp. 82-94, 2000.
[28] R. Gendron, J. Tatibouet, J. Guevremont, M. Dumoulin, and L. Piche, "Ultrasonic behavior of polymer blends," *Polymer Engineering & Science,* vol. 35, pp. 79-91, 1995.
[29] I. H. Witten, E. Frank, M. A. Hall, and C. J. Pal, *Data Mining: Practical machine learning tools and techniques*: Morgan Kaufmann, 2016.
[30] R. S. Michalski, J. G. Carbonell, and T. M. Mitchell, *Machine learning: An artificial intelligence approach*: Springer Science & Business Media, 2013.
[31] S. Shalev-Shwartz and S. Ben-David, *Understanding machine learning: From theory to algorithms*: Cambridge university press, 2014.
[32] Y. Baştanlar and M. Özuysal, "Introduction to machine learning," *miRNomics: MicroRNA Biology and Computational Analysis*, pp. 105-128, 2014.
[33] S. Chakrabarti, E. Cox, E. Frank, R. H. Güting, J. Han, X. Jiang, *et al.*, *Data mining: know it all*: Morgan Kaufmann, 2008.
[34] F. Dunn, W. Hartmann, D. Campbell, and N. H. Fletcher, *Springer handbook of acoustics*: Springer, 2015.
[35] P. Laugier and G. Haïat, *Bone quantitative ultrasound* vol. 576: Springer, 2011.
[36] C.-H. Chen, *Ultrasonic and advanced methods for nondestructive testing and material characterization*: World Scientific, 2007.
[37] P. J. Shull, *Nondestructive evaluation: theory, techniques, and applications*: CRC press, 2016.

[38] B. T. Khuri-Yakub and Ö. Oralkan, "Capacitive micromachined ultrasonic transducers for medical imaging and therapy," *Journal of micromechanics and microengineering,* vol. 21, p. 054004, 2011.
[39] J. Krautkrämer and H. Krautkrämer, *Ultrasonic testing of materials*: Springer Science & Business Media, 2013.
[40] A. Castellano, P. Foti, A. Fraddosio, S. Marzano, and M. D. Piccioni, "Mechanical characterization of CFRP composites by ultrasonic immersion tests: Experimental and numerical approaches," *Composites Part B: Engineering,* vol. 66, pp. 299-310, 2014.
[41] C. Carpentier and J. Rudlin, "Manual ultrasonic inspection of thin metal welds," in *11th European Conference on Non-Destructive Testing, Prague, Czech Republic*, 2014.
[42] A. Kapadia, "Non destructive testing of composite materials," *National Composites Network*, pp. 1-4, 2007.
[43] A. S. Birks, R. E. Green, and P. McIntire, *Ultrasonic testing*: American Society for Nondestructive Testing, 1991.
[44] E. Brown, P. Olley, and P. Coates, "In line melt temperature measurement during real time ultrasound monitoring of single screw extrusion," *Plastics, rubber and composites,* vol. 29, pp. 3-13, 2000.
[45] S. D. Milić, A. D. Žigić, and M. M. Ponjavić, "Online temperature monitoring, fault detection, and a novel heat run test of a water-cooled rotor of a hydrogenerator," *IEEE Transactions on Energy Conversion,* vol. 28, pp. 698-706, 2013.
[46] P. K. Rao, J. P. Liu, D. Roberson, Z. J. Kong, and C. Williams, "Online real-time quality monitoring in additive manufacturing processes using heterogeneous sensors," *Journal of Manufacturing Science and Engineering,* vol. 137, p. 061007, 2015.
[47] J. Brizuela, J. Camacho, T. G. Álvarez-Arenas, J. Cruza, and E. Poodts, "Air-coupled ultrasound inspection of complex aluminium-CFRP components," in *Ultrasonics Symposium (IUS), 2016 IEEE International*, 2016, pp. 1-4.
[48] C. Zhou, Y. Wang, C. Qiao, S. Zhao, and Z. Huang, "High-accuracy ultrasonic temperature measurement based on MLS-modulated continuous wave," *Measurement,* vol. 88, pp. 1-8, 2016.
[49] M. Xiao-Bing, Z. Shu-Yi, Z. Jun-Jian, and Y. Yue-Tao, "Automatic ultrasonic thermometry," *JOURNAL-NANJING UNIVERSITY NATURAL SCIENCES EDITION,* vol. 39, pp. 517-524, 2003.
[50] I. Bazán, M. Vazquez, A. Ramos, A. Vera, and L. Leija, "A performance analysis of echographic ultrasonic techniques for non-invasive temperature estimation in hyperthermia range using phantoms with scatterers," *Ultrasonics,* vol. 49, pp. 358-376, 2009.
[51] Y. Wei, Y. Gao, Z. Xiao, G. Wang, M. Tian, and H. Liang, "Ultrasonic Al2O3 Ceramic Thermometry in High-Temperature Oxidation Environment," *Sensors,* vol. 16, p. 1905, 2016.
[52] M. D. Abolhassani, A. Norouzy, A. Takavar, and H. Ghanaati, "Noninvasive temperature estimation using sonographic digital images," *Journal of ultrasound in medicine,* vol. 26, pp. 215-222, 2007.
[53] K. Masumnia-Bisheh, M. Ghaffari-Miab, and B. Zakeri, "Evaluation of Different Approximations for Correlation Coefficients in Stochastic FDTD to Estimate SAR Variance in a Human Head Model," *IEEE Transactions on Electromagnetic Compatibility,* 2016.

[54] T. T. Soong, *Fundamentals of probability and statistics for engineers*: John Wiley & Sons, 2004.
[55] K. Bauters, J. Cottyn, D. Claeys, M. Slembrouck, P. Veelaert, and H. van Landeghem, "Automated work cycle classification and performance measurement for manual work stations," *Robotics and Computer-Integrated Manufacturing,* vol. 51, pp. 139-157, 2018.
[56] Y. Shaban and S. Yacout, "Visual data mining of faults in machining process based on machine learning."
[57] M. Aksoy, O. Torkul, and I. H. Cedimoglu, "An industrial visual inspection system that uses inductive learning," *Journal of Intelligent Manufacturing,* vol. 15, pp. 569-574, 2004.
[58] A. M. Almana and M. Aksoy, "An overview of inductive learning algorithms," *International Journal of Computer Applications,* vol. 88, 2014.
[59] D. Cogoljević, M. Alizamir, I. Piljan, T. Piljan, K. Prljić, and S. Zimonjić, "A machine learning approach for predicting the relationship between energy resources and economic development," *Physica A: Statistical Mechanics and its Applications,* 2017.
[60] D.-M. Chun, S.-H. Ahn, and J.-D. Jang, "Construction of web-based material database and case study of material selection for automotive engine pulley," *Transactions of the Korean Society of Automotive Engineers,* vol. 14, pp. 107-114, 2006.
[61] A. Mosavi, T. Rabczuk, and A. R. Varkonyi-Koczy, "Reviewing the novel machine learning tools for materials design," in *International Conference on Global Research and Education*, 2017, pp. 50-58.
[62] A. Mosavi and A. Vaezipour, "Reactive search optimization; application to multiobjective optimization problems," *Applied Mathematics,* vol. 3, p. 1572, 2012.
[63] A. Mosavi, "A multicriteria decision making environment for engineering design and production decision-making," *International Journal of Computer Applications,* vol. 69, 2013.
[64] H. Shi and J. Zeng, "Real-time prediction of remaining useful life and preventive opportunistic maintenance strategy for multi-component systems considering stochastic dependence," *Computers & Industrial Engineering,* vol. 93, pp. 192-204, 2016.
[65] E. F. Alsina, M. Chica, K. Trawiński, and A. Regattieri, "On the use of machine learning methods to predict component reliability from data-driven industrial case studies," *The International Journal of Advanced Manufacturing Technology,* vol. 94, pp. 2419-2433, 2018.
[66] H.-I. Lin, "Development of an intelligent transformer insertion system using a robot arm," *Robotics and Computer-Integrated Manufacturing,* vol. 51, pp. 209-221, 2018.
[67] S. M. Iveson, J. D. Litster, K. Hapgood, and B. J. Ennis, "Nucleation, growth and breakage phenomena in agitated wet granulation processes: a review," *Powder technology,* vol. 117, pp. 3-39, 2001.
[68] A. Wafa'H, B. Khorsheed, M. Mahfouf, I. Gabbott, G. K. Reynolds, and A. D. Salman, "Transparent Predictive Modelling of the Twin Screw Granulation Process using a Compensated Interval Type-2 Fuzzy System," *European Journal of Pharmaceutics and Biopharmaceutics,* 2017.
[69] Y. Shaban, S. Yacout, M. Balazinski, and K. Jemielniak, "Cutting tool wear detection using multiclass logical analysis of data," *Machining Science and Technology,* vol. 21, pp. 526-541, 2017.

[70] P. G. Nieto, E. García-Gonzalo, J. Á. Antón, V. G. Suárez, R. M. Bayón, and F. M. Martín, "A comparison of several machine learning techniques for the centerline segregation prediction in continuous cast steel slabs and evaluation of its performance," *Journal of Computational and Applied Mathematics,* vol. 330, pp. 877-895, 2018.
[71] A. Ragab, M. El-Koujok, B. Poulin, M. Amazouz, and S. Yacout, "Fault diagnosis in industrial chemical processes using interpretable patterns based on Logical Analysis of Data," *Expert Systems with Applications,* vol. 95, pp. 368-383, 2018.
[72] P. Yildirim, D. Birant, and T. Alpyildiz, "Data mining and machine learning in textile industry," *Wiley Interdisciplinary Reviews: Data Mining and Knowledge Discovery,* vol. 8, 2018.
[73] D. C. Sing, L. N. Metz, and S. Dudli, "Machine learning-based classification of 38 years of spine-related literature into 100 research topics," *Spine,* vol. 42, pp. 863-870, 2017.
[74] I. Podolak, A. Roman, M. Szykuła, and B. Zieliński, "A machine learning approach to synchronization of automata," *Expert Systems with Applications,* 2017.
[75] N. I. Yassin, S. Omran, E. M. El Houby, and H. Allam, "Machine Learning Techniques for Breast Cancer Computer Aided Diagnosis Using Different Image Modalities: A Systematic Review," *Computer Methods and Programs in Biomedicine,* 2017.
[76] V. Matz, M. Kreidl, and R. Smid, "Classification of ultrasonic signals," *International Journal of Materials and Product Technology,* vol. 27, pp. 145-155, 2006.
[77] H. Mo and Y. Zhao, "Motor Imagery Electroencephalograph Classification Based on Optimized Support Vector Machine by Magnetic Bacteria Optimization Algorithm," *Neural Processing Letters,* vol. 44, pp. 185-197, 2016.
[78] O. Faruk, A. K. Bledzki, H.-P. Fink, and M. Sain, "Biocomposites reinforced with natural fibers: 2000–2010," *Progress in Polymer Science,* vol. 37, pp. 1552-1596, 2012.
[79] A. Karmaker and J. Shneider, "Mechanical performance of short jute fibre reinforced polypropylene," *Journal of materials science letters,* vol. 15, pp. 201-202, 1996.
[80] C. Correa, C. Razzino, and E. Hage Jr, "Role of maleated coupling agents on the interface adhesion of polypropylene—wood composites," *Journal of Thermoplastic Composite Materials,* vol. 20, pp. 323-339, 2007.
[81] N. Ranganathan, K. Oksman, S. K. Nayak, and M. Sain, "Effect of long fiber thermoplastic extrusion process on fiber dispersion and mechanical properties of viscose fiber/polypropylene composites," *Polymers for Advanced Technologies,* vol. 27, pp. 685-692, 2016.
[82] H. Hajiha and M. Sain, "High toughness hybrid biocomposite process optimization," *Composites Science and Technology,* vol. 111, pp. 44-49, 2015.
[83] X. Shen, J. Jia, C. Chen, Y. Li, and J.-K. Kim, "Enhancement of mechanical properties of natural fiber composites via carbon nanotube addition," *Journal of materials science,* vol. 49, pp. 3225-3233, 2014.
[84] S. Mathurosemontri, P. Uawongsuwan, S. Nagai, and H. Hamada, "The Effect of Processing Parameter on Mechanical Properties of Short Glass Fiber Reinforced Polyoxymethylene Composite by Direct Fiber Feeding Injection Molding Process," *Energy Procedia,* vol. 89, pp. 255-263, 2016.
[85] Y.-T. Cheng, W. Ni, and C.-M. Cheng, "Determining the instantaneous modulus of viscoelastic solids using instrumented indentation measurements," *Journal of materials research,* vol. 20, pp. 3061-3071, 2005.

[86] Y. Liu and S. Kumar, "Polymer/carbon nanotube nano composite fibers–a review," *ACS applied materials & interfaces,* vol. 6, pp. 6069-6087, 2014.
[87] A. Amash and P. Zugenmaier, "Morphology and properties of isotropic and oriented samples of cellulose fibre–polypropylene composites," *Polymer,* vol. 41, pp. 1589-1596, 2000.
[88] R. Reixach Corominas, J. Puig Serramitja, J. A. Méndez González, J. Gironès i Molera, X. Espinach Orús, G. Arbat Pujolràs, *et al.*, "Orange Wood Fiber Reinforced Polypropylene Composites: Thermal Properties," *© Bioresources, 2015, vol. 10, núm. 2, p. 2156-2166,* 2015.
[89] S. Patlazhan and Y. Remond, "Structural mechanics of semicrystalline polymers prior to the yield point: a review," *Journal of Materials Science,* vol. 47, pp. 6749-6767, 2012.
[90] A. R. Clarke and C. N. Eberhardt, *Microscopy techniques for materials science*: Woodhead Publishing, 2002.
[91] I. Severina, J. Sadler, and E. Maeva, "Acoustic Microscopy Study of Properties and Microstructure of Synthetic and Natural Fiber Composite Materials," in *Acoustical Imaging*, ed: Springer, 2011, pp. 143-150.
[92] L. C. Mendes and S. P. Cestari, "Printability of HDPE/natural fiber composites with high content of cellulosic industrial waste," *Materials Sciences and Applications,* vol. 2, p. 1331, 2011.
[93] P. Joseph, K. Joseph, S. Thomas, C. Pillai, V. Prasad, G. Groeninckx, *et al.*, "The thermal and crystallisation studies of short sisal fibre reinforced polypropylene composites," *Composites Part A: Applied Science and Manufacturing,* vol. 34, pp. 253-266, 2003.
[94] E. Jose, A. Joseph, M. Skrifvars, S. Thomas, and K. Joseph, "Thermal and crystallization behavior of cotton—Polypropylene commingled composite systems," *Polymer Composites,* vol. 31, pp. 1487-1494, 2010.
[95] J. Golebiewski and A. Galeski, "Thermal stability of nanoclay polypropylene composites by simultaneous DSC and TGA," *Composites Science and Technology,* vol. 67, pp. 3442-3447, 2007.
[96] S. T. Huxtable, D. G. Cahill, S. Shenogin, L. Xue, R. Ozisik, P. Barone, *et al.*, "Interfacial heat flow in carbon nanotube suspensions," *Nature materials,* vol. 2, pp. 731-734, 2003.
[97] H.-S. Yang, A. Kiziltas, and D. J. Gardner, "Thermal analysis and crystallinity study of cellulose nanofibril-filled polypropylene composites," *Journal of thermal analysis and calorimetry,* vol. 113, pp. 673-682, 2013.
[98] S. Spoljaric, A. Genovese, and R. A. Shanks, "Polypropylene–microcrystalline cellulose composites with enhanced compatibility and properties," *Composites Part A: Applied Science and Manufacturing,* vol. 40, pp. 791-799, 2009.
[99] M. Pracella, D. Chionna, I. Anguillesi, Z. Kulinski, and E. Piorkowska, "Functionalization, compatibilization and properties of polypropylene composites with hemp fibres," *Composites Science and Technology,* vol. 66, pp. 2218-2230, 2006.
[100] D. Ndiaye, V. Verney, H. Askanian, S. Commereuc, and A. Tidjani, "Morphology, Thermal Behavior and Dynamic Rheological Properties of Wood Polypropylene Composites," *Materials Sciences and Applications,* vol. 4, p. 730, 2013.
[101] U. Somnuk, G. Eder, P. Phinyocheep, N. Suppakarn, W. Sutapun, and Y. Ruksakulpiwat, "Quiescent crystallization of natural fibers–polypropylene composites," *Journal of applied polymer science,* vol. 106, pp. 2997-3006, 2007.

[102] K. Na, H. S. Park, H. Y. Won, J. K. Lee, K. H. Lee, J. Y. Nam, *et al.*, "SALS study on transcrystallization and fiber orientation in glass fiber/polypropylene composites," *Macromolecular research,* vol. 14, pp. 499-503, 2006.
[103] A. Arbelaiz, B. Fernandez, J. Ramos, and I. Mondragon, "Thermal and crystallization studies of short flax fibre reinforced polypropylene matrix composites: Effect of treatments," *Thermochimica Acta,* vol. 440, pp. 111-121, 2006.
[104] N. Ranganathan, K. Oksman, S. K. Nayak, and M. Sain, "Regenerated cellulose fibers as impact modifier in long jute fiber reinforced polypropylene composites: Effect on mechanical properties, morphology, and fiber breakage," *Journal of Applied Polymer Science,* vol. 132, 2015.
[105] R. Abu-Zurayk, E. Harkin-Jones, T. McNally, G. Menary, P. Martin, C. Armstrong, *et al.*, "Structure–property relationships in biaxially deformed polypropylene nanocomposites," *Composites Science and Technology,* vol. 70, pp. 1353-1359, 2010.
[106] J. Fritsch, S. Hiermaier, and G. Strobl, "Characterizing and modeling the non-linear viscoelastic tensile deformation of a glass fiber reinforced polypropylene," *Composites Science and Technology,* vol. 69, pp. 2460-2466, 2009.
[107] Y. Men and G. Strobl, "Critical strains determining the yield behavior of s-PP," *Journal of Macromolecular Science, Part B,* vol. 40, pp. 775-796, 2001.
[108] V. Oshmyan, S. Patlazhan, and Y. Remond, "Simulation of small-strain deformations of semi-crystalline polymer: Coupling of structural transformations with stress-strain response," *Journal of materials science,* vol. 39, pp. 3577-3586, 2004.
[109] H. Chang, J. Luo, H. C. Liu, A. A. B. Davijani, P.-H. Wang, and S. Kumar, "Orientation and interfacial stress transfer of cellulose nanocrystal nanocomposite fibers," *Polymer,* vol. 110, pp. 228-234, 2017.
[110] Y. Men, J. Rieger, and G. Strobl, "Role of the entangled amorphous network in tensile deformation of semicrystalline polymers," *Physical review letters,* vol. 91, p. 095502, 2003.
[111] J. Jarzynski, "Mechanisms of sound attenuation in materials," ed: ACS Publications, 1990.
[112] A. C. Lorena, L. F. Jacintho, M. F. Siqueira, R. De Giovanni, L. G. Lohmann, A. C. De Carvalho, *et al.*, "Comparing machine learning classifiers in potential distribution modelling," *Expert Systems with Applications,* vol. 38, pp. 5268-5275, 2011.

Vita auctoris

NAME:	Ahmed Elseddawy
PLACE OF BIRTH:	Cairo, Egypt
YEAR OF BIRTH :	1986
EDUCATION:	Bachelor of Mechatronis Engineering 2003-2008 Ain Shams University Master of Engineering Physics 2009-2013 Ain Shams University Ph. D of Electrical Engineering 2014-2018 University of Windsor